FINAL RESULTS FROM PROSPECT

"It doesn't matter what happens to me, just get my presentation to the ~~9 A.M. meeting at 562 West Ninth Street, conference room C!"~~
3 pm seminar in building 510, small seminar room

David Jaffe, BNL

25 July 2024

What I’m going to talk about

Neutrinos: Early history

Neutrinos: Early 2010s

PROSPECT motivation, design, construction

Final results with PROSPECT-I

Last words

I have borrowed or adapted numerous slides from PROSPECT colleagues.
Thanks to Karsten Heeger, Tom Langford, Bryce Littlejohn, Danielle Norcini, Pravana Surukuchi, Diego Venegas Vargas

Neutrinos: Early history

Ref: A.Pais, Rev.Mod.Phys. **49** (1977) 925.

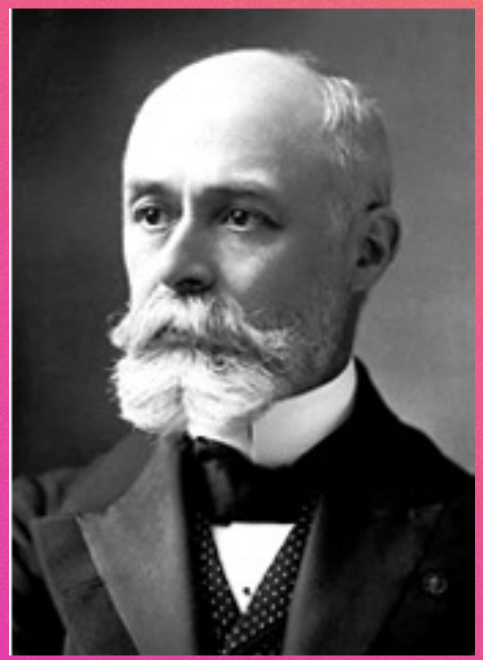

1896 Becquerel discovers radioactivity

1914 Chadwick observes continues β-ray energy spectrum

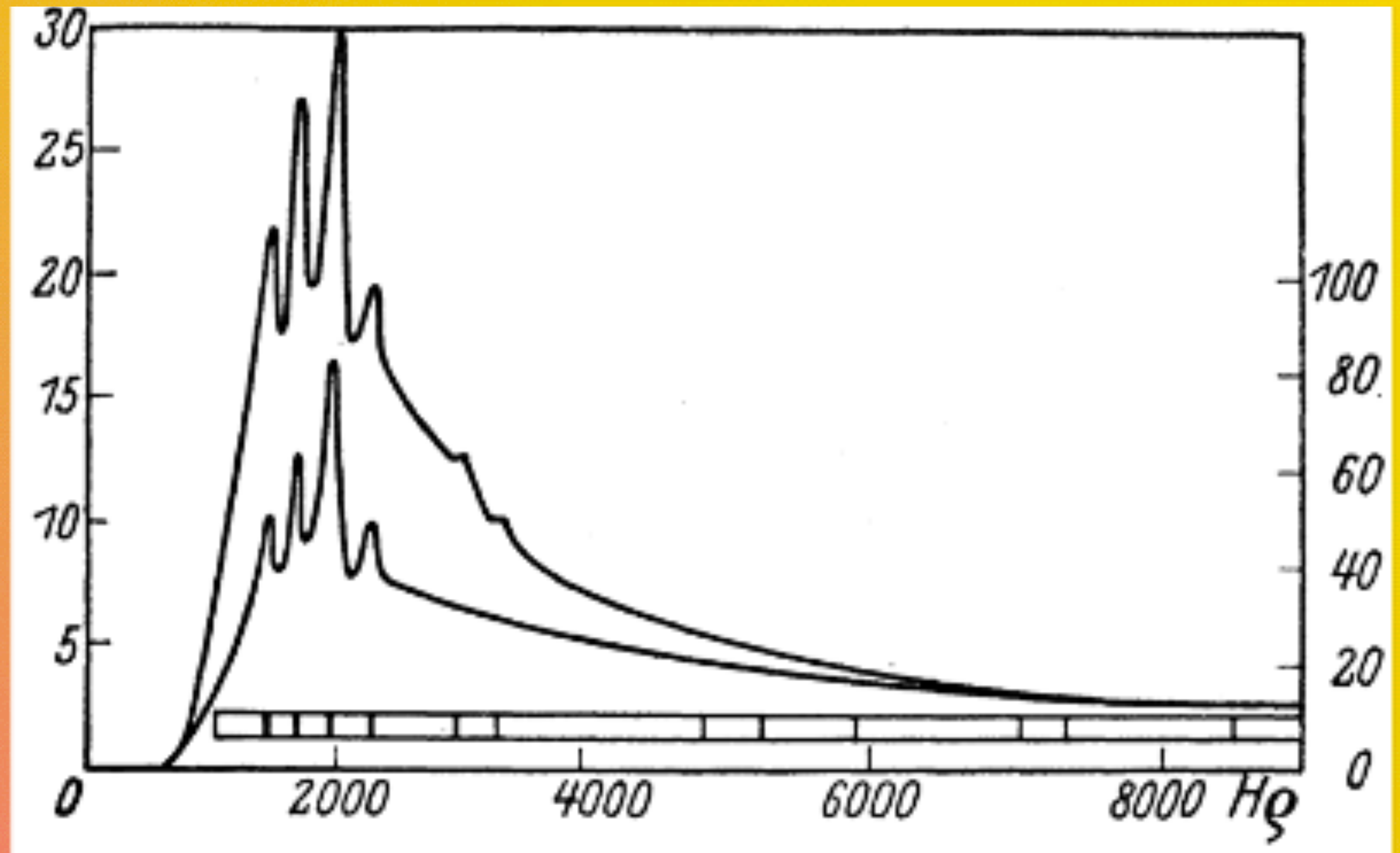

Fig. 3. Chadwick's measurement of β-spectrum of Ra B + C.

James Chadwick, Maurice Goldhaber's PhD advisor

Boating on Lake Como 1927

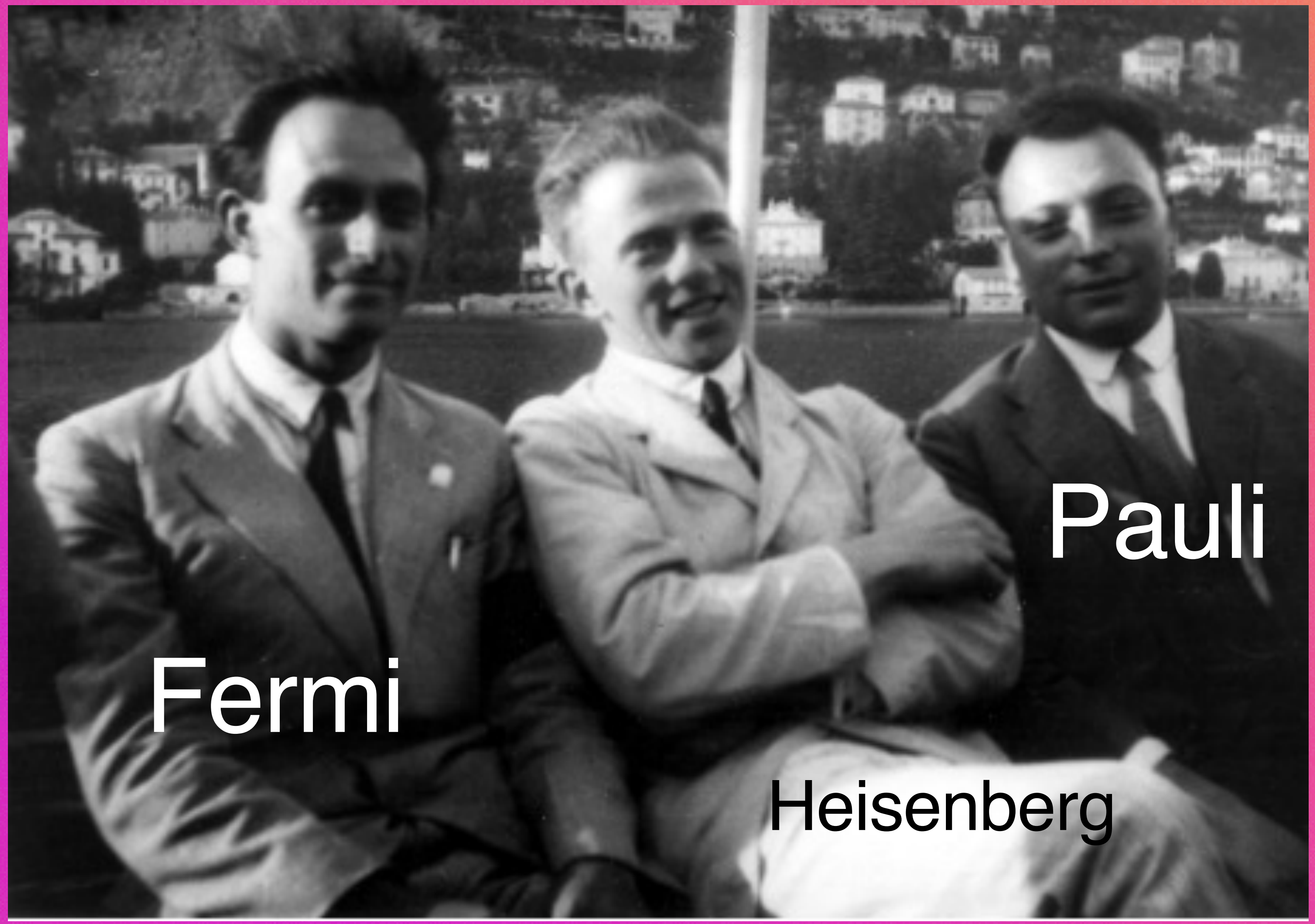

1930 Pauli proposes “a desperate remedy to save… the law of conservation of energy:a light (mass < m(e)), neutral, highly penetrating particle with spin 1/2.” Pauli dubs it the “neutron”. Laments that it is unobservable.

1932 Chadwick discovers the neutron (not Pauli’s)

1932-3 Fermi dubs Pauli’s particle the “neutrino” ν. Develops theory of β decay and concludes $m(\nu) \ll m(e)$.

Neutrinos: Early history

Reines and Cowan exploit the inverse beta decay (IBD) reaction $\bar{\nu}_e p \to e^+ n$ using liquid scintillator (LS) detector and Cd-doped water. The positron annihilation is detected in the LS and the neutron captures on Cd to produce ~6 MeV of gamma energy, also detected in the LS. The spatial and temporal correlation suppresses background.

The detector is located 12m underground to shield from cosmogenic background and 11m from a nuclear reactor.

Triad	$\bar{\nu}$ flux factor	Run length (hr)	Counts from 0.75–7 μsec	Counts from 11–25 μsec	Accidental background (hr^{-1})	Net rate (hr^{-1})
Top	1.13	379.1	919	427	0.50±0.02	1.92±0.09
	0	38.8	27	40	0.46±0.07	0.23±0.15
Bottom	1.12	383.5	815	398	0.46±0.02	1.66±0.08
	0	128.0	119	145	0.50±0.04	0.42±0.09

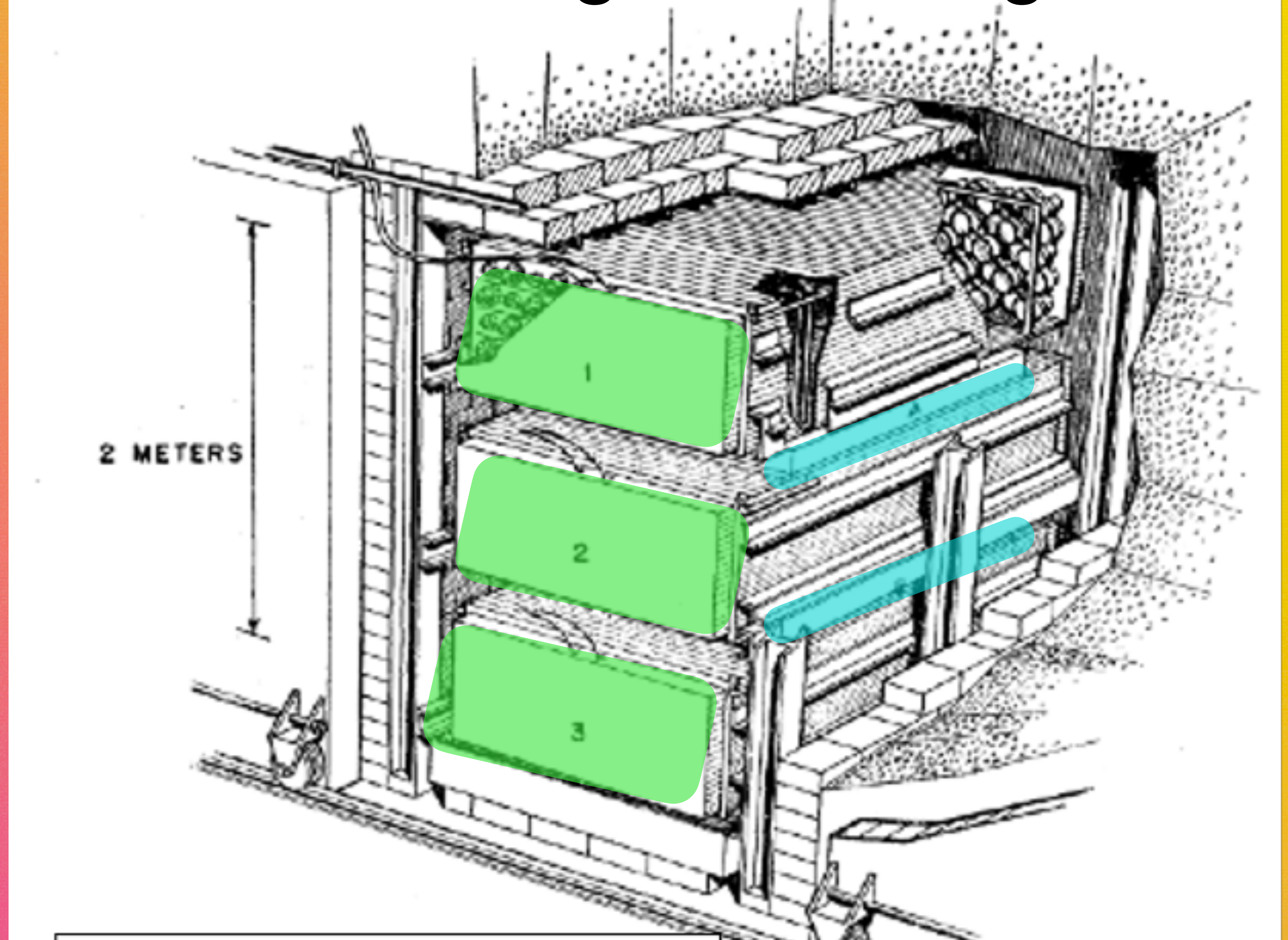

Reines et al.,Phys.Rev.**117** (1960) 1.

Neutrinos oscillation was confirmed in the 1990s.

Determined $N_\nu = 2.9840 \pm 0.0082$

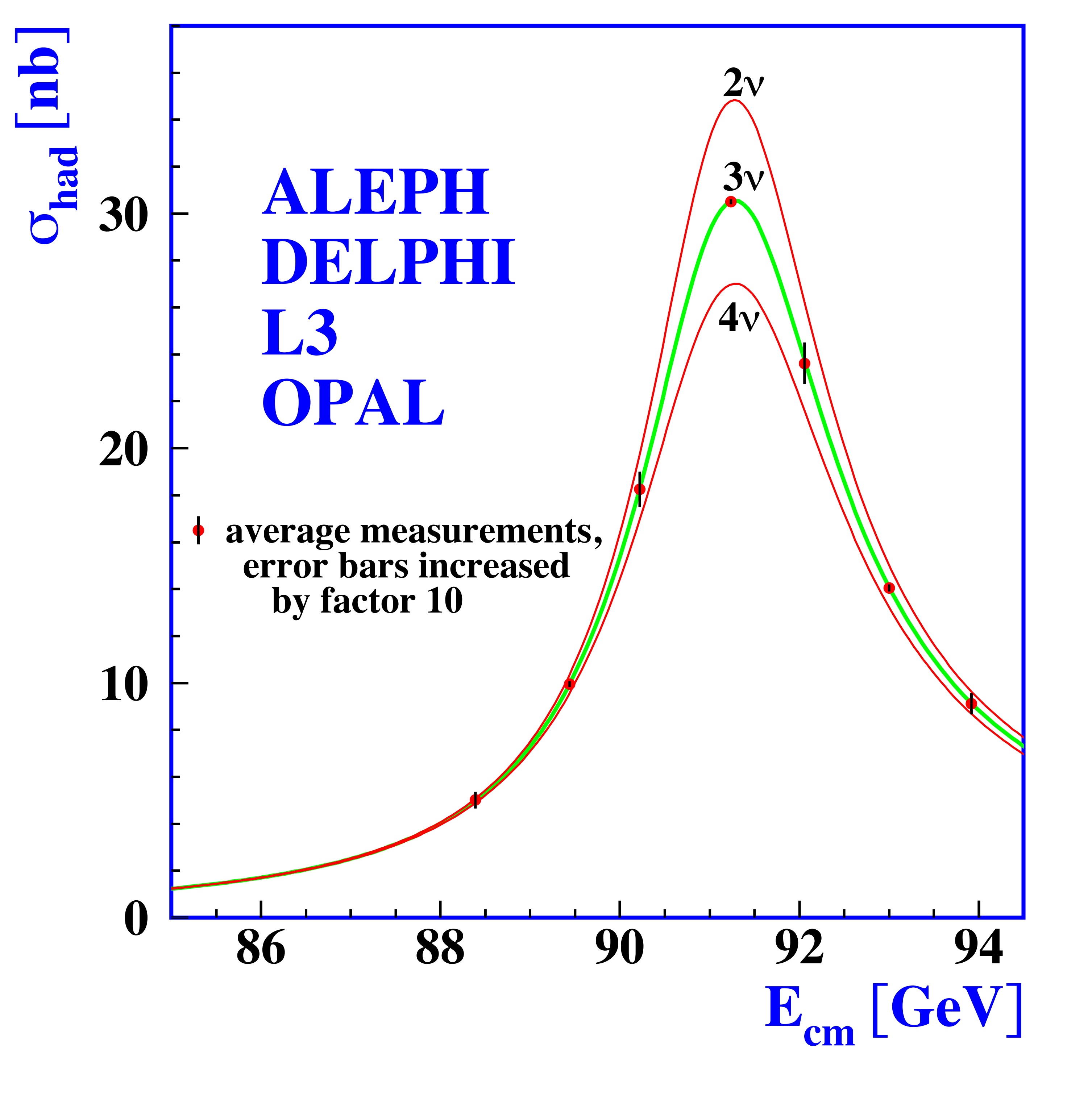

Phys.Rept. 427 (2006) 257

As of today: Oscillation of 3 massive active neutrinos is clearly the dominant effect:

If neutrinos have mass: $$|\nu_l\rangle = \sum U_{li} |\nu_i\rangle$$

Flavor (e, μ, τ) — Mass 1,2.3

For 3 Active neutrinos.

Pontecorvo-Maki-Nakagawa-Sakata matrix

$$U_{li} = \begin{pmatrix} U_{e1} & U_{e2} & U_{e3} \\ U_{\mu 1} & U_{\mu 2} & U_{\mu 3} \\ U_{\tau 1} & U_{\tau 2} & U_{\tau 3} \end{pmatrix}$$

(Double β decay only)

$$= \begin{pmatrix} 1 & 0 & 0 \\ 0 & c_{23} & s_{23} \\ 0 & -s_{23} & c_{23} \end{pmatrix} \cdot \begin{pmatrix} 1 & 0 & 0 \\ 0 & 1 & 0 \\ 0 & 0 & e^{-i\delta} \end{pmatrix} \cdot \begin{pmatrix} c_{13} & 0 & s_{13} \\ 0 & 1 & 0 \\ -s_{13} & 0 & c_{13} \end{pmatrix} \cdot \begin{pmatrix} c_{12} & s_{12} & 0 \\ -s_{12} & c_{12} & 0 \\ 0 & 0 & 1 \end{pmatrix} \cdot \begin{pmatrix} 1 & 0 & 0 \\ 0 & e^{-i\alpha_2/2} & 0 \\ 0 & 0 & e^{-i\alpha_3/2+i\delta} \end{pmatrix}$$

✔ Atmospheric, Accel. | ? CP Violating Phase | ✔ Reactor, Accel. | ✔ Solar,Reactor | ? Majorana CP Phases

Credit: Art McDonald Neutrino 2024

Additional light neutrinos must have little or no coupling to the Z and W, hence “sterile”. Evidence of sterile neutrinos can be sought in the electron neutrino “disappearance”. In a model with one additional light sterile neutrino the antineutrino survival rate is (L = baseline, E_ν = energy)

$$P(\bar{\nu}_e \rightarrow \bar{\nu}_e) \approx 1 - \sin^2 2\theta_{14} \sin^2 \frac{\Delta m_{41}^2 L}{4E_\nu}$$

Neutrinos early 2010s Reactor Antineutrino "Anomalies"

Phys. Rev D 95, 072006 (2017).
Daya Bay collaboration

Spectral Deviation

Flux Deficit

PR**D83** (2011) 073006

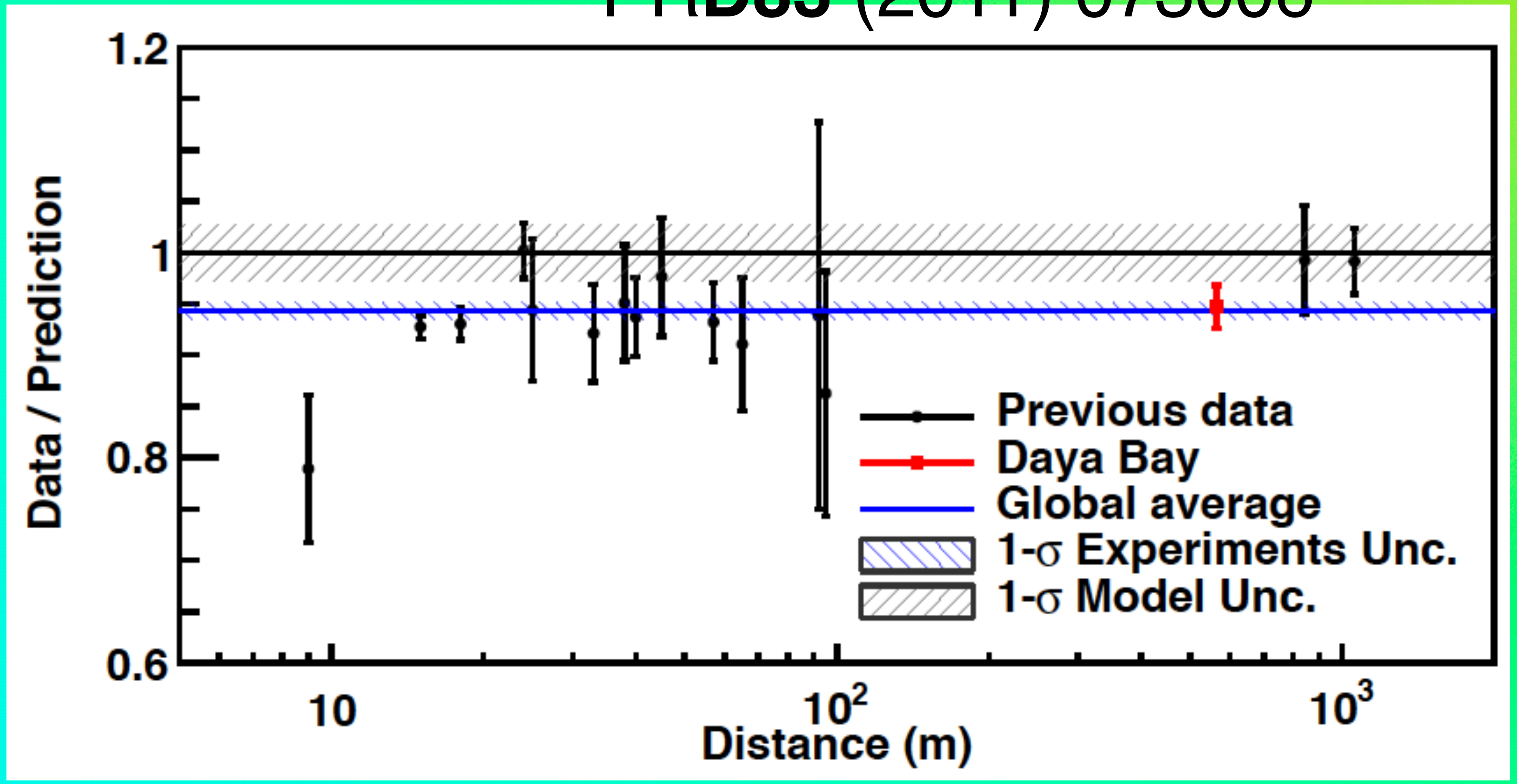

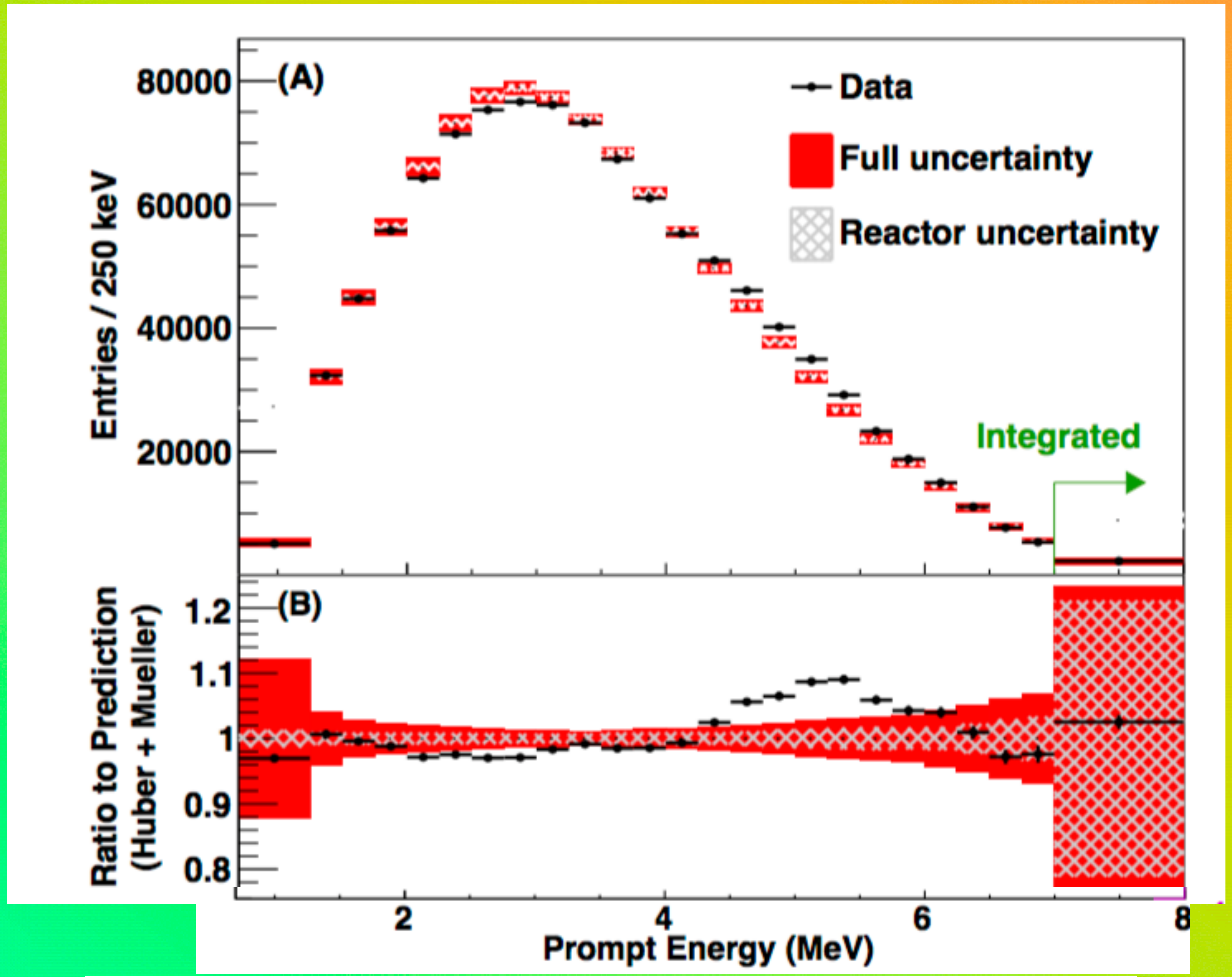

Extra (sterile) neutrino oscillations or artifact of flux predictions?

Understanding reactor flux and spectrum anomalies requires additional data

Measured spectrum does not agree with predictions.

PROSPECT goals:

1. **Reactor-model-independent eV-scale sterile neutrino search at short baselines**
2. **Precisely measure the antineutrino spectrum from ^{235}U fission products**

Reactor neutrinos: powerful source of pure $\bar{\nu}_e$

- reactors are a powerful source: generate a lot of pure electron antineutrinos
- e.g. generation in a PWR* reactor: ^{235}U, ^{238}U, ^{239}Pu, ^{241}Pu
- fission produces neutron-rich daughters that beta decay ~6 times until stable
- >99.9% flux $\bar{\nu}_e$- only from this process
- 1 GW_{th}~10^{20} $\bar{\nu}_e$/second
- detection: inverse beta decay (IBD), coincidence tag

$$\bar{\nu}_e p \rightarrow e^+ n$$

$$E_{\text{prompt}} \approx E_\nu - 0.8 \text{ MeV}$$

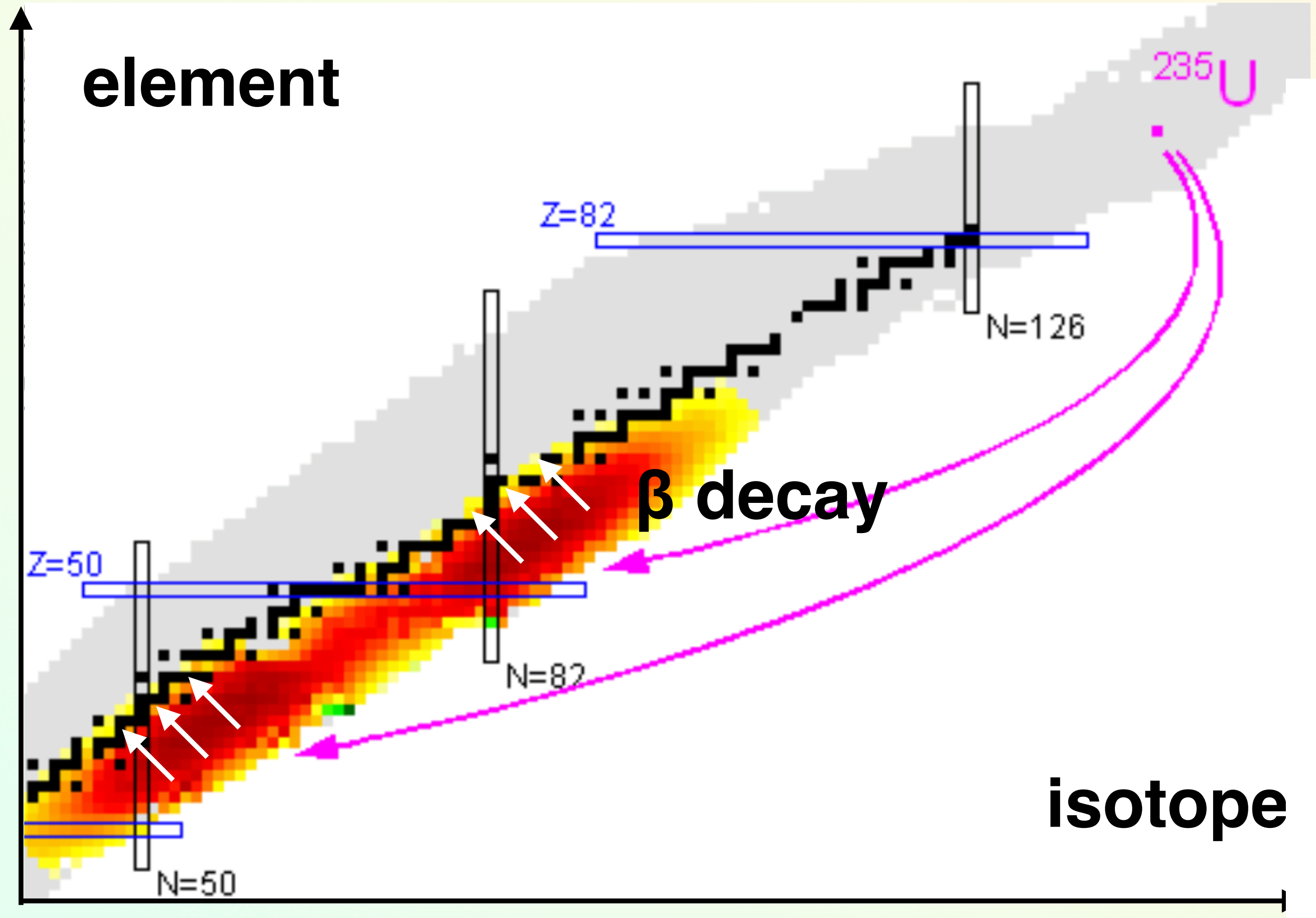

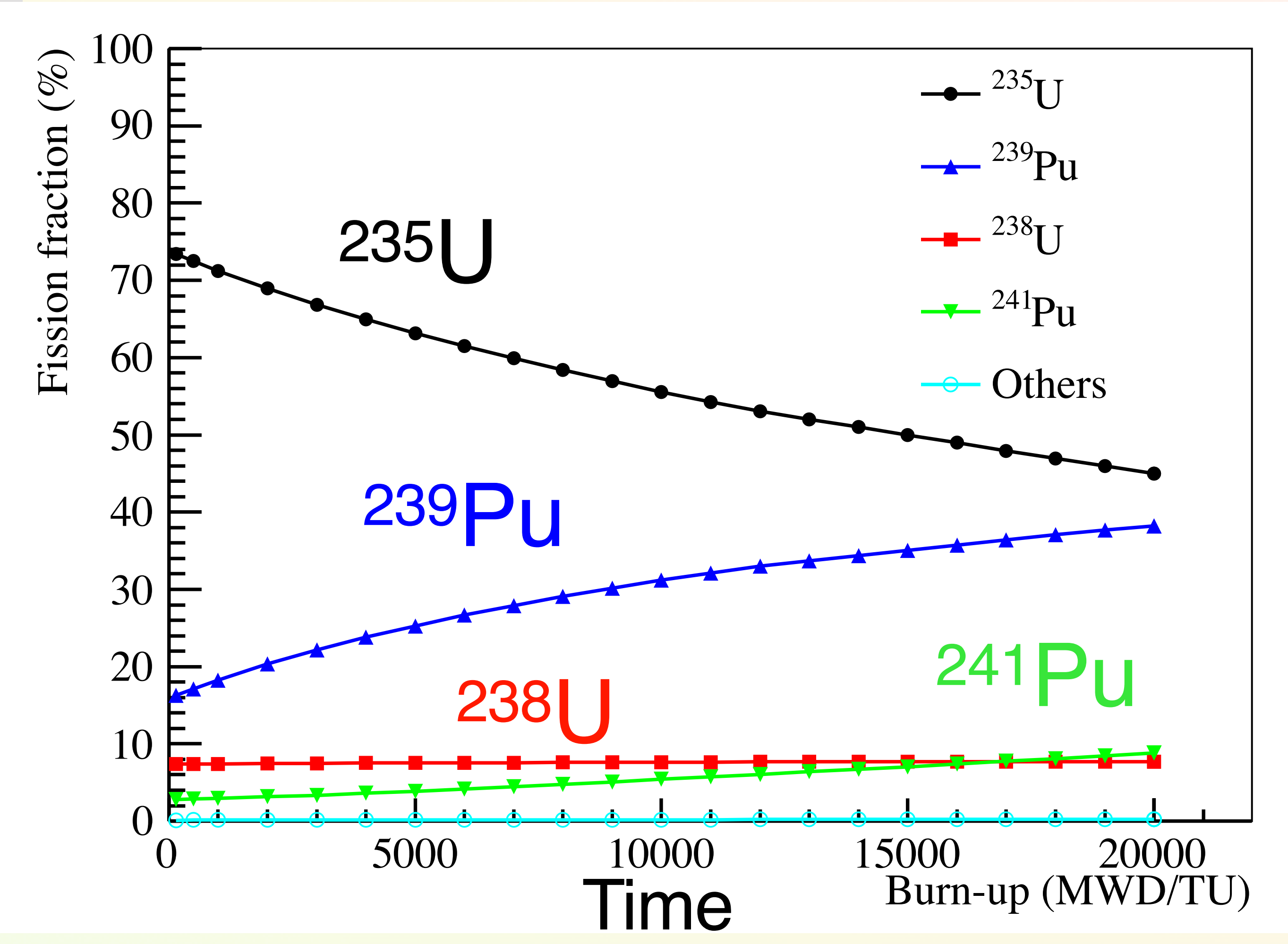

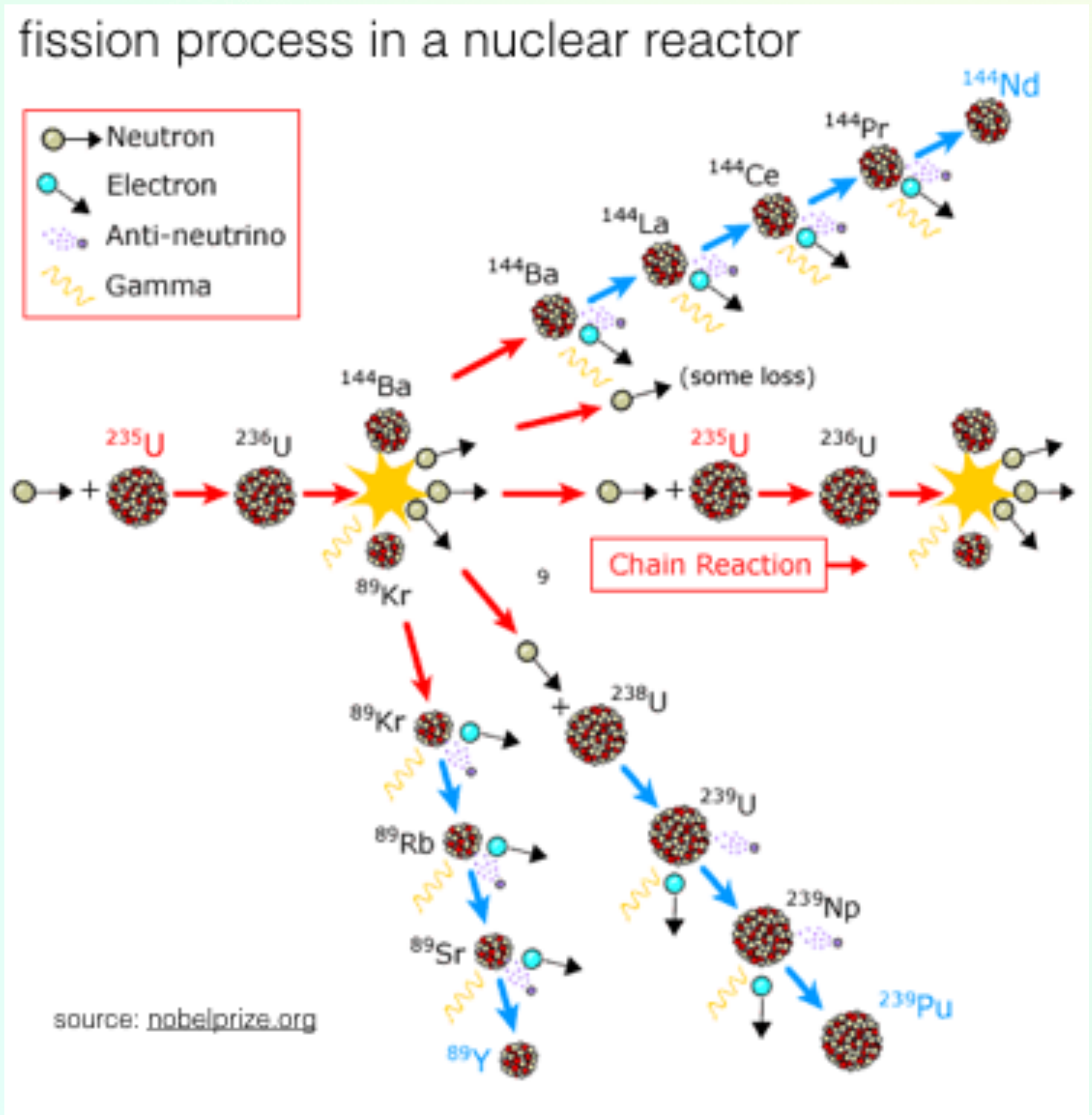

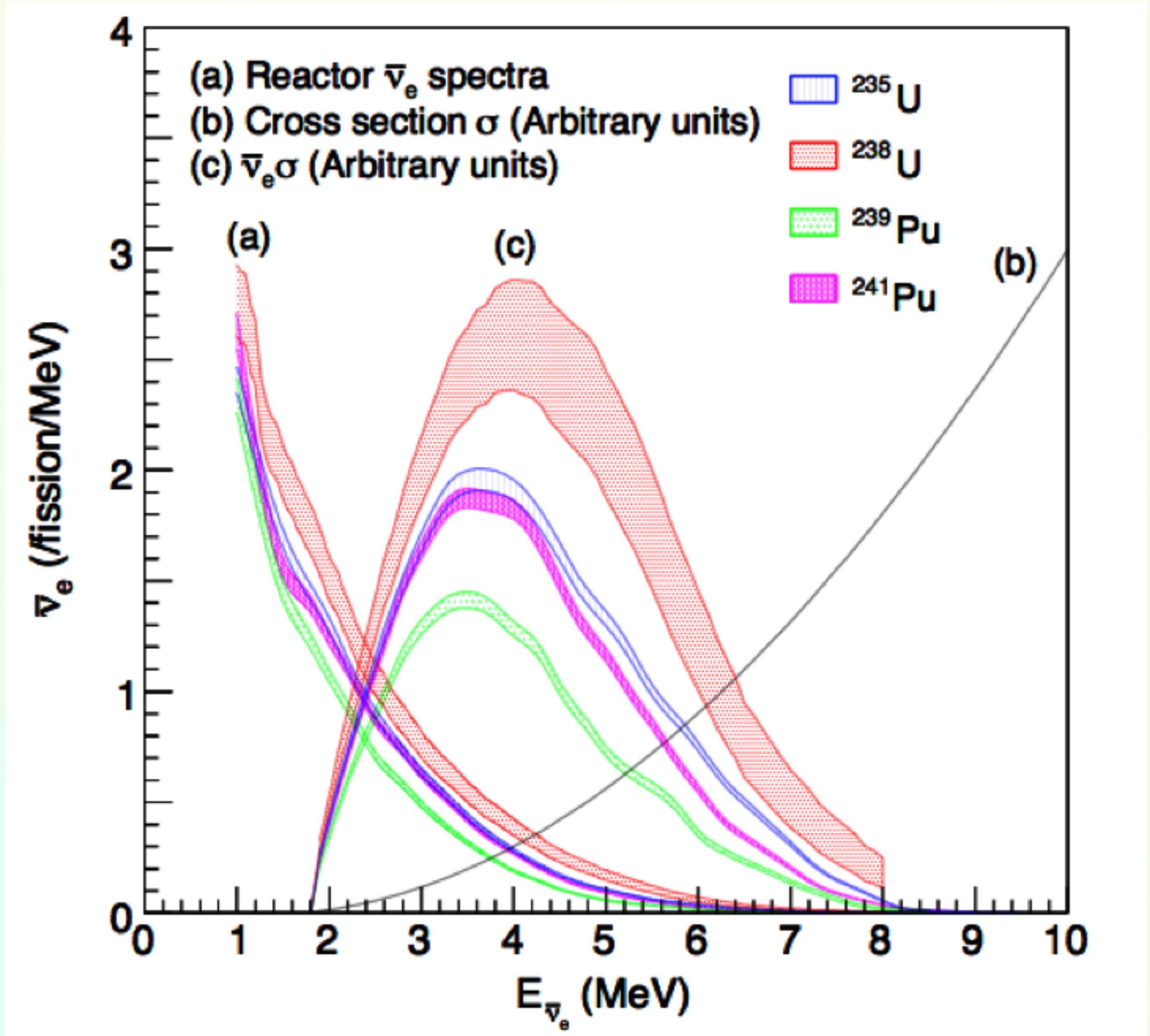

pure, prolific source of neutrinos with a workhorse detection mechanism

*PWR = Pressurized Water Reactor (typical commercial reactor)

Neutrino source: High Flux Isotope Reactor @ ORNL

- 85MW highly enriched uranium reactor
- >99% of $\bar{\nu}_e$ from ^{235}U fissions, effectively no isotopic evolution
- compact core (44cm diameter, 51cm tall),
- compact source of $\bar{\nu}_e$
- 24 day cycles, 46% reactor up time
- detailed study of surface cosmogenic backgrounds (PROSPECT: NIMA A806 (2016) 401)

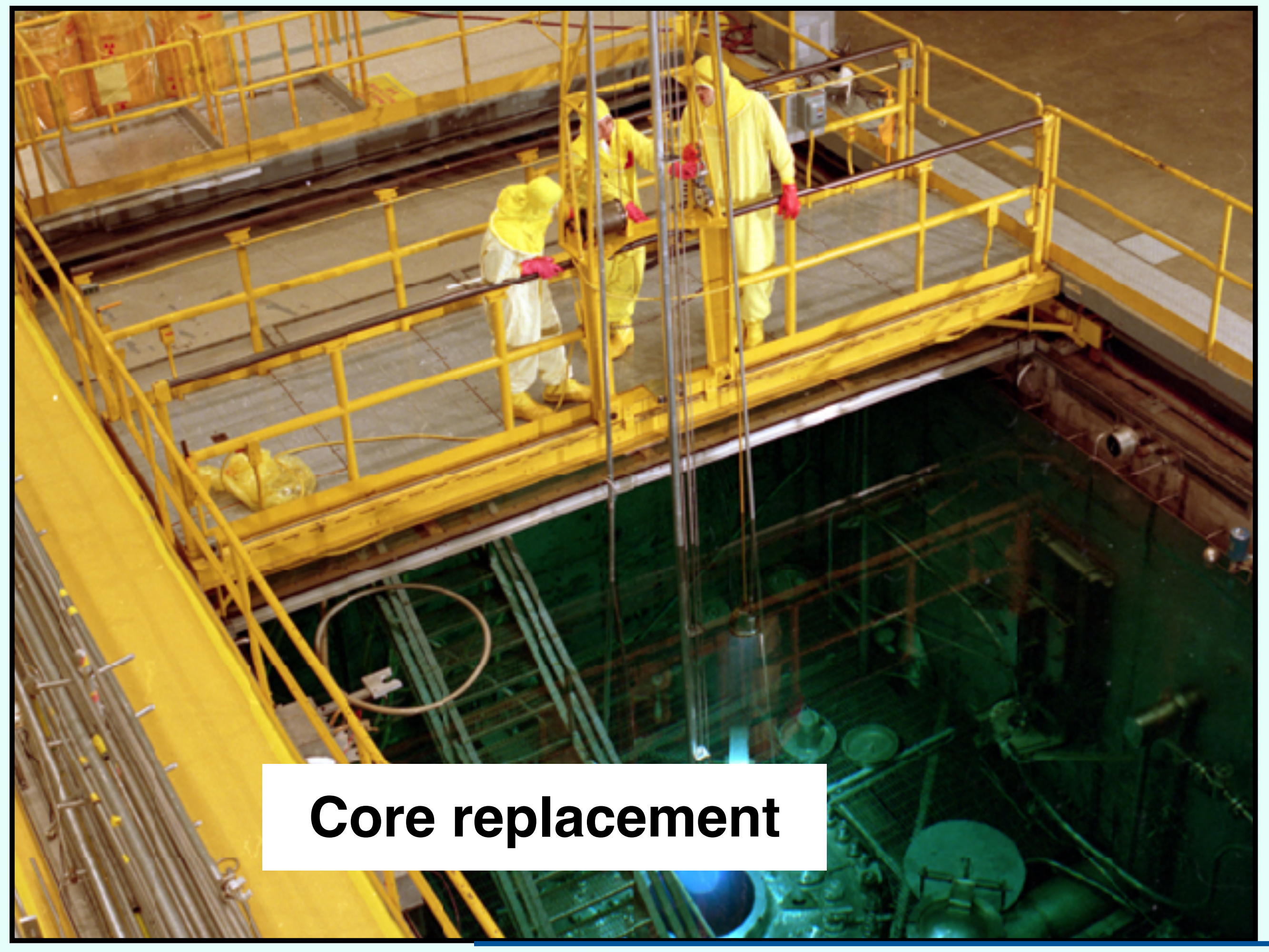

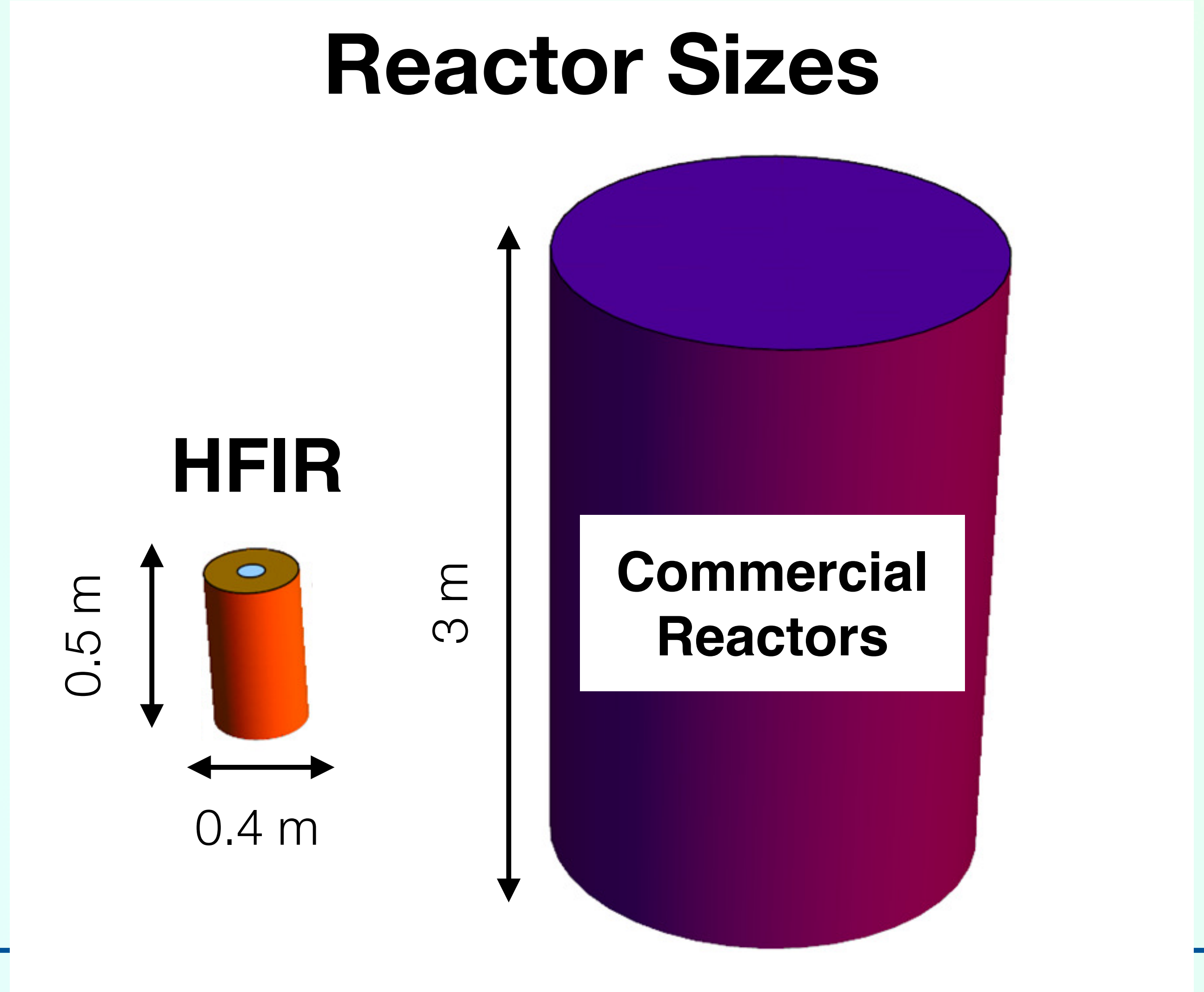

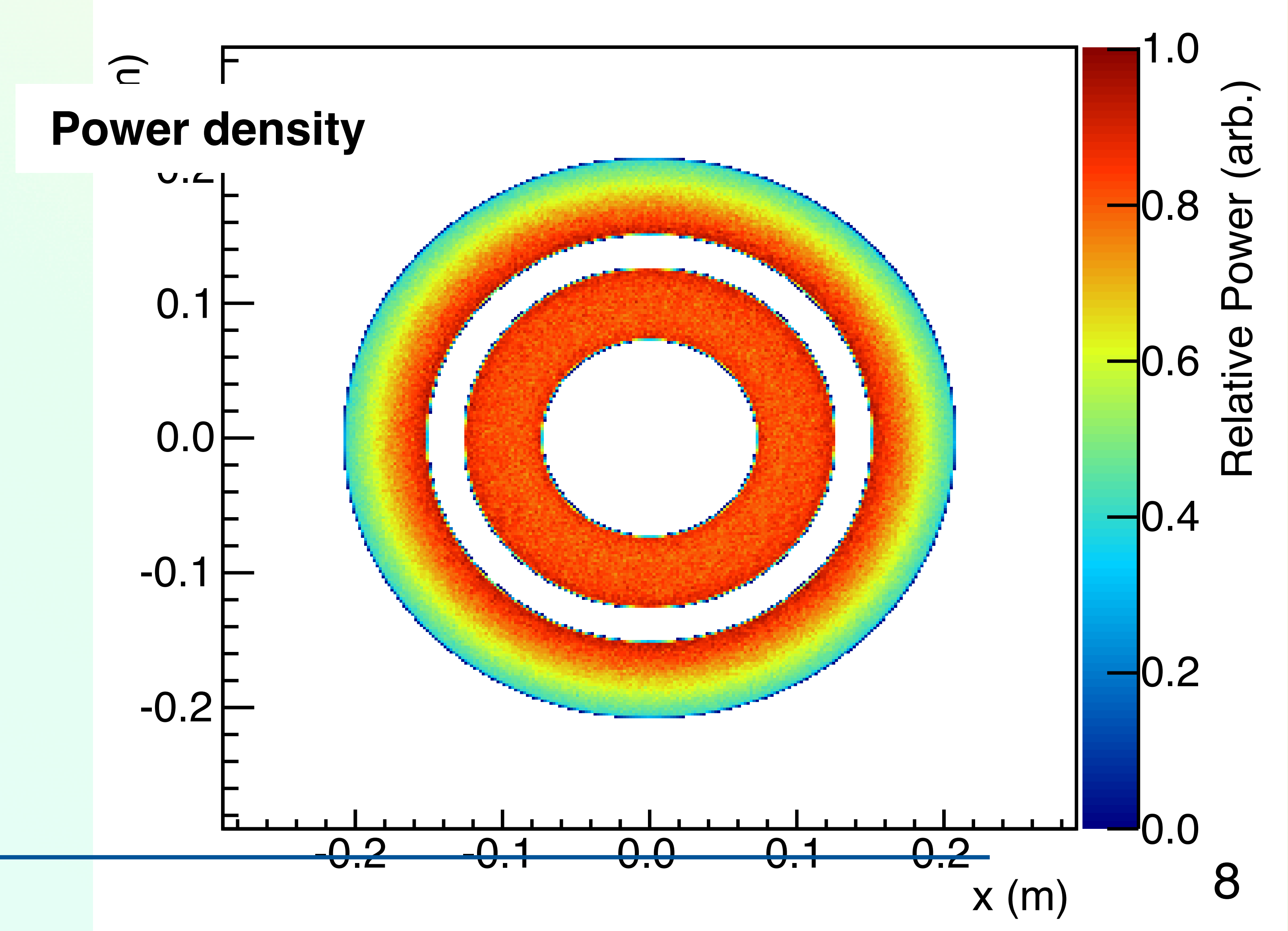

Experimental strategy at HFIR

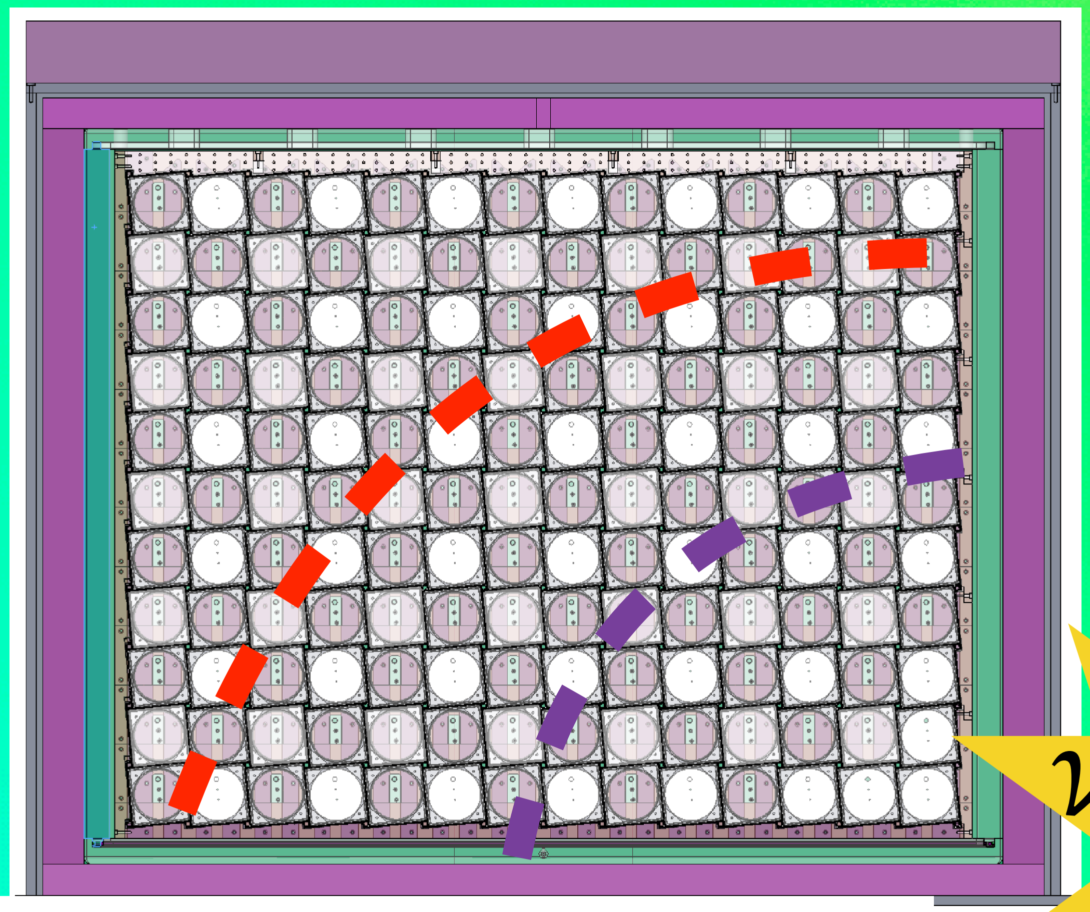

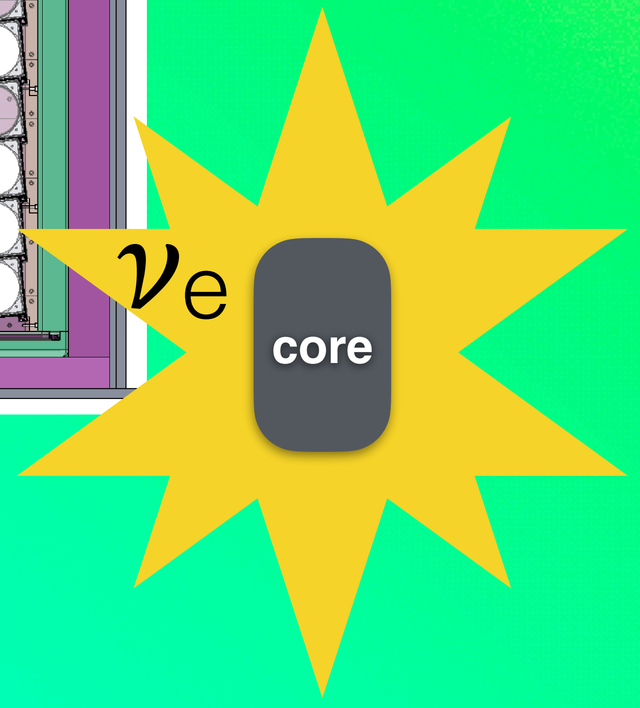

Goal - spectrum measurement:
✓single isotope ^{235}U (most abundant in PWR)

Goal - sterile neutrino search:
✓access to short baselines
✓compact core
✓static IBD yield
✓segmented detector = relative measurement

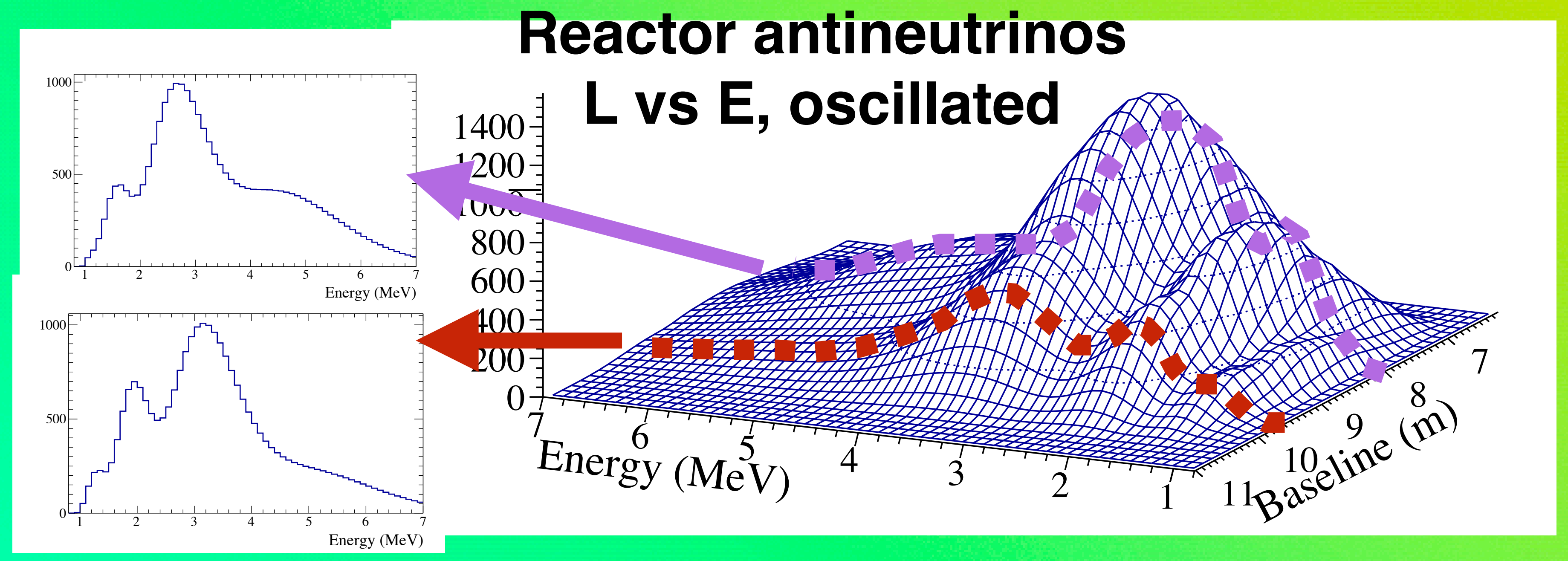

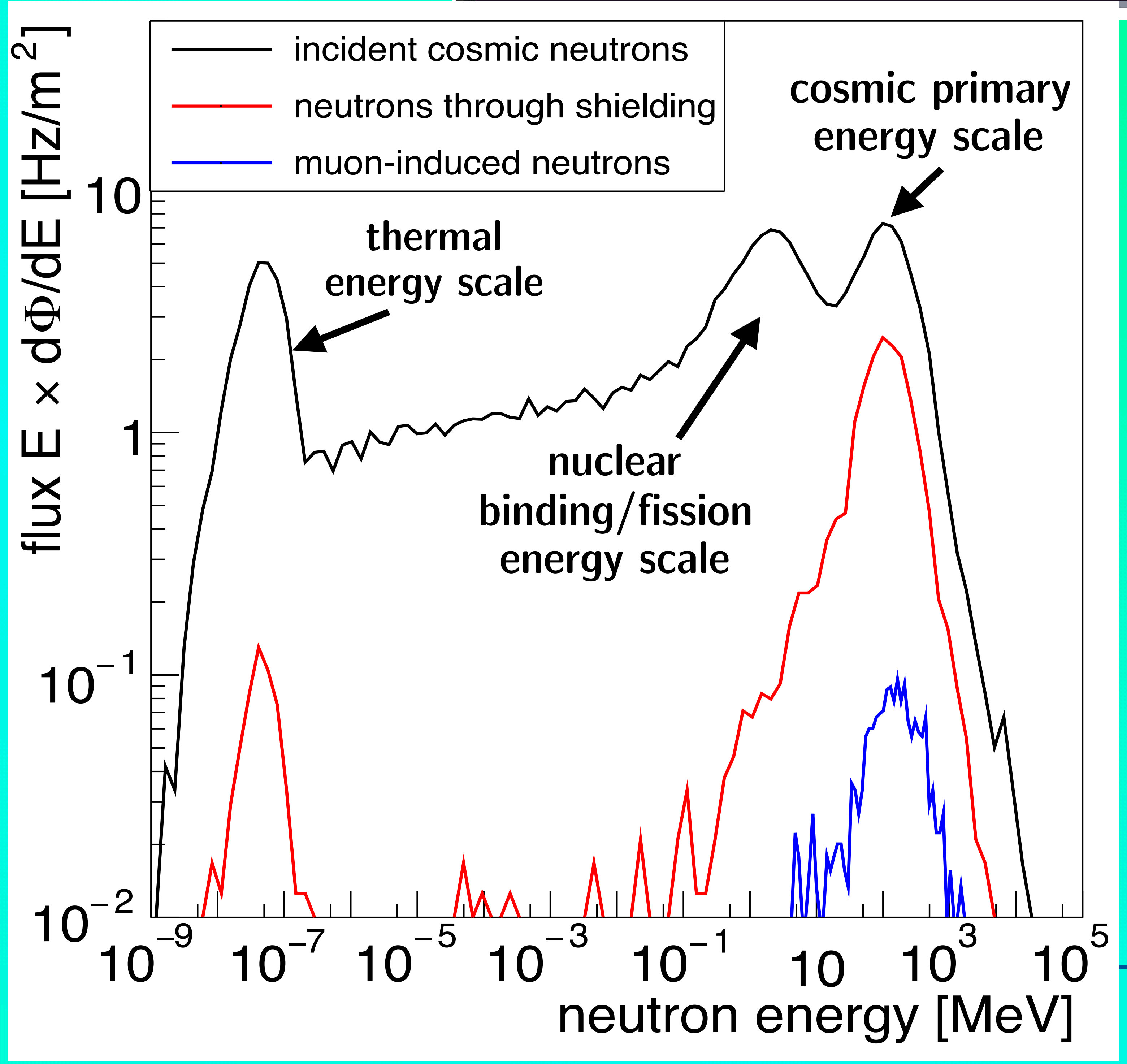

Nothing is perfect…

- limited overburden = cosmogenic fast neutrons are dominant IBD-like background
- possible reactor generated accidental backgrounds

PROSPECT segmented detector design

Realization of experiment strategy:

- target/detection: ^{6}Li-loaded liquid scintillator
- 154 segments, 119cm × 15cm × 15cm
- thin (1.5mm) optical panels held in place by 3D printed support rods
- 25 liters/segment, **total mass: ~4 tons**
- segmentation enables:
  - calibration access throughout volume
  - 3D position reconstruction (X, Y) with (Z) from double-ended PMT readout
  - fiducialization
- optimized shield for cosmogenics

Reflective panels

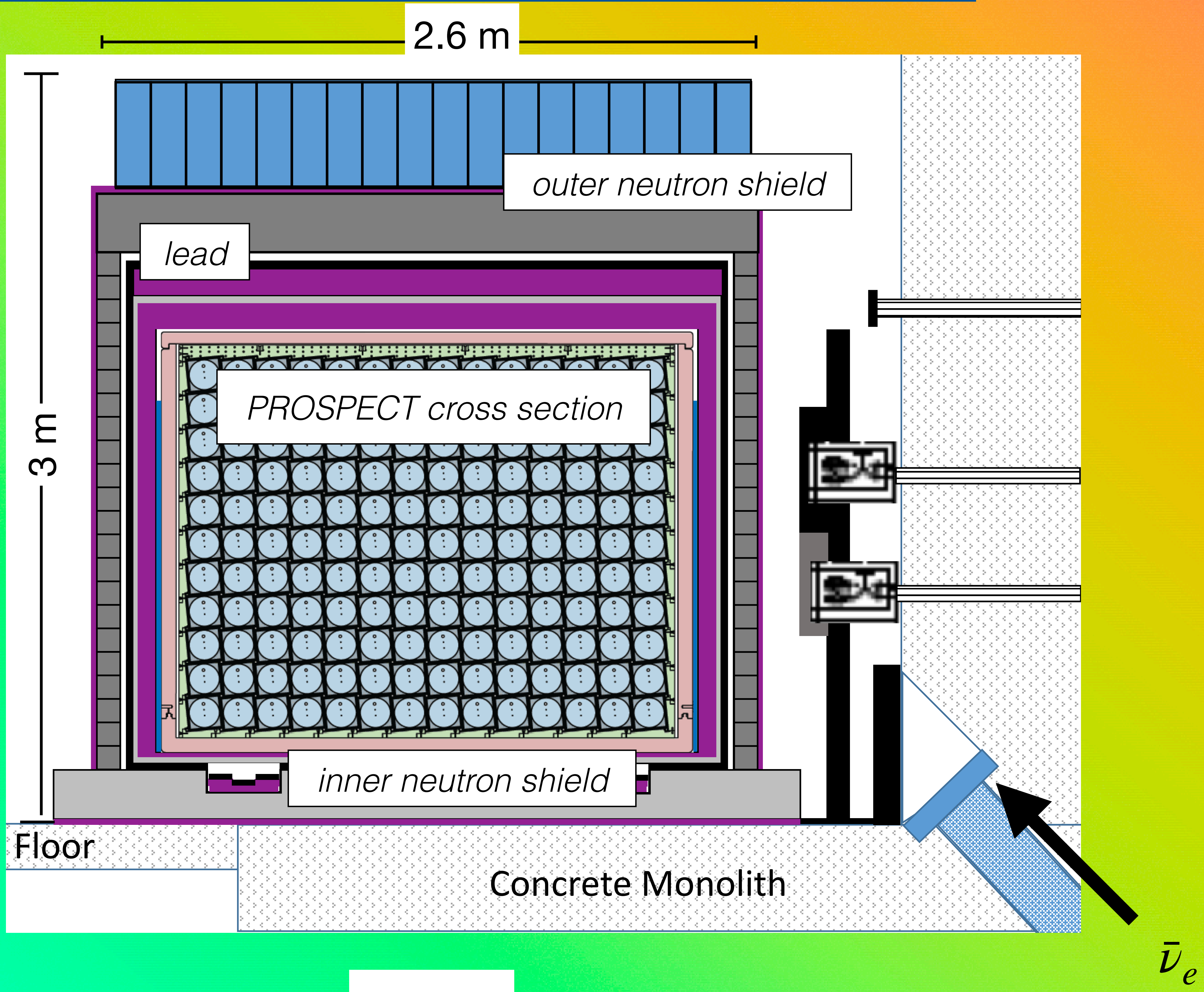

tilt for calibration access

3D printed support rod

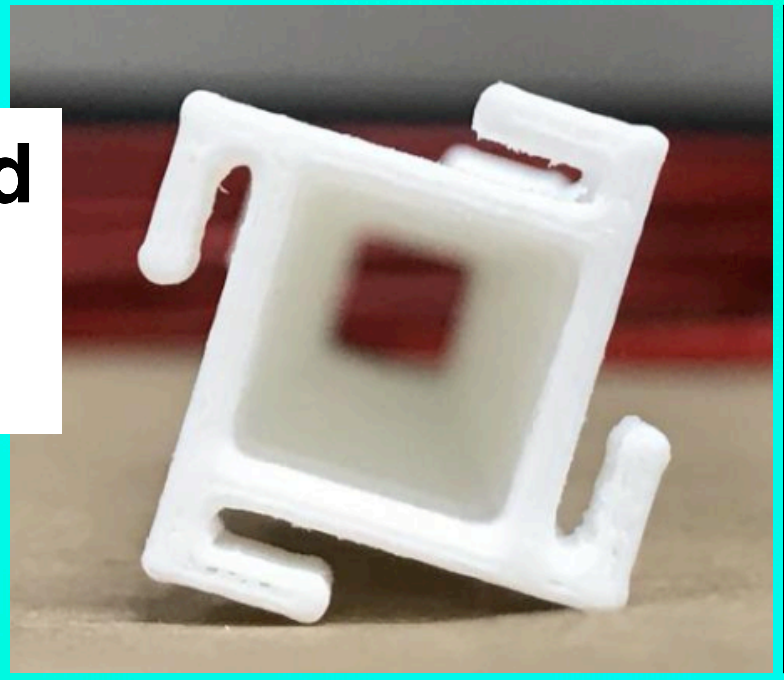

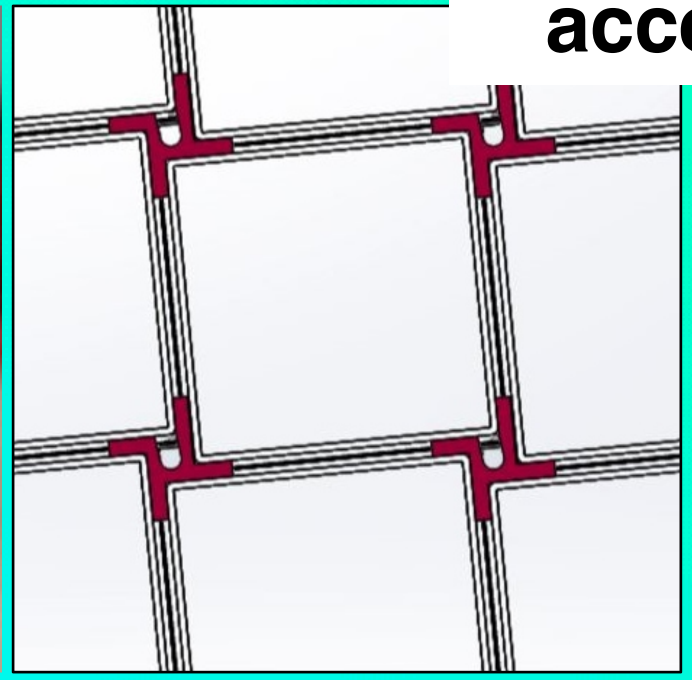

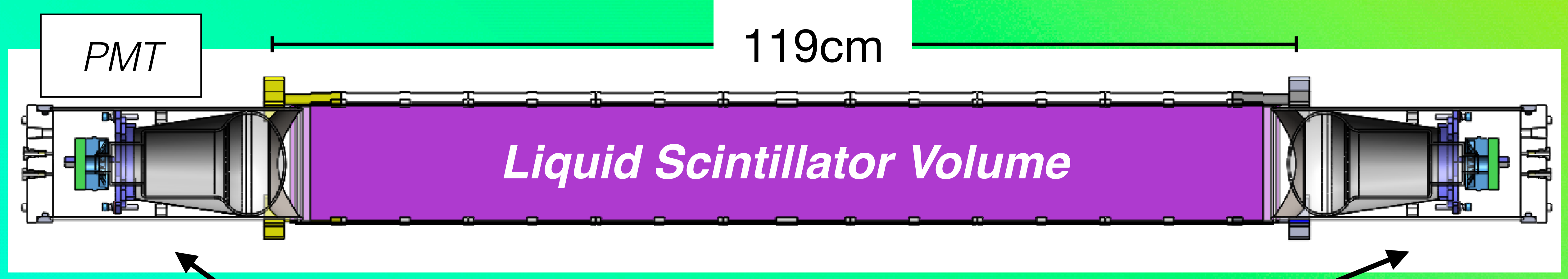

PMT housings filled with mineral oil

Detection with ^{6}Li-loaded liquid scintillator (LiLS)

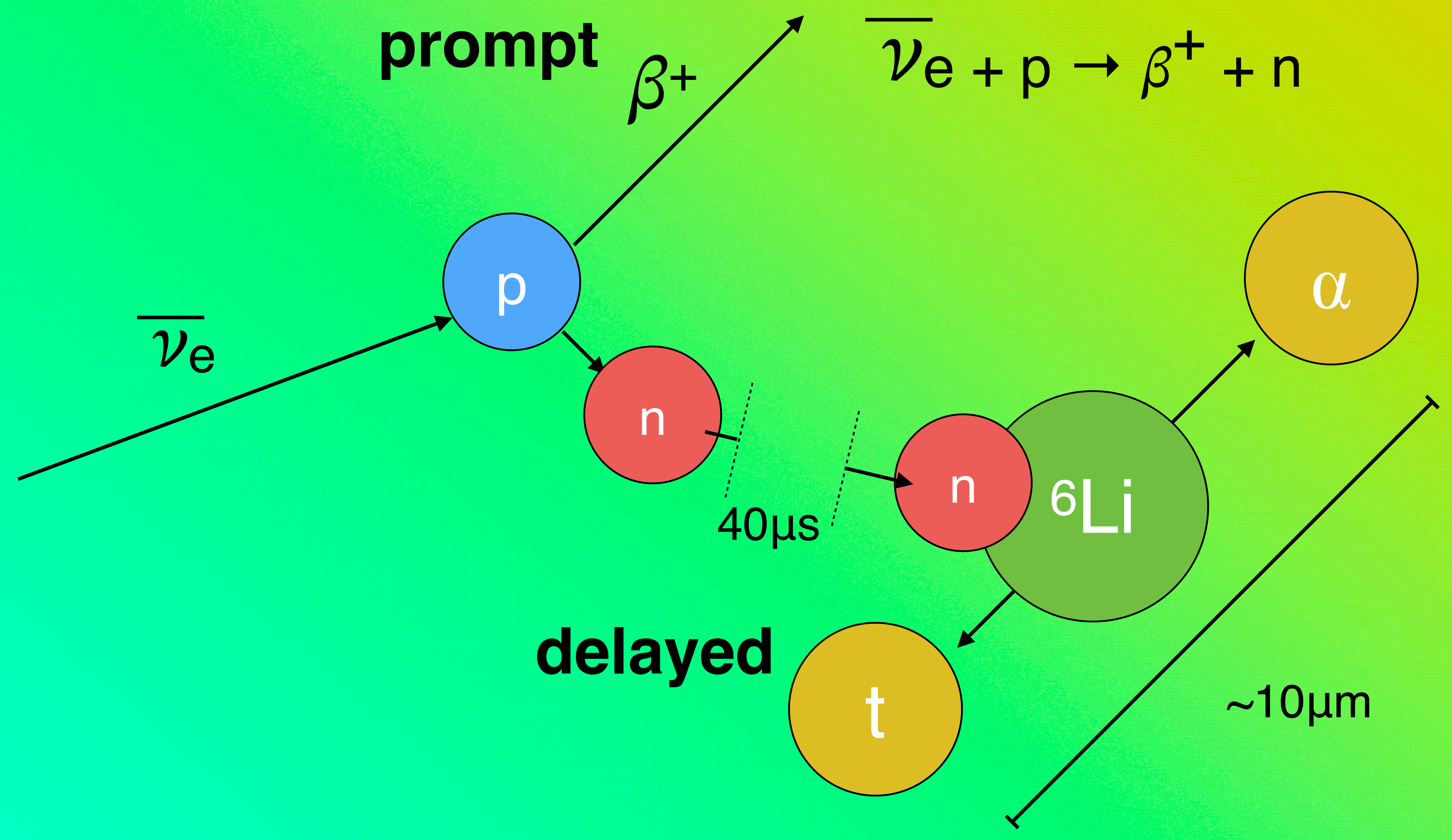

- custom developed ^{6}LiLS based on EJ-309, non-toxic and non-flammable
- compact detector needs a capture agent that is highly localized, within segments
- minimize position dependent efficiency
- spatial and temporal cuts to identify IBDs and reject backgrounds

^{6}LiLS provides event localization and identification required for a compact detector

Pulse shape discrimination (PSD)

LiLS provides capability of pulse-shape discrimination.

Even better handle on IBD acceptance and background rejection with particle ID.

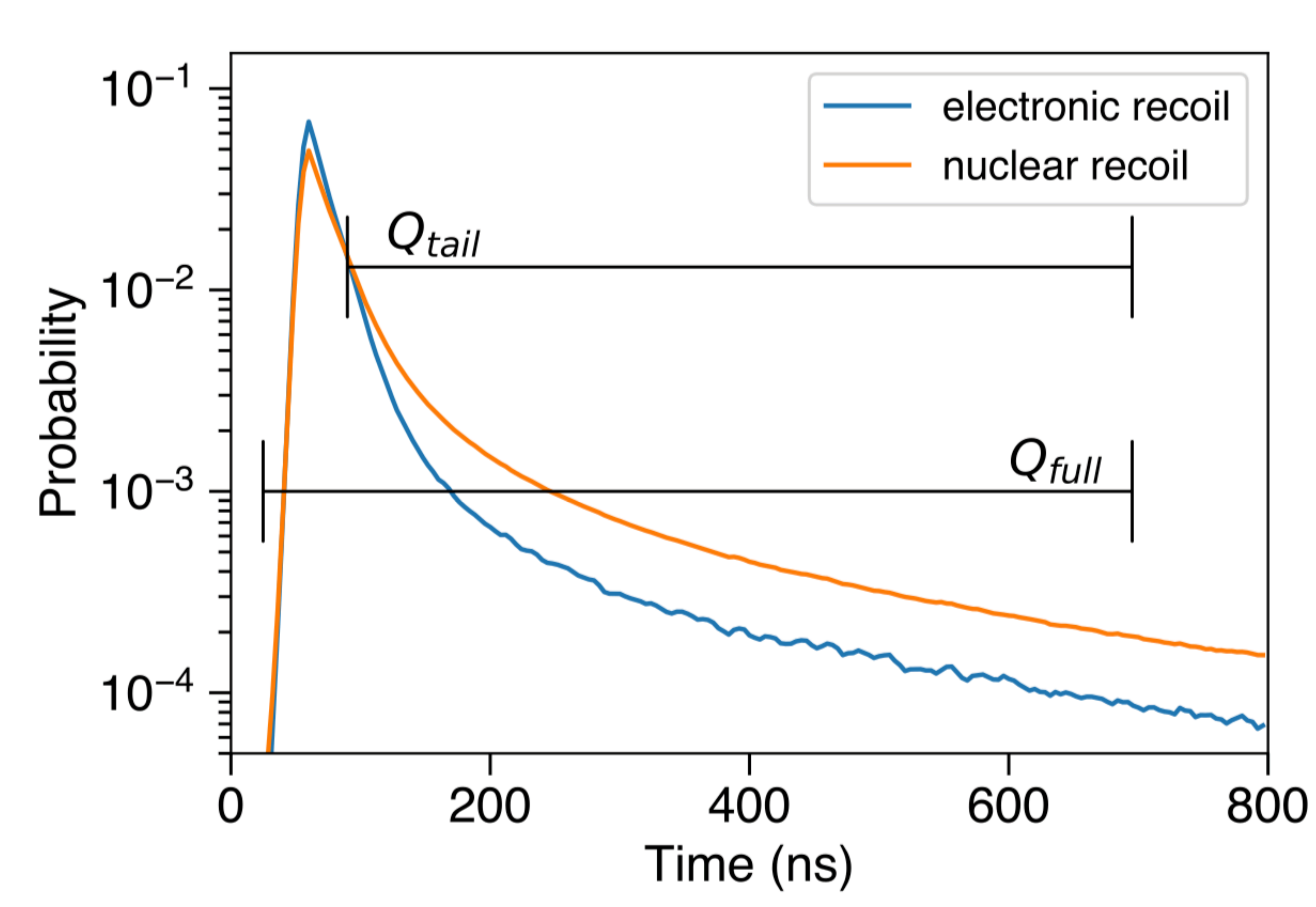

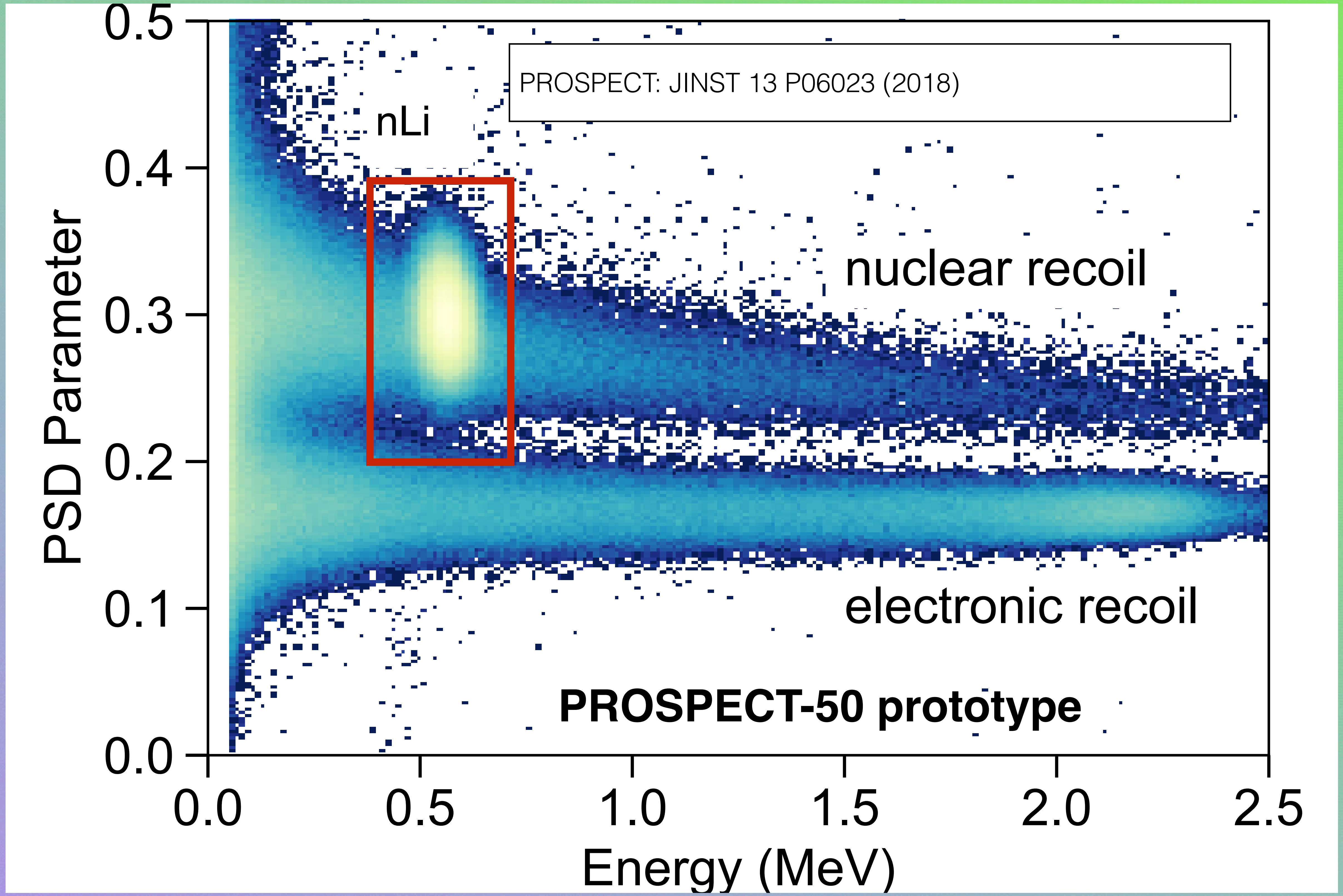

PSD can identify particle type through shape of pulse

Active Shielding

- Segmentation provides a way to concretely define fiducial volume
- A combination of PSD, topology, shower veto and fiducialization cuts provide active background suppression

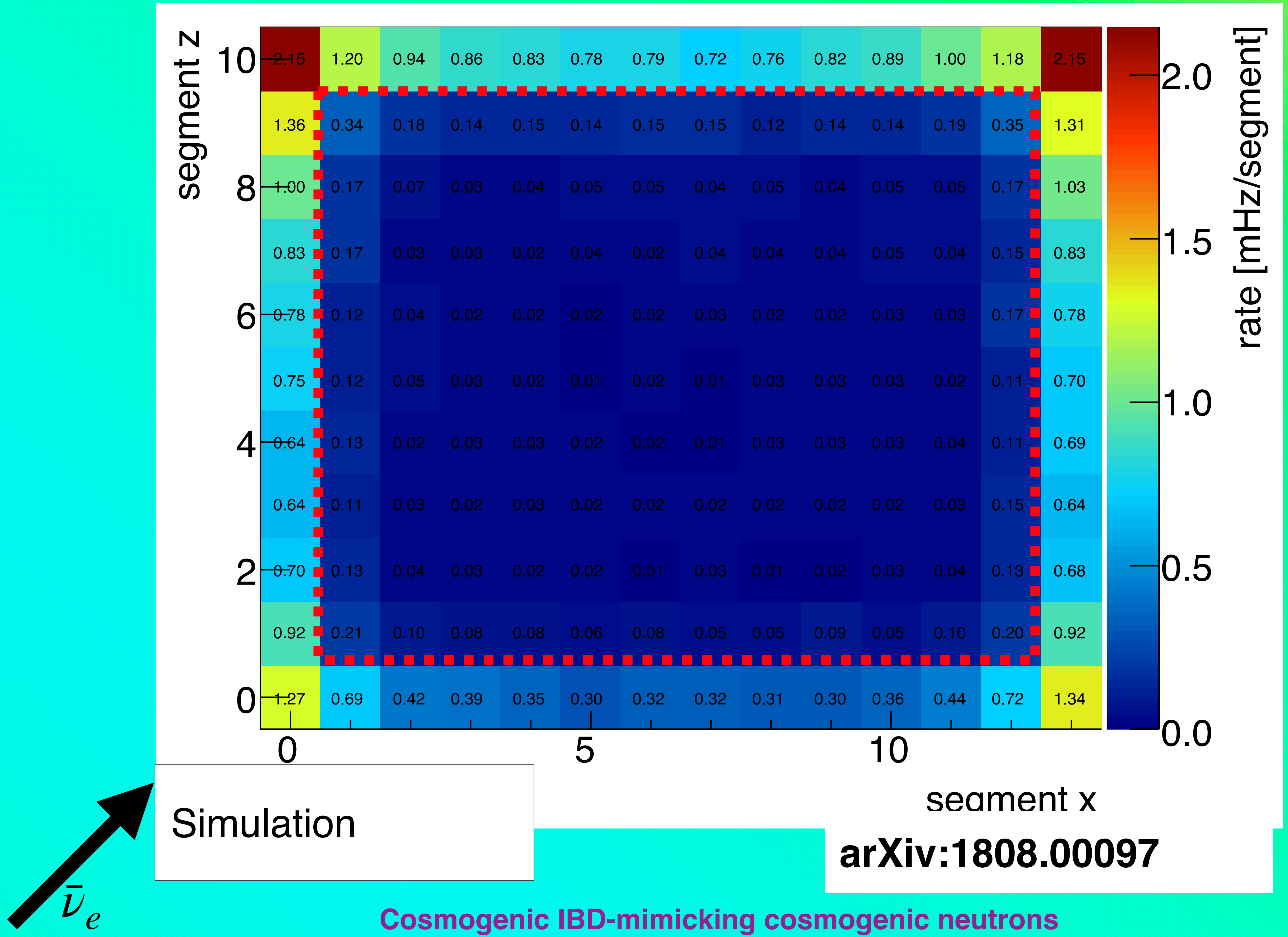

arXiv:1808.00097

Cosmogenic IBD-mimicking cosmogenic neutrons

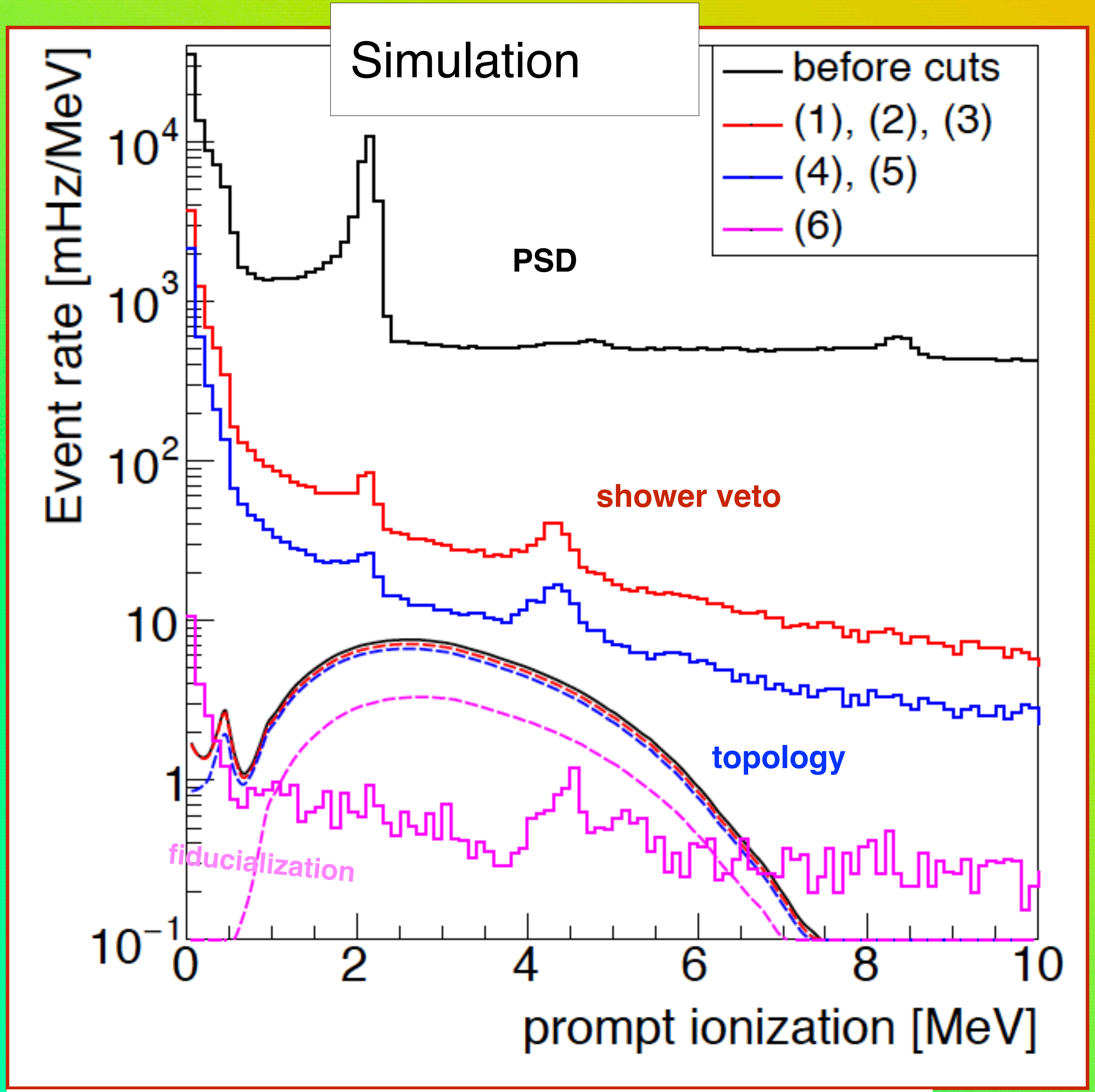

PROSPECT Collaboration, J. Phys. G: 43 (2016)

A combination of active and passive shielding enables a surface neutrino experiment

Some fabrication and construction images

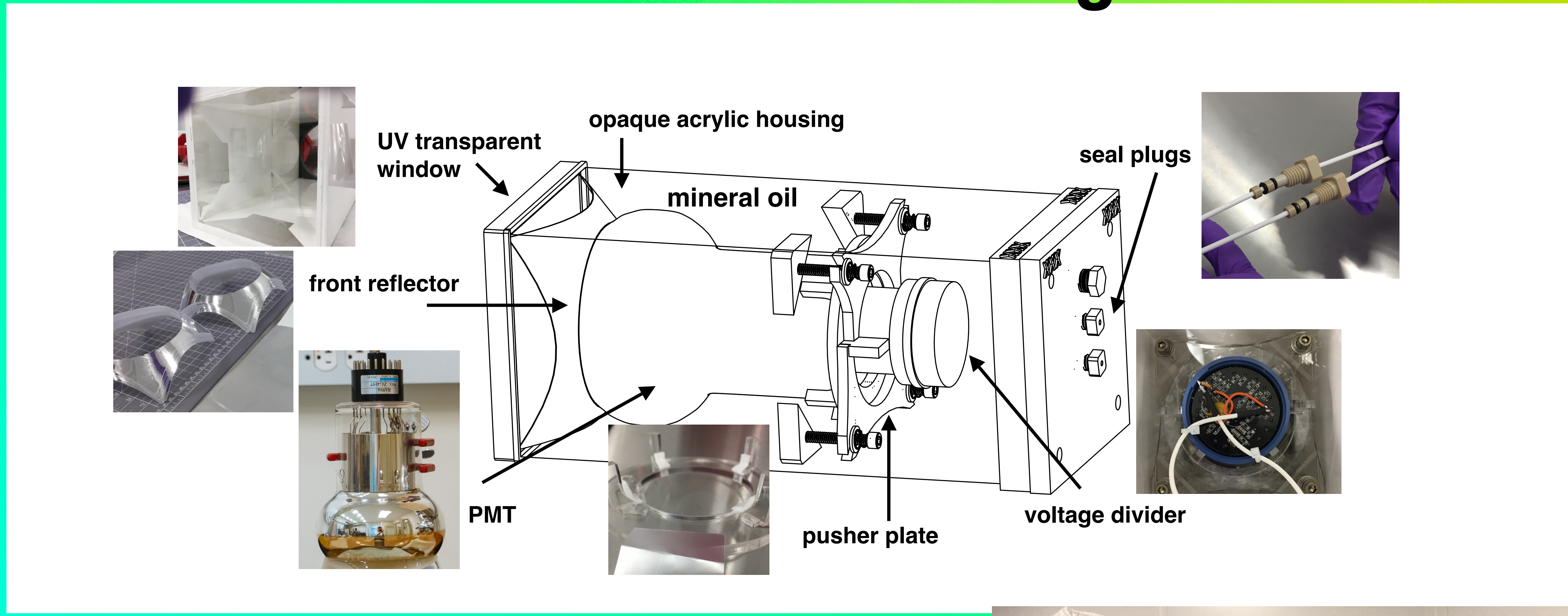

NOVEMBER 2016- NOVEMBER 2017


PMT testing


First PMT module


Production reflector


Liquid scintillator production


ASSEMBLY OF FIRST ROW
NOVEMBER 1, 2017
YALE WRIGHT LAB

NOVEMBER 17, 2017
FINAL ROW INSTALLATION


AHHHHH!


6½ TON CAP
DEC 2017 - JAN 2018
DRY COMMISSIONING AT YALE

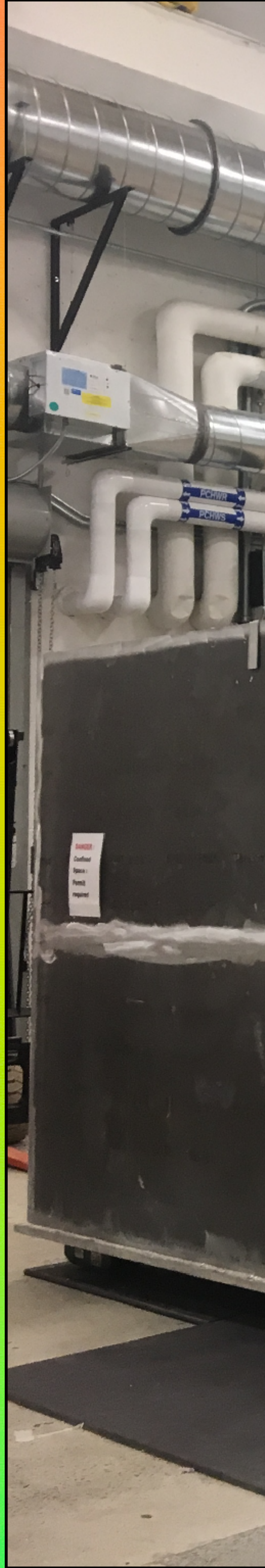


FEBRUARY 2018
ARRIVAL AT ORNL

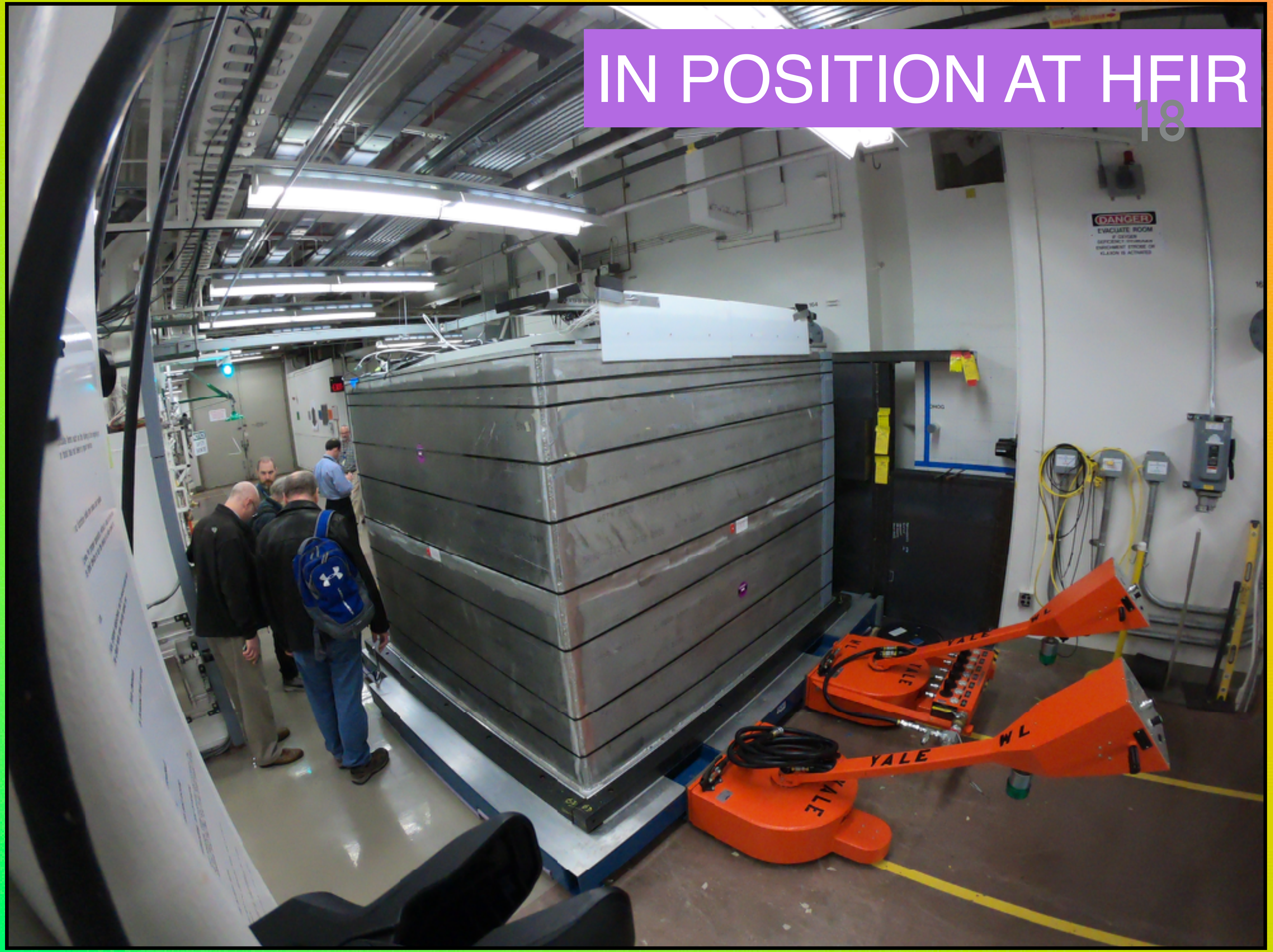
IN POSITION AT HFIR
YALE


TARE
DANGER
NOMINAL
CAPACITY
4 BAR
FILLING FROM
MIXING TANK

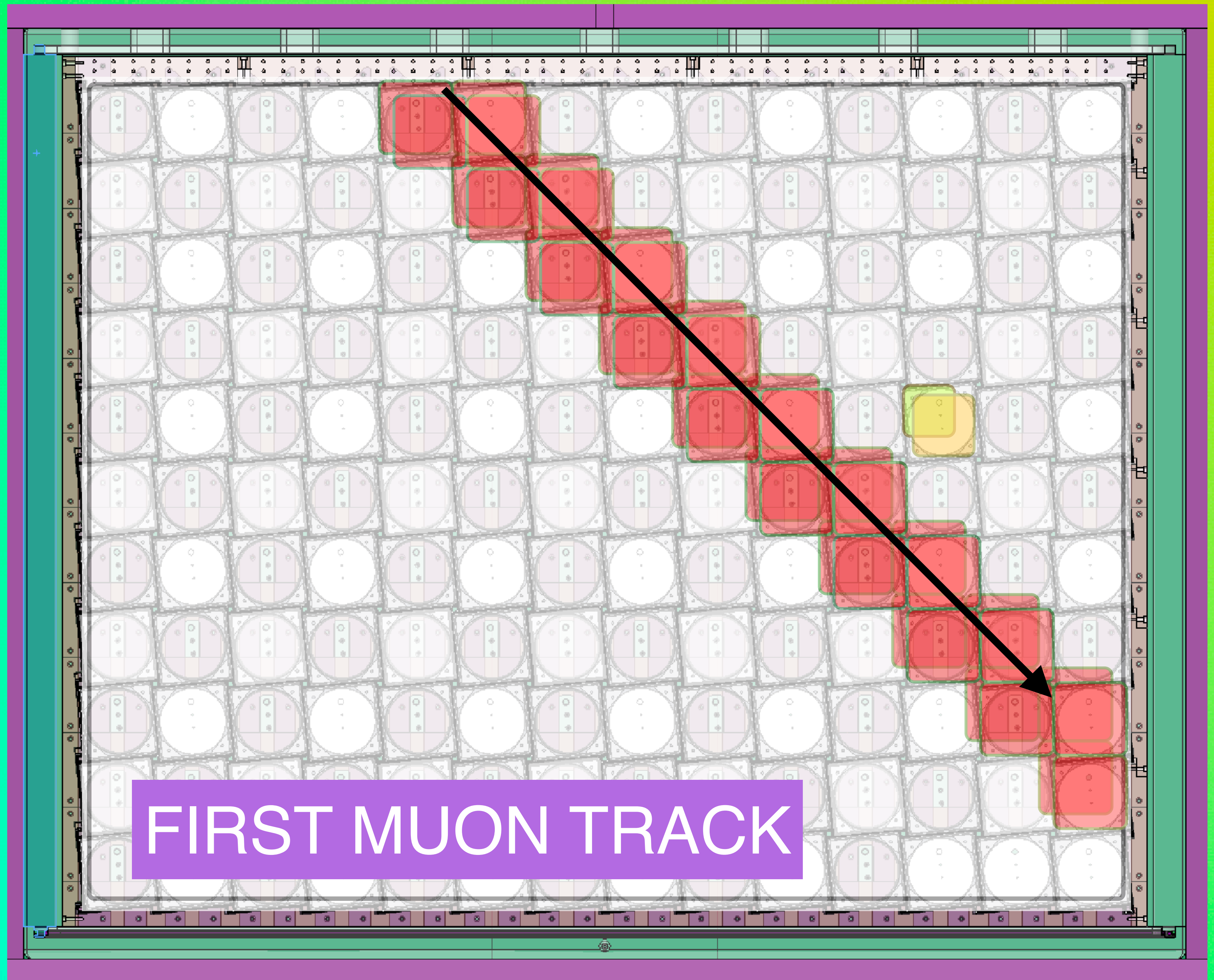
FIRST MUON TRACK

FEBRUARY 2018
ARRIVAL AT ORNL

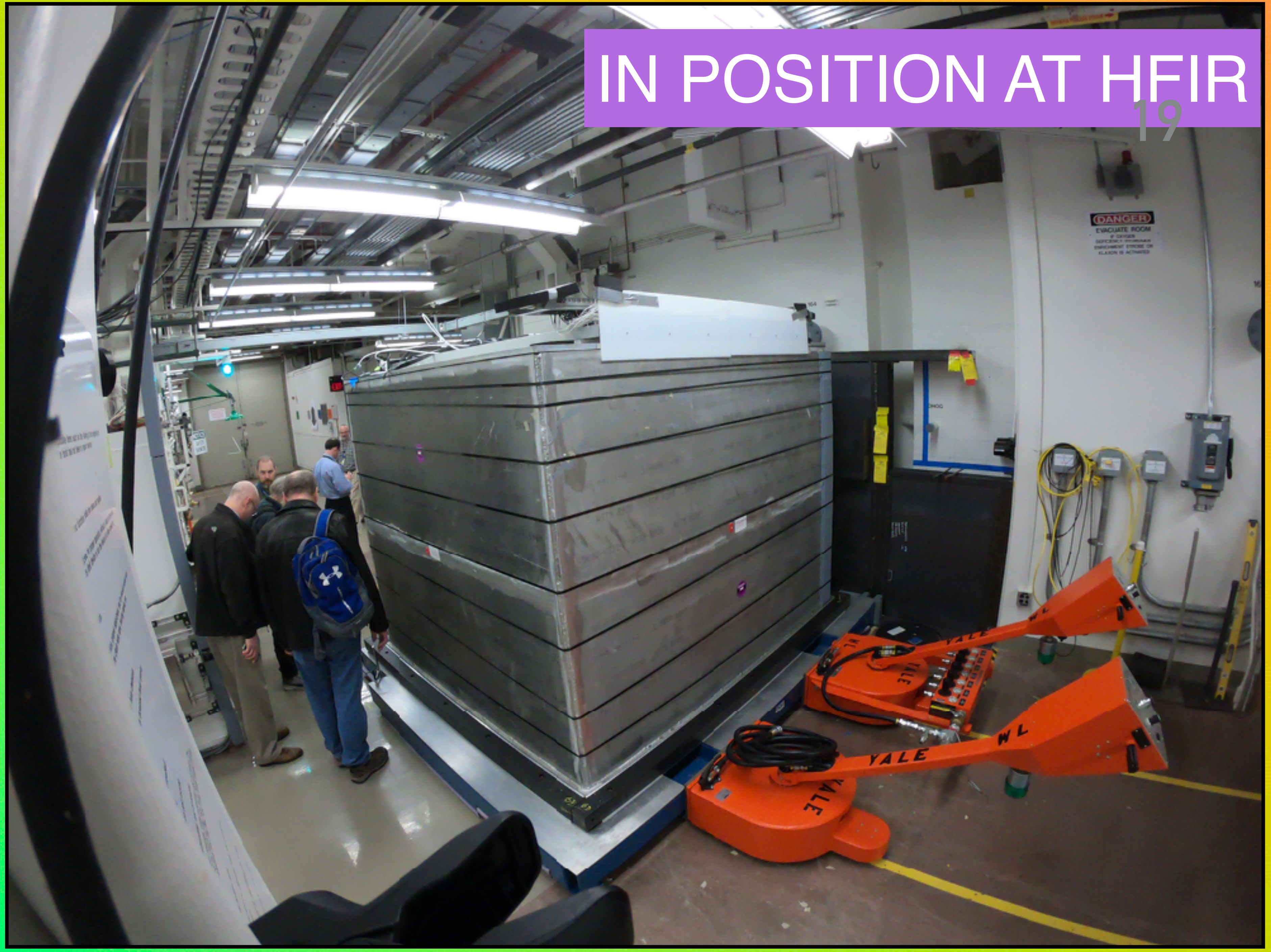

IN POSITION AT HFIR

FILLING FROM
MIXING TANK

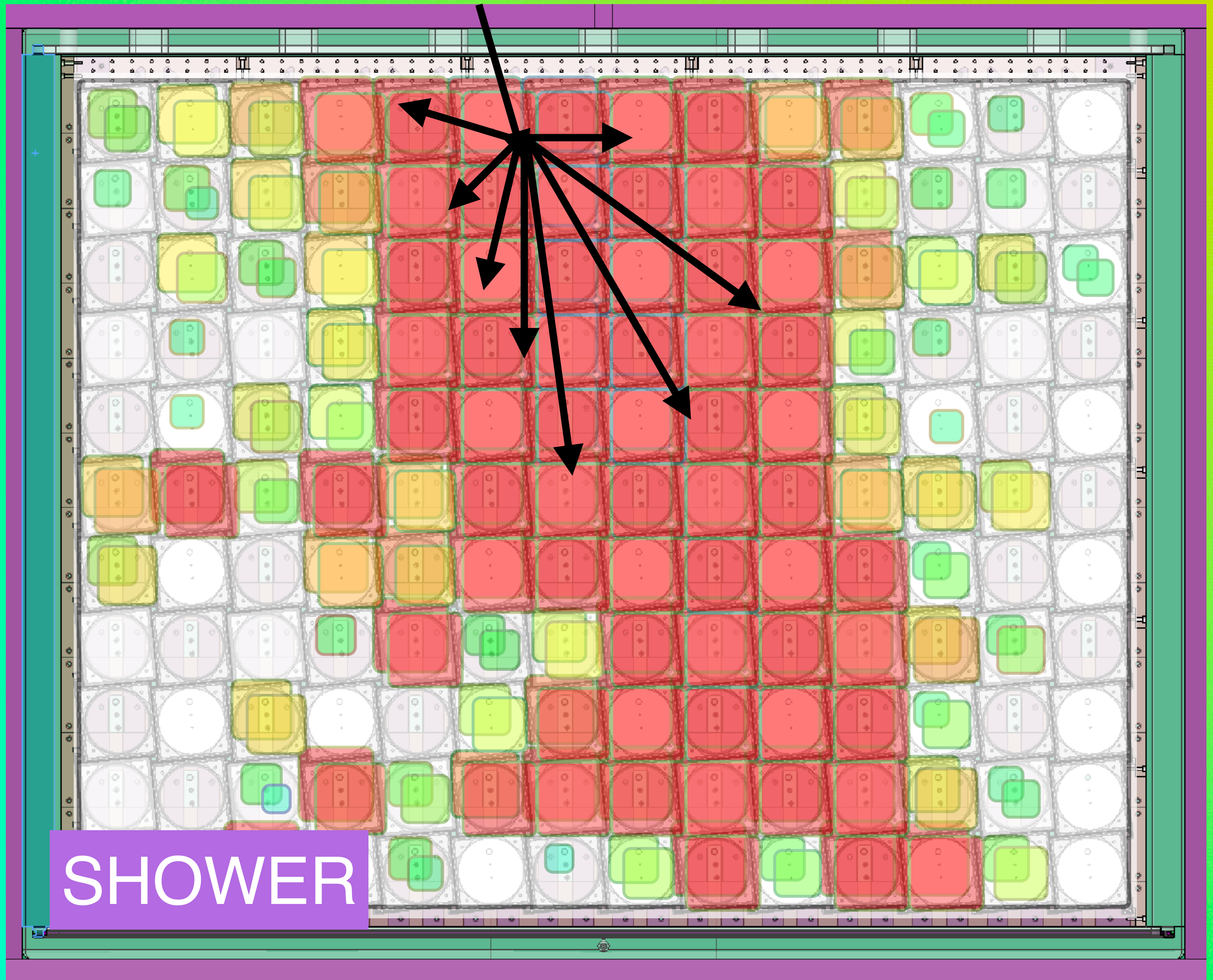

SHOWER


FEBRUARY 2018
ARRIVAL AT ORNL

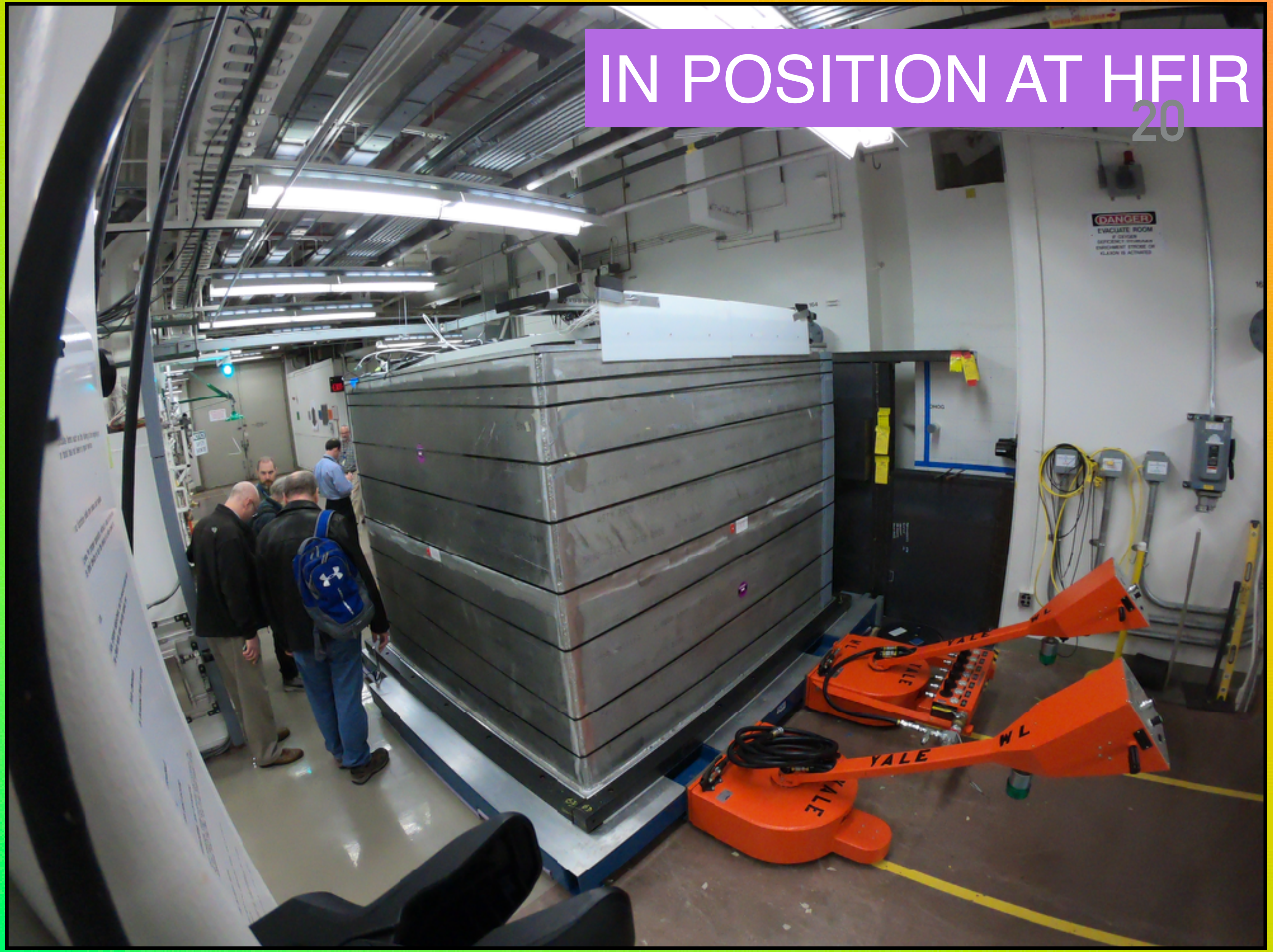
IN POSITION AT HFIR


FILLING FROM
MIXING TANK

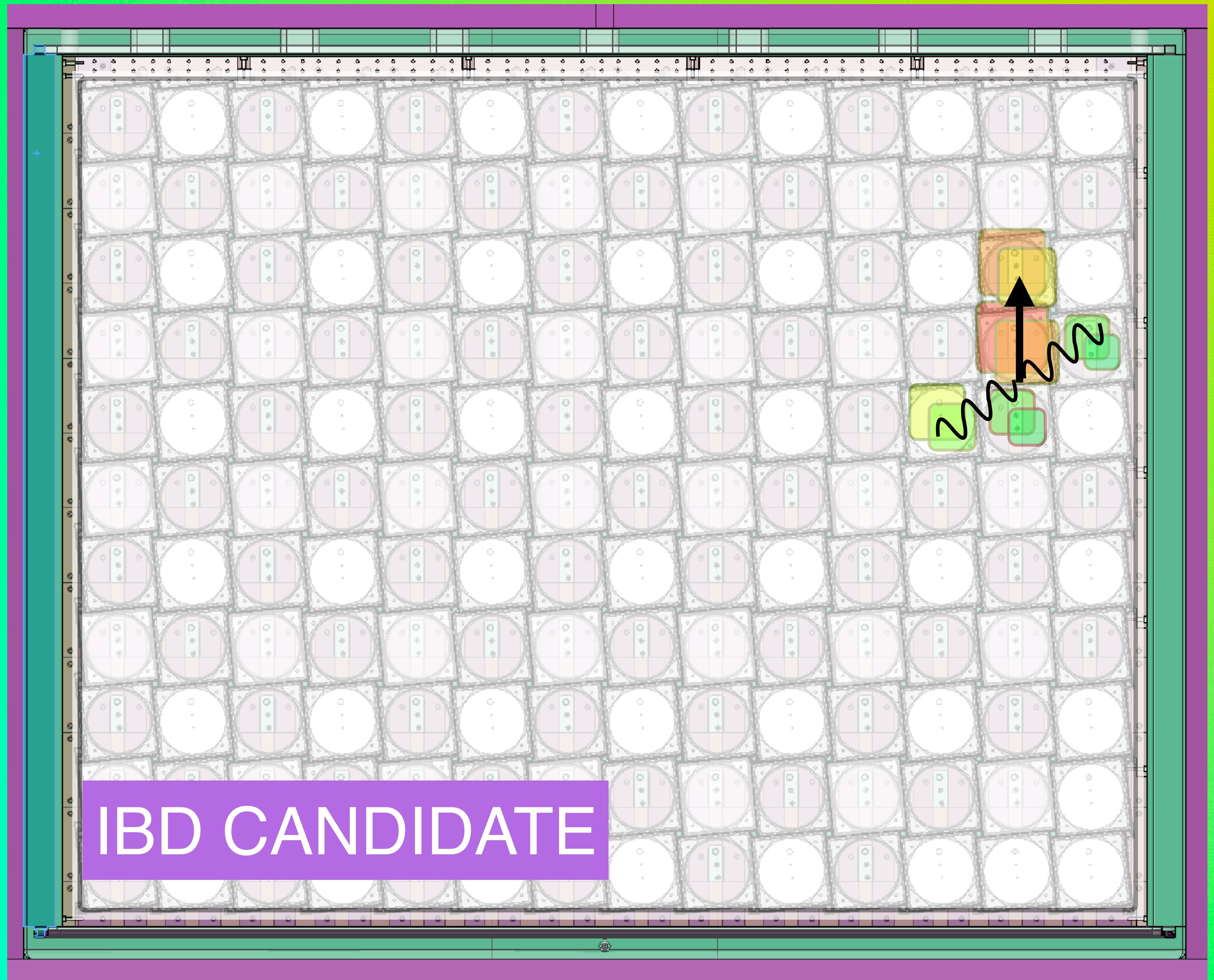
IBD CANDIDATE

PROSPECT ENERGY RESPONSE

Calibration with deployed sources (^{60}Co, ^{137}Cs, ^{22}Na) and cosmogenically produced $^{1}\mathrm{H}(n,\gamma)^{2}\mathrm{H}$ and $^{12}\mathrm{C}(n,p)^{12}\mathrm{B}$

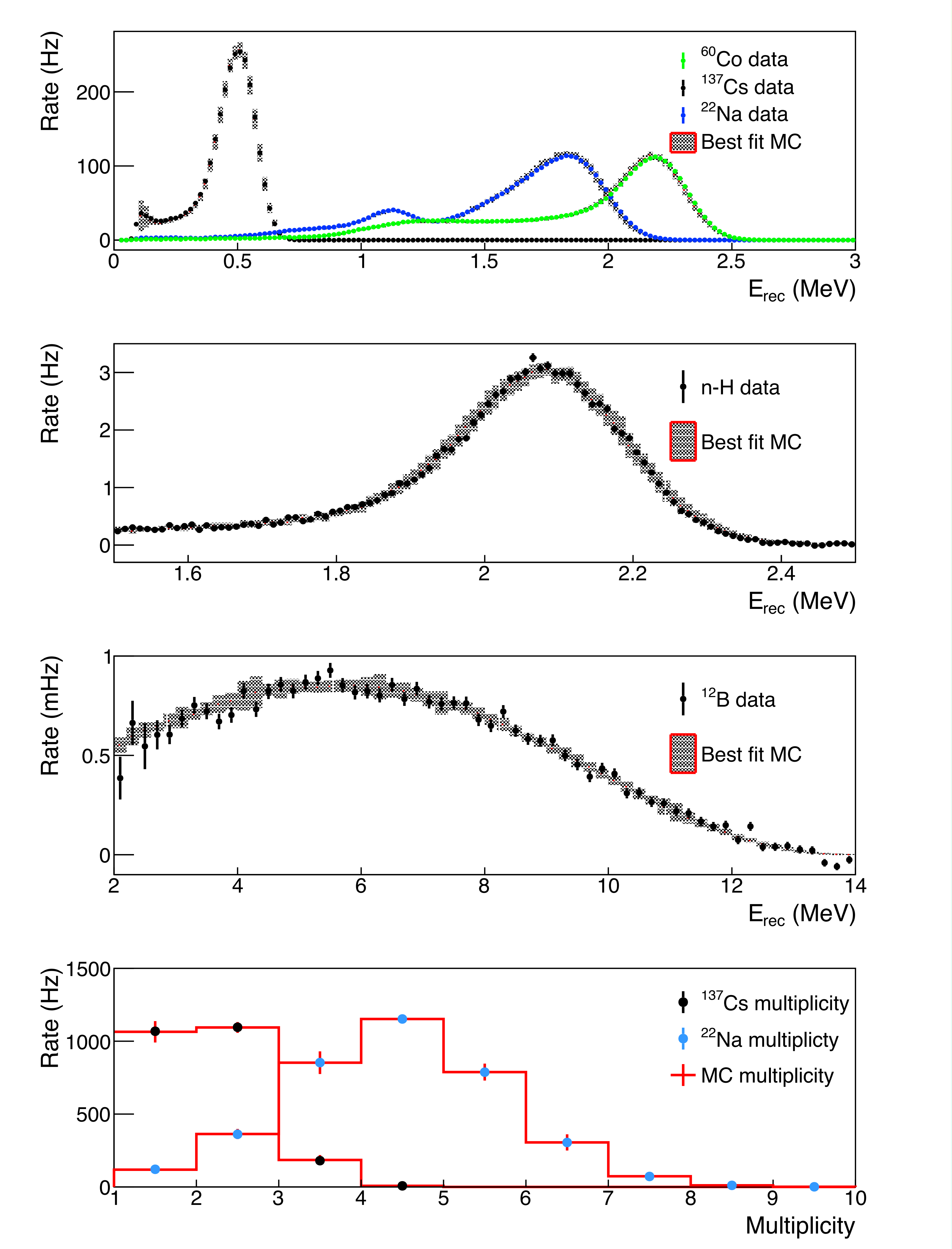

SIMULATED RESPONSE TO A MONO-ENERGETIC 4.0 MEV $\bar{\nu}_e$

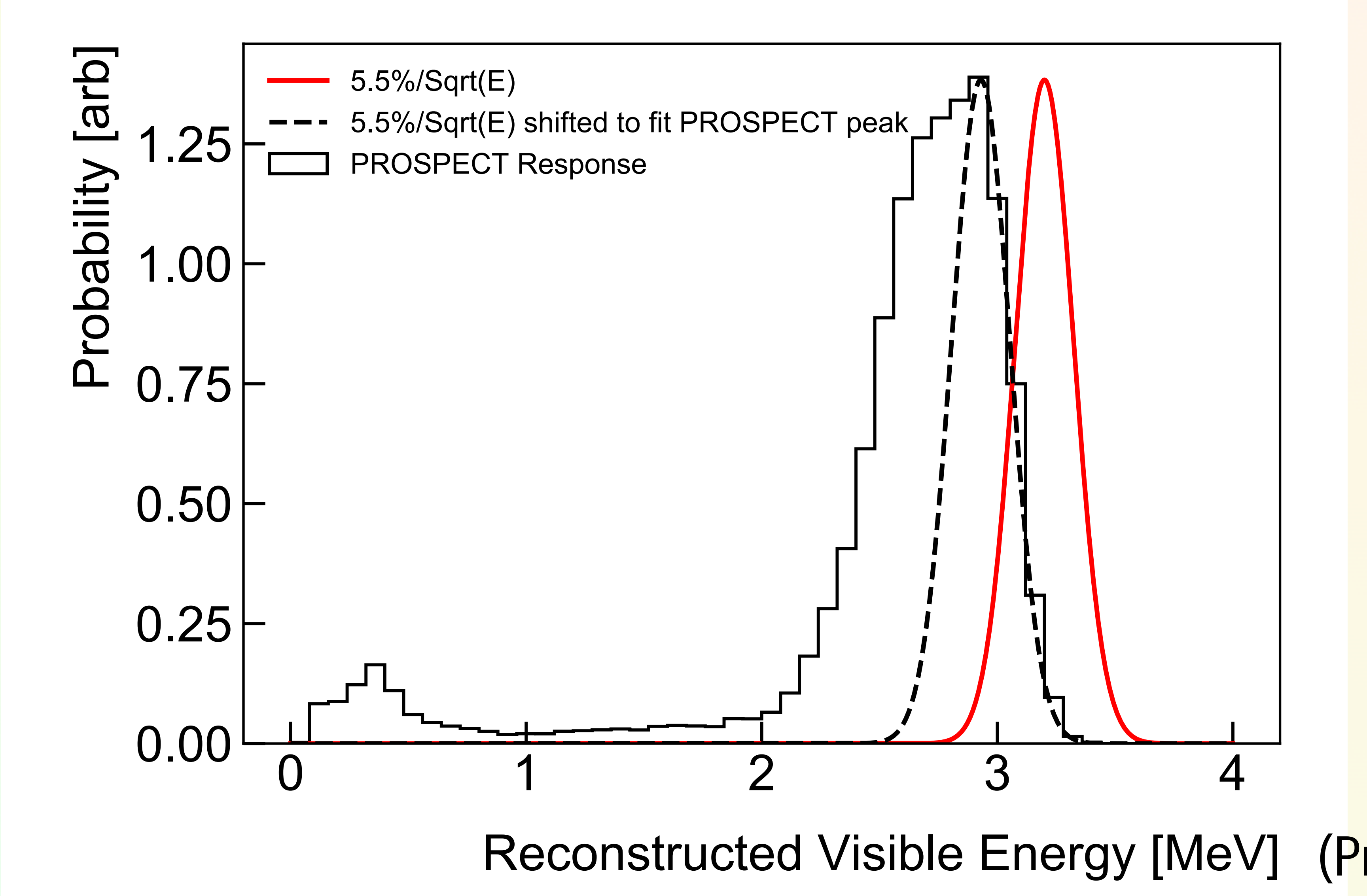

(Prompt energy)

SIMULATED RESPONSE TO A FLAT $\bar{\nu}_e$ SPECTRUM

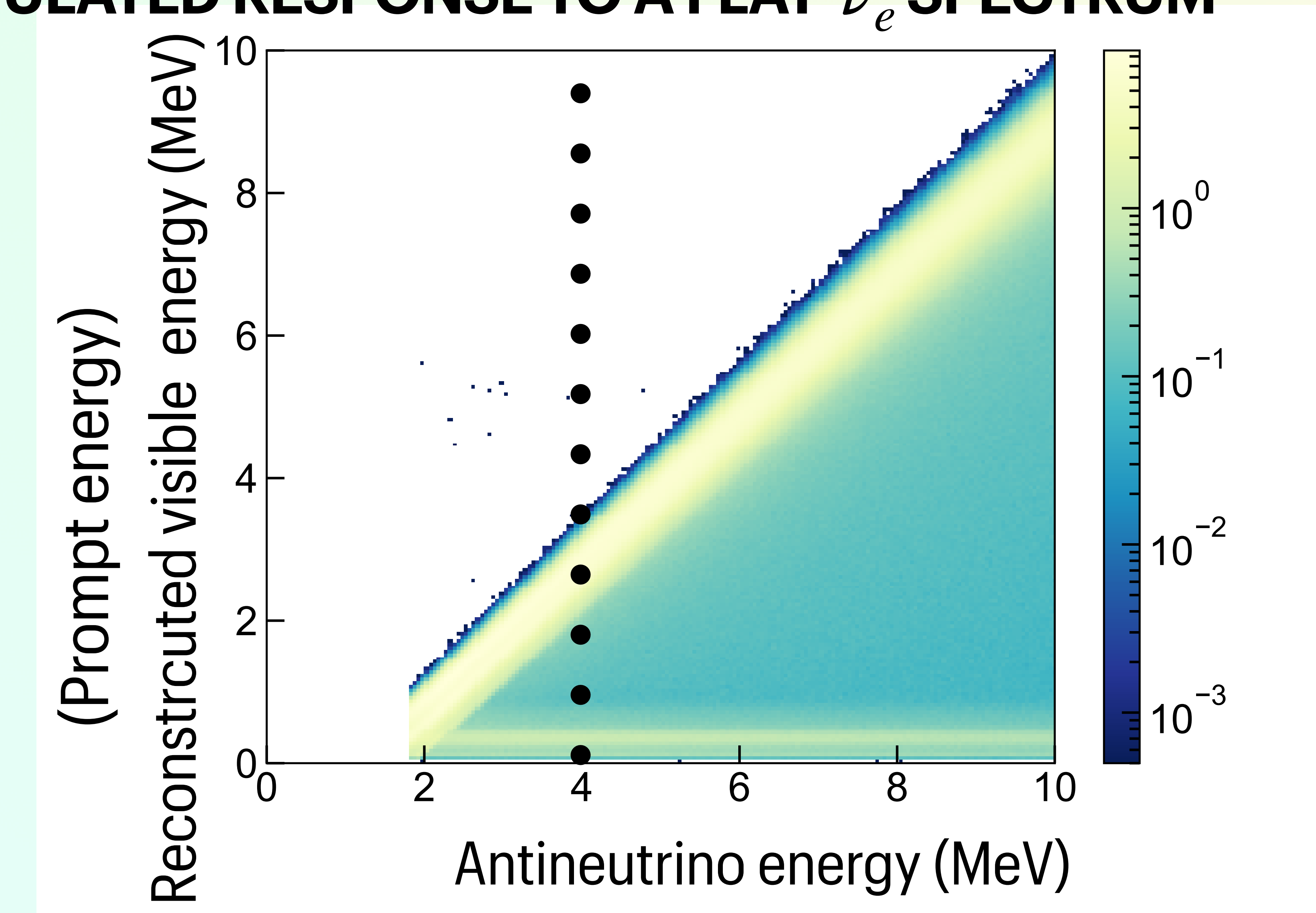

Within a few hours.. neutrinos!

- **March 5, 2018:** fully assembled detector began operation
- **Reactor On:** 1254±30 correlated events between [.8, 7.2] MeV per day
- **Reactor Off**: 614±20 correlated events (first off day March 16)
  benefit of being at a research reactor!
- subtract RxOn and RxOff for antineutrino spectrum
- distinct peaks in background from neutron interactions with H and ^{12}C

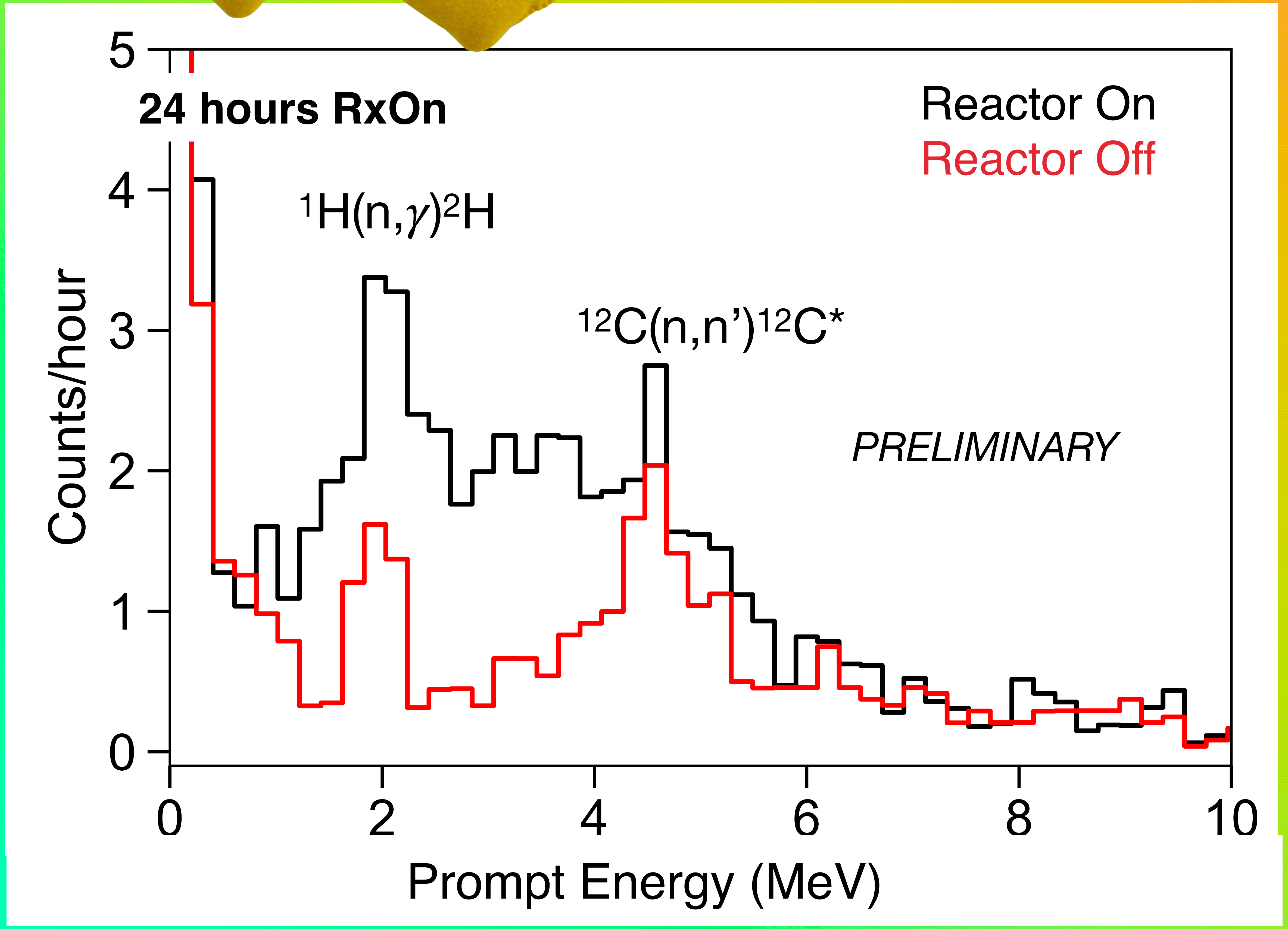

time to 5σ reactor antineutrino detection at Earth's surface: < 2 hours

OPERATION OF PROSPECT-I

The PROSPECT-I detector acquired data from 5 March to 6 October 2018 spanning five 24-day HFIR fuel cycles. We acquired 96 and 73 days of reactor-on (RxOn) and reactor-off (RxOff) data, respectively. An unscheduled HFIR outage of >1 year began in November 2018.

From the start of data taking, PMT HV began to exhibit current instabilities that gradually affected 64 of the 154 detector segments. We later established that these instabilities were caused by LiLS intrusion into the PMT housings that damaged the PMT bases. We also observed a gradual decrease in LiLS light yield which we attribute to oxygen contamination of the cover gas.

PROSPECT-I's final results are based on different detector configurations for each of five fuel cycles. For each configuration, segments with both PMTs operative (DE = Double End) are used to register IBD interactions, segments with only a single PMT operative (SE = Single End) are used to veto backgrounds.

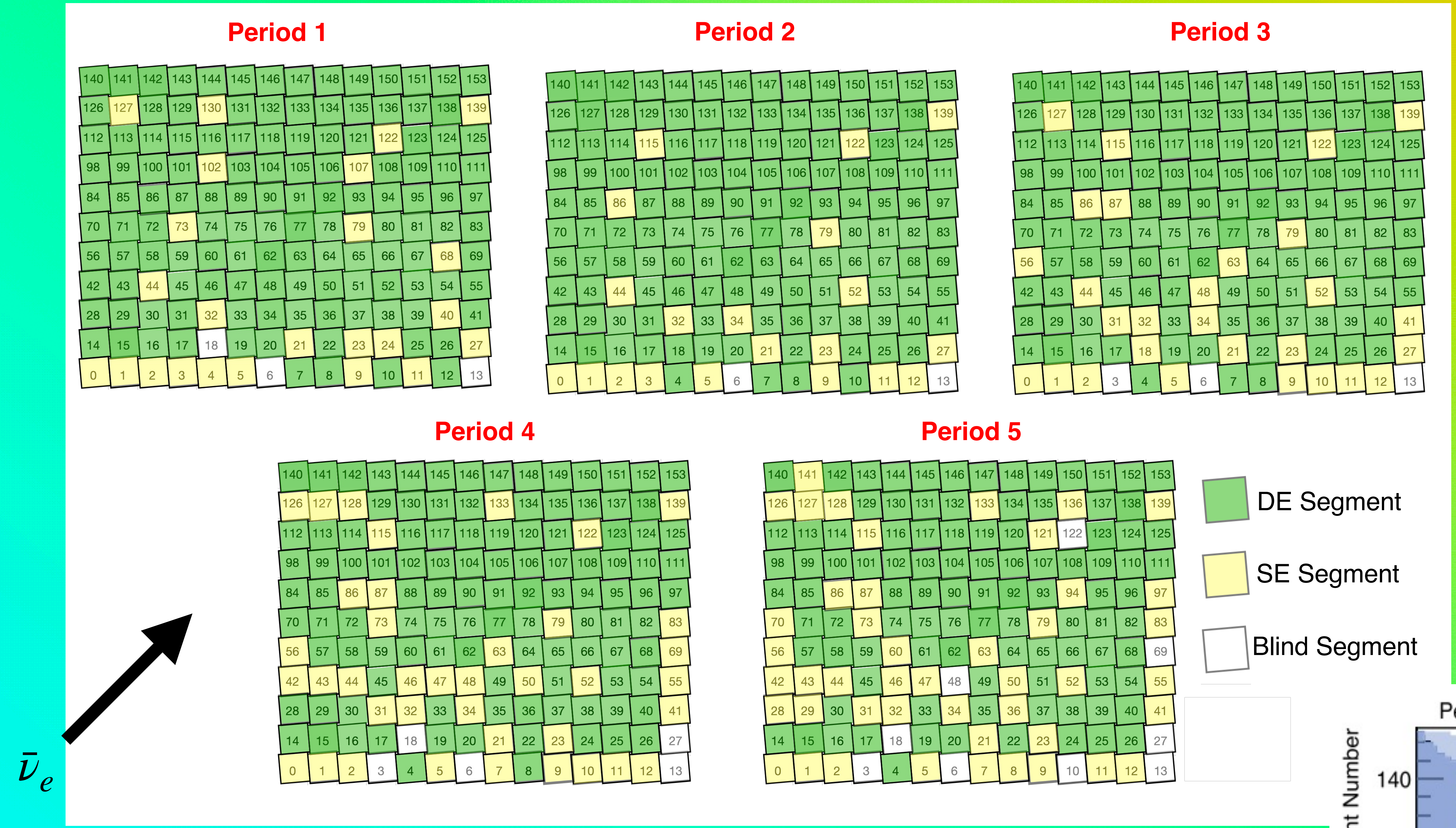

Data Set	Rx-On(Off) Days	N_{IBD}	N_{eff}	S:CB(AB)
Prev. Analysis	95.65(73.09)	50560 ± 406	18100	1.37(1.78)
This Analysis	95.62(72.69)	61029 ± 338	36204	3.90(4.31)
Period 1	9.54(14.58)	6357 ± 100	4328	4.03(6.21)
Period 2	22.83(15.71)	16546 ± 172	10259	4.35(4.64)
Period 3	23.20(16.40)	15094 ± 166	9050	4.04(4.44)
Period 4	22.29(16.79)	13486 ± 161	7742	3.72(3.39)
Period 5	17.76(9.21)	9546 ± 146	4825	3.38(2.88)

TABLE I. Final IBD event statistics for the previous and current analysis. Reactor-on (RxOn) and -off (RxOff) data taking time is presented in units of calendar days. N_{IBD}, N_{eff} and both signal to cosmogenic background (S:CB) and signal to accidental background (S:AB) ratios are calculated over the IBD energy region of [0.8, 7.2] MeV for previous analysis in [10] and [0.8, 7.4] MeV for the current analysis.

- Analysis with five different configurations using both SE and DE segments was substantially more complex than the initial analyses.
- As shown in the table, the average signal (S) to Cosmogenic Background (CB) and Accidental Background (AB) increased by over a factor of two.
- The effective number of IBDs doubled with respect to the previous analysis.

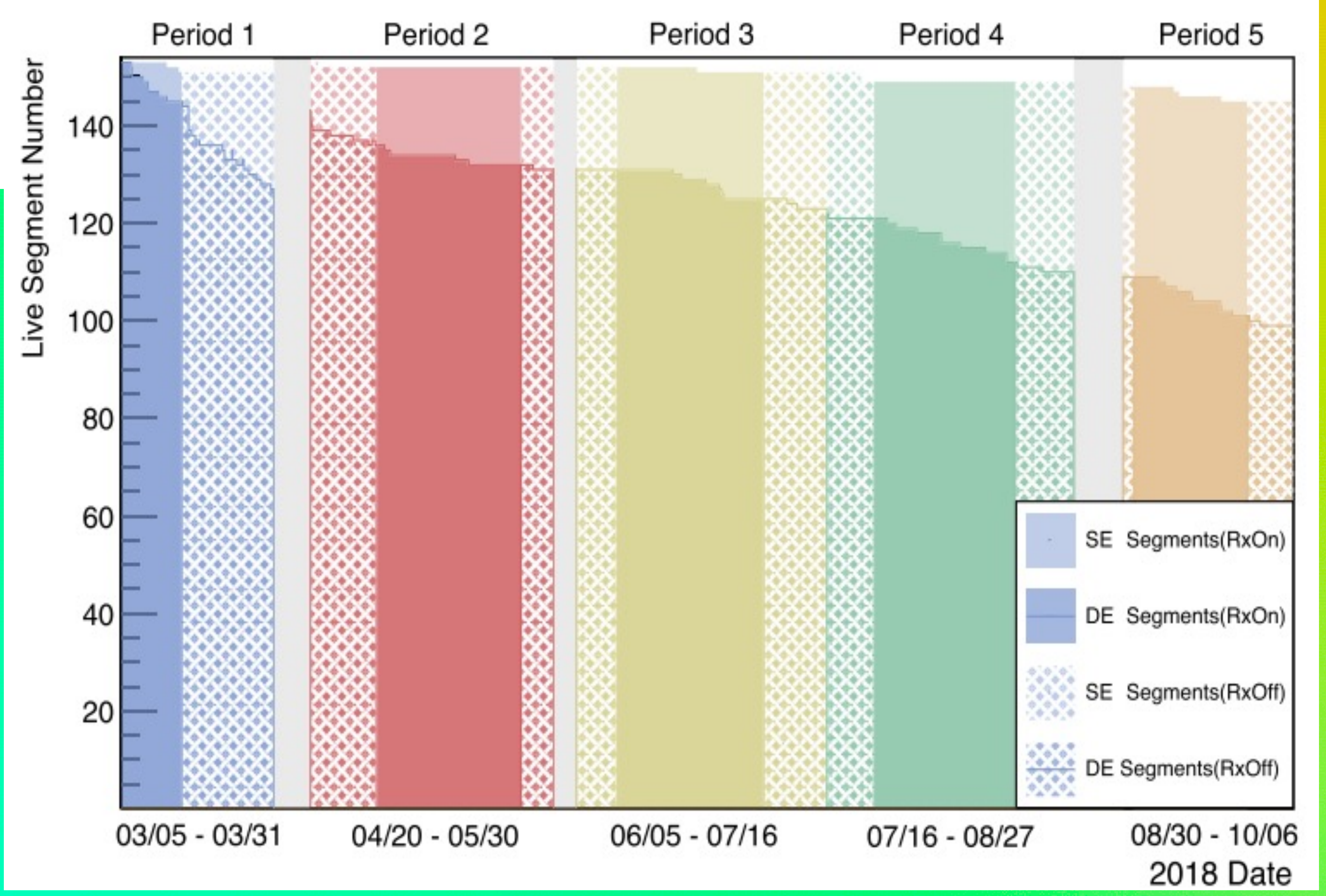

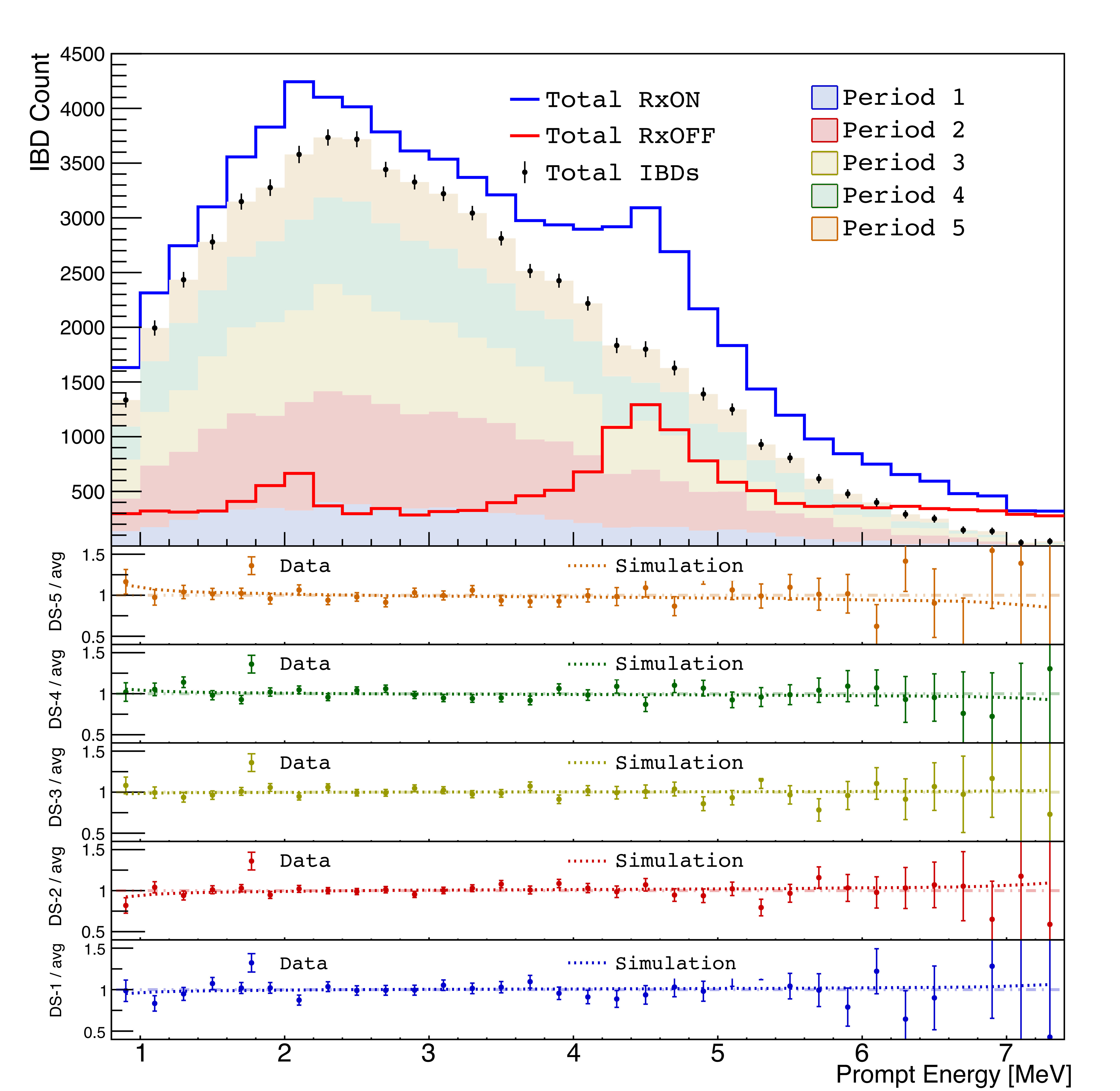

- Measured Total RxON and RxOFF data summed over all periods, and the calculated IBD prompt spectrum for each period as a function of the observed prompt energy in the top panel.
- The lower panels show the ratio of the IBD counts for each period compared to the average and compared to simulation of each period.
- The peaks at ~2 and ~4.5 MeV are cosmogenically induced background from double neutrons and inelastic neutron-^{12}C interactions, respectively.
- The IBD spectra are consistent between all periods.

Top panel:
The unfolded antineutrino energy spectrum compared to the shape of the calculated Huber-Mueller spectrum.

The correction for IBD counts from non-fission antineutrinos (mainly from ^{28}Al decay) is indicated [*Phys.Rev.C* 101 (2020) 5, 054605].

Bottom panel:
The local p-value from a comparison of the observed and calculated Huber-Mueller shape with a 1.25 MeV-wide sliding window.

Middle panel:
Gaussian fit to the excess in data compared to the HM model near 6 MeV.

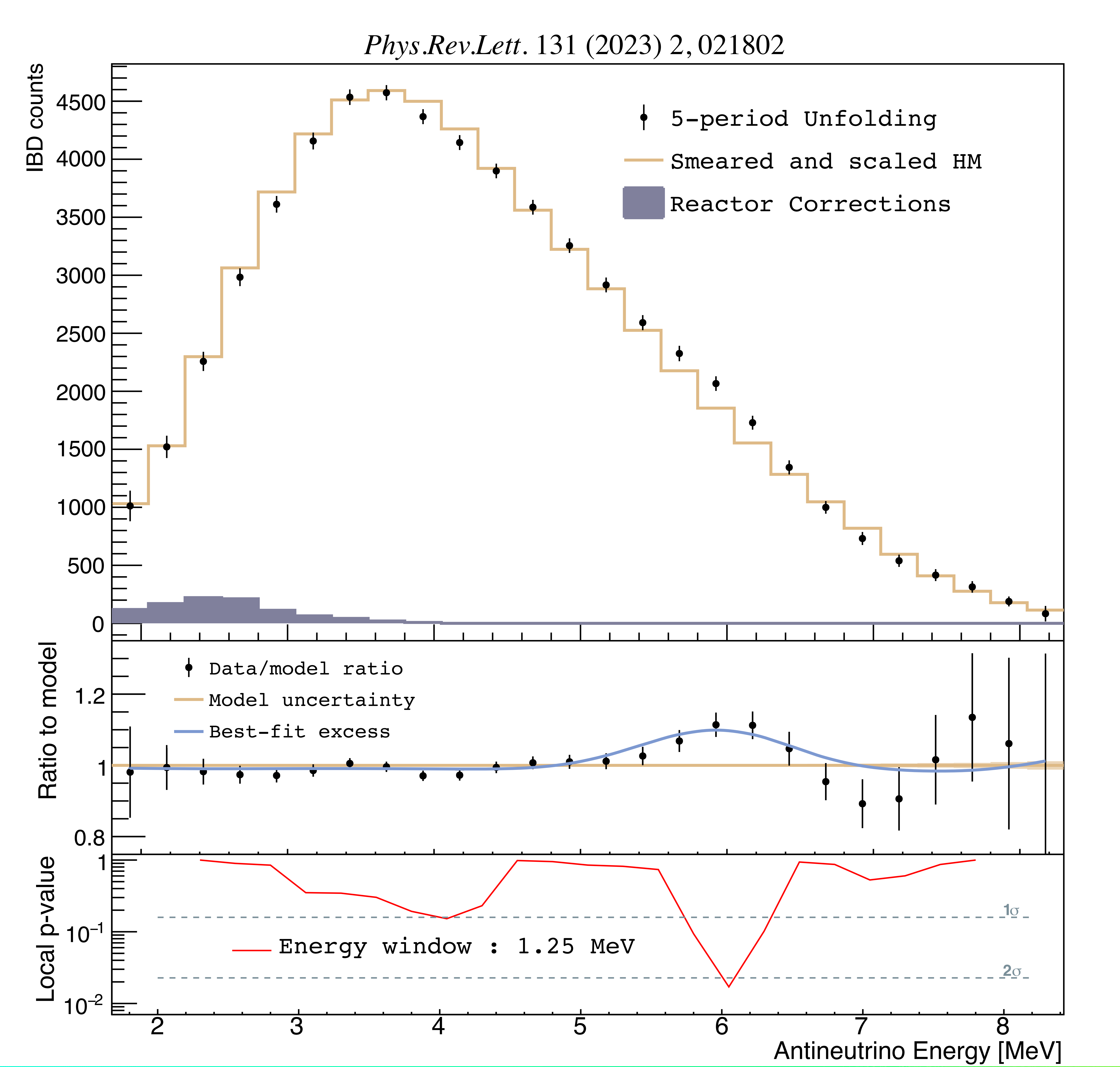

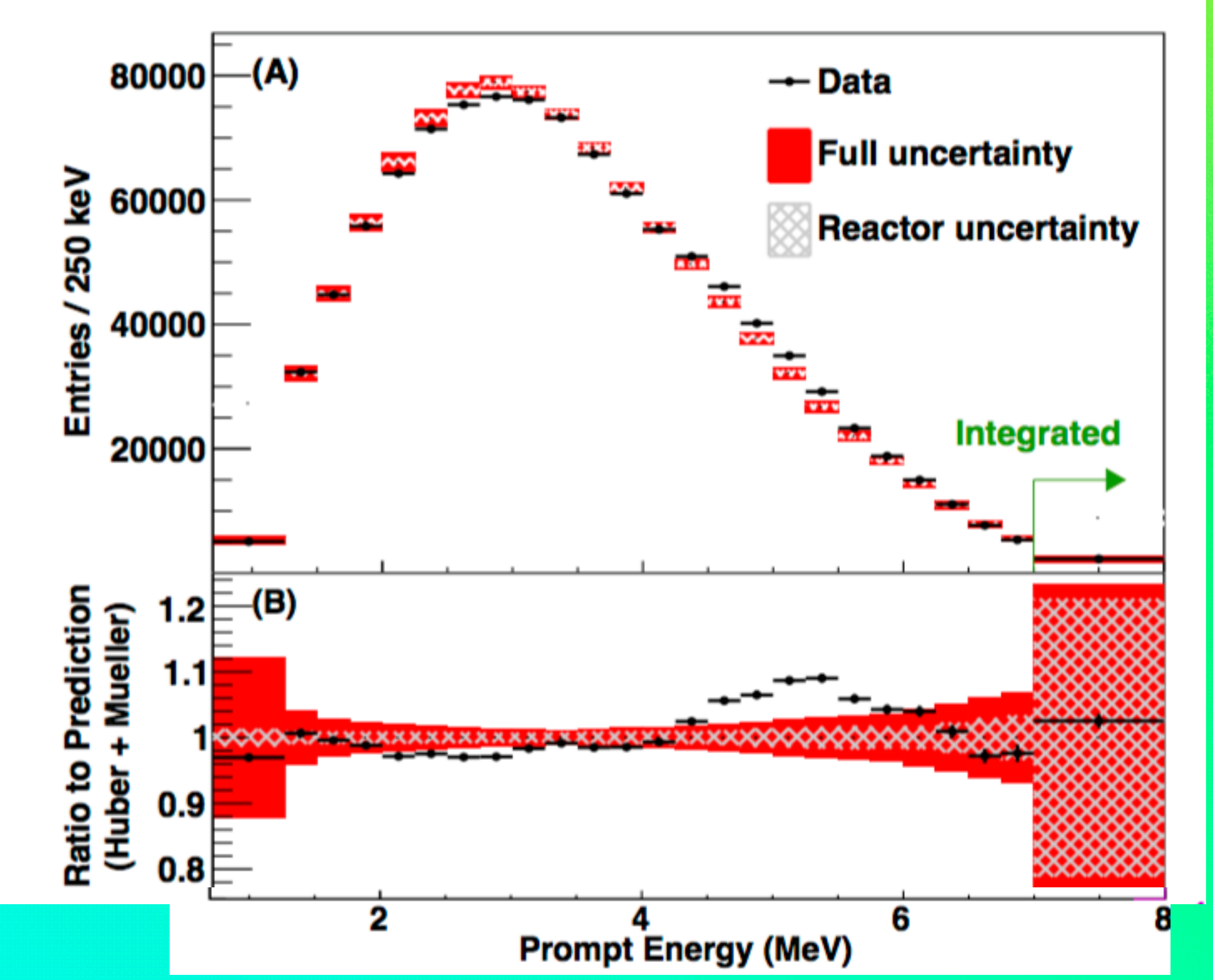

Test three hypotheses using PROSPECT and Daya Bay spectra (CPC45, 073001 (2021)):

1. The excess is not due to ^{235}U, other fission isotopes are responsible for the observed excess,
   - Disfavored at $\Delta\chi^2 = 13.6 \text{ or } 3.7\sigma$
2. All isotopes contribute equally to the excess
   - Most likely, $\Delta\chi^2 = 0.4$
3. ^{235}U is solely responsible for the excess.
   - Disfavored at $\Delta\chi^2 = 3.9 \text{ or } 2\sigma$ when Daya Bay detector systematics are taken into account (solid line)

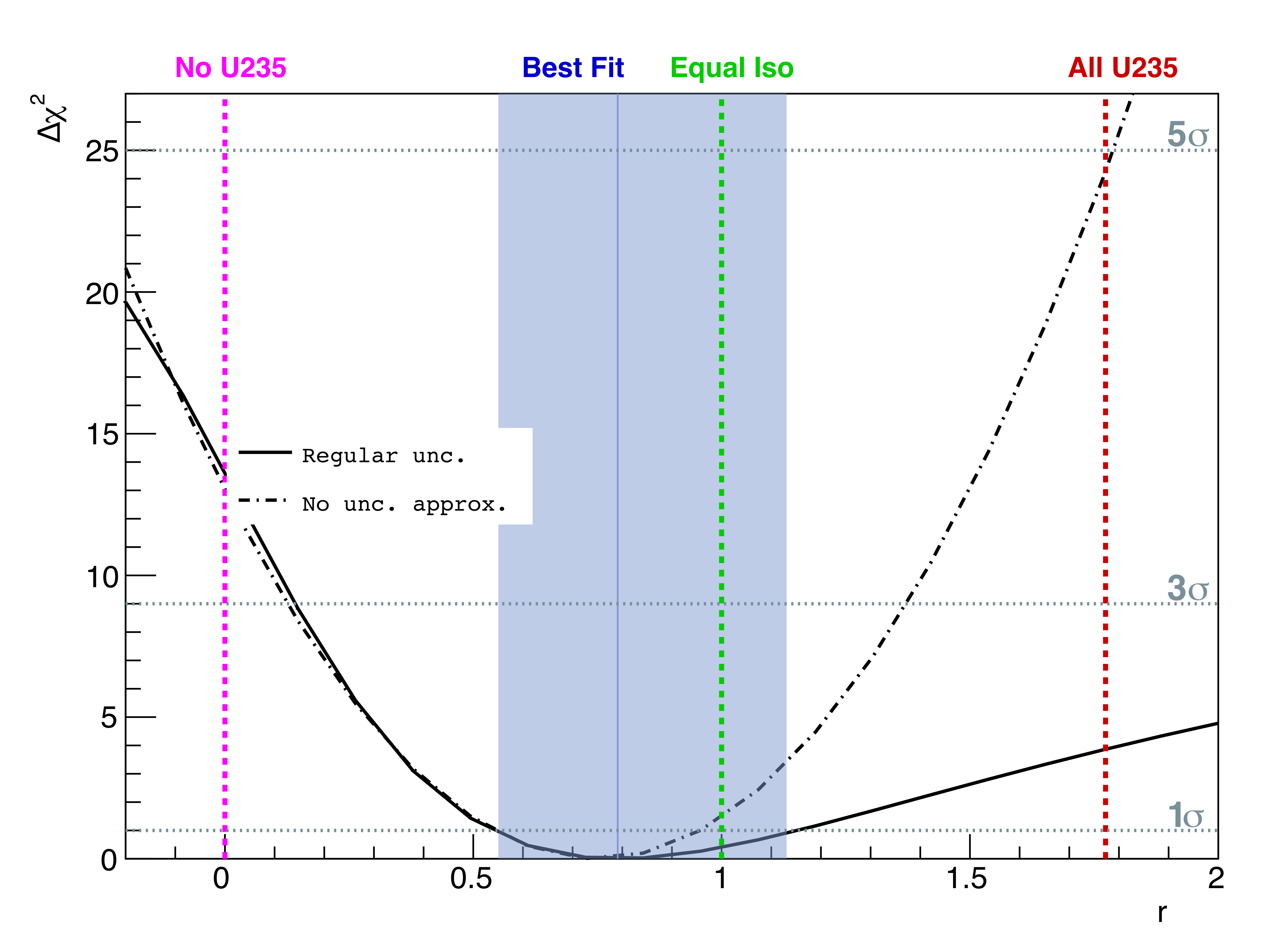

Final search for short-baseline neutrino oscillation with PROSPECT-I

We used the same five-period analysis with 0.2 MeV-width prompt-energy bins from 0.8 to 7.4 MeV and divided the detector into six baseline bins.

This tests for sterile neutrinos using a total of 990 bins (33 energy x 6 baseline x 5 periods).

Finer baseline binning gave minimal improvement in sensitivity.

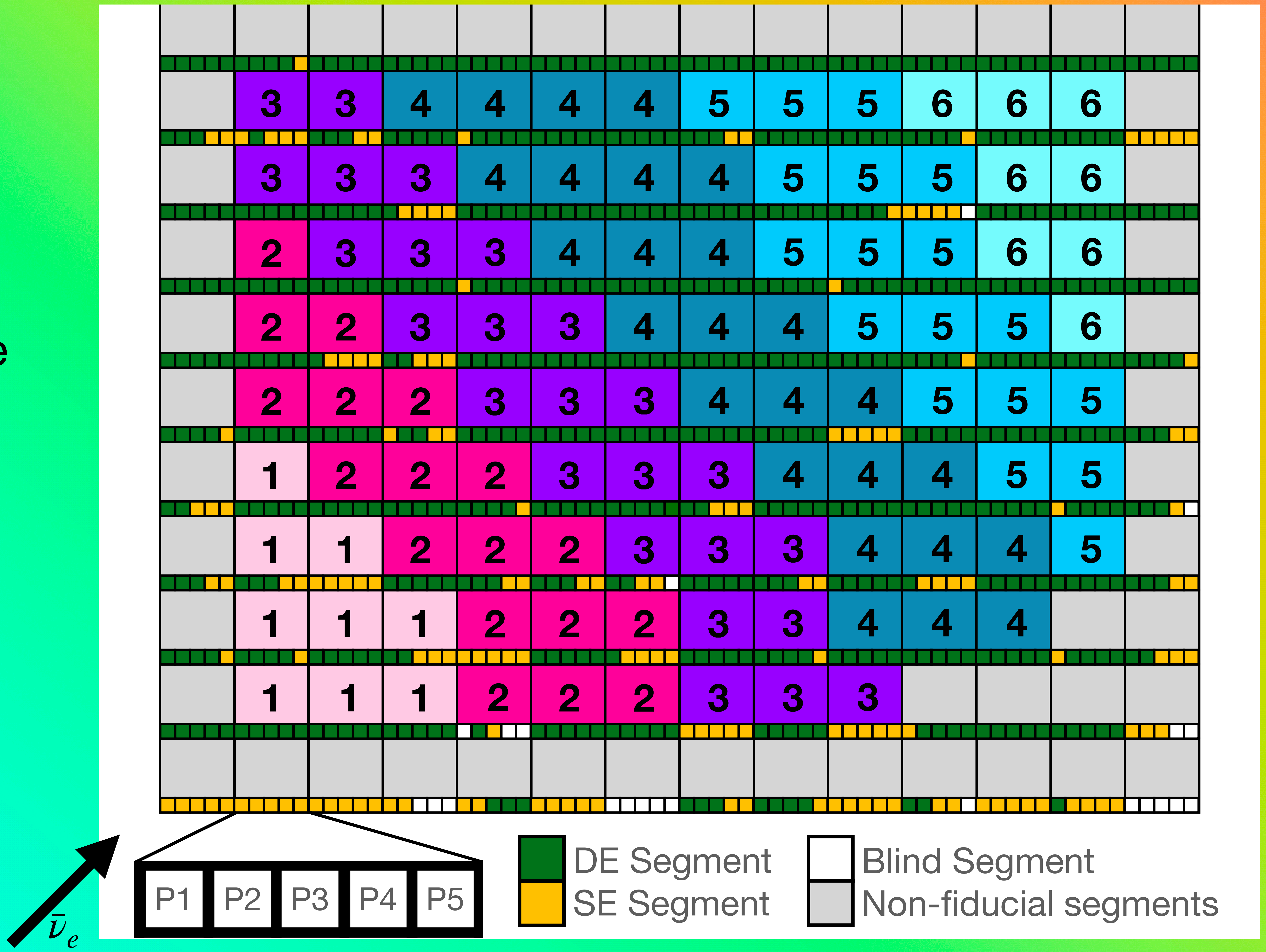

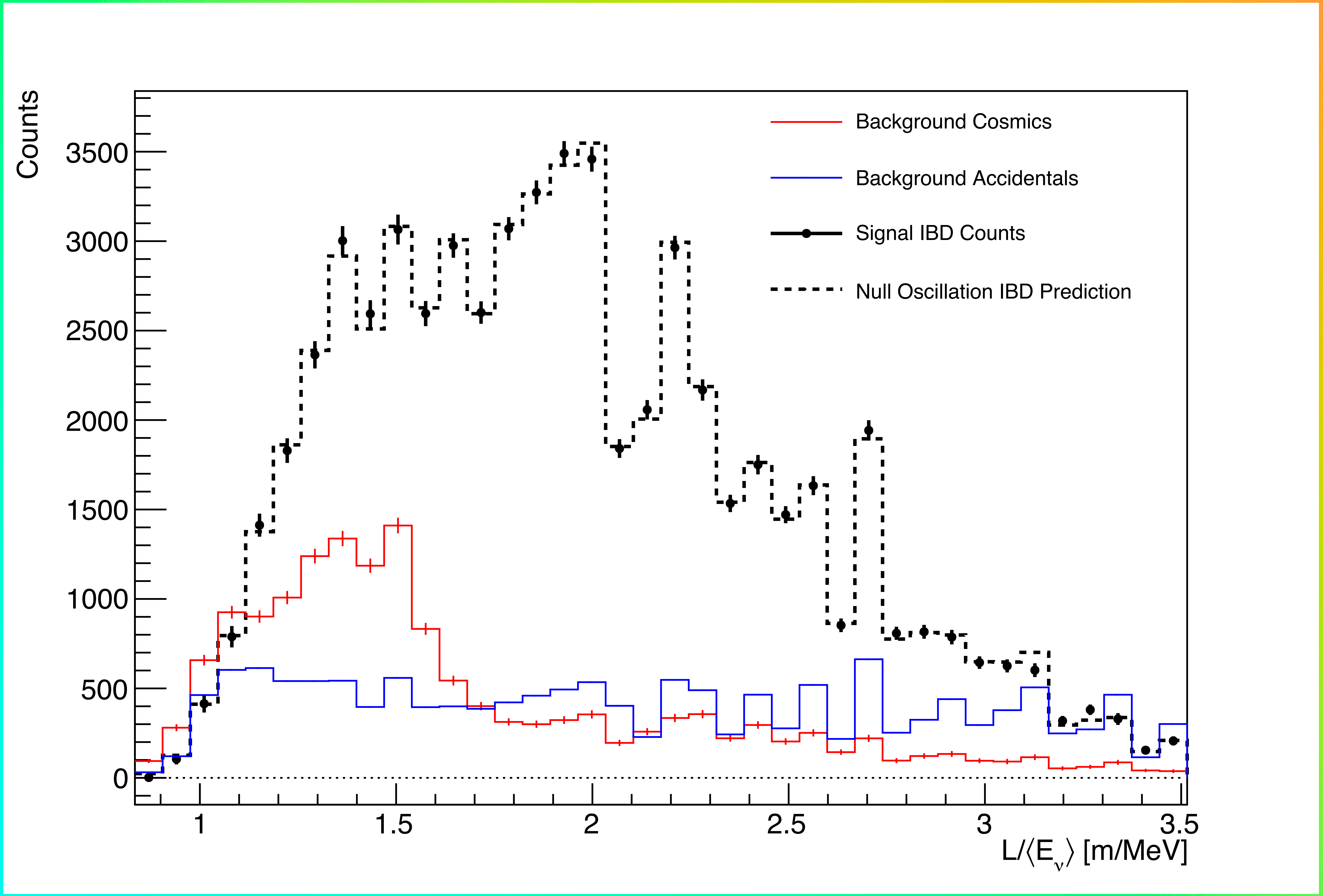

We grouped the data in bins of $L/<E_\nu>$ (m/MeV) in comparison to the backgrounds.

The largest background at low $L/<E_\nu>$ is due to cosmics which contribute at high energy; accidental backgrounds are larger at larger $L/<E_\nu>$.

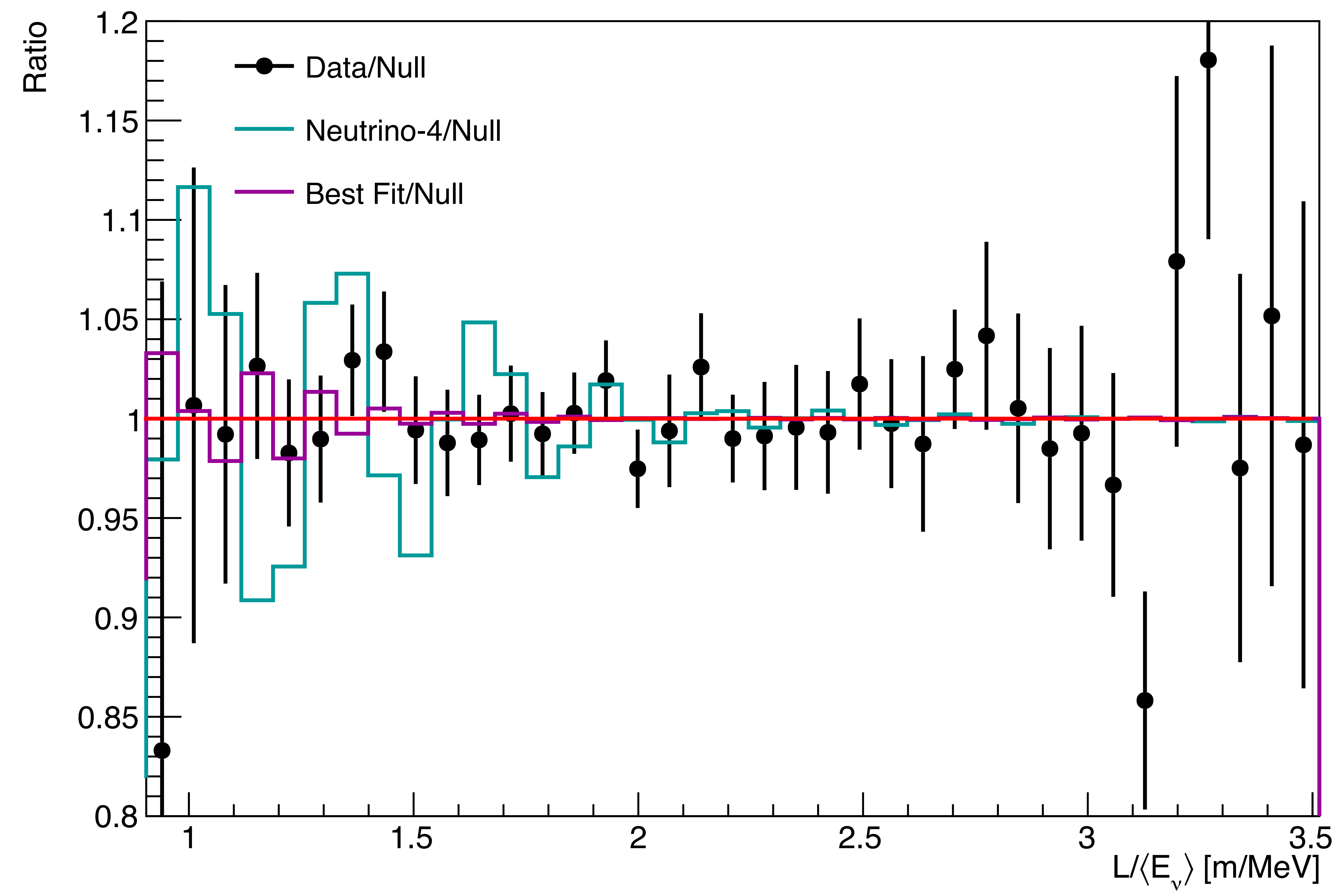

The ratio of the PROSPECT-I IBD data with the null (no-oscillation) hypothesis in $L/<E_\nu>$ compared to the ratio of the best-fit oscillation result from the Neutrino-4 to the null hypothesis.

The ratio of the PROSPECT best fit to the null hypothesis is also shown.

arXiv:2406.10408

PROSPECT-I exclusion in the 3+1 sterile neutrino oscillation phase space.

The dotted line shows the 95% CL sensitivity. The solid line shows the excluded region at 95% CL.

The dashed line shows the region excluded at 5σ.

PROSPECT results are consistent with the null (non-oscillation) hypothesis with a *p* value of 73% based 2000 simulated "toy" experiments.

Best fit at $(\sin^2 2\theta_{14}, \Delta m^2_{41}) = (0.42, 15.2\ \mathrm{eV}^2)$

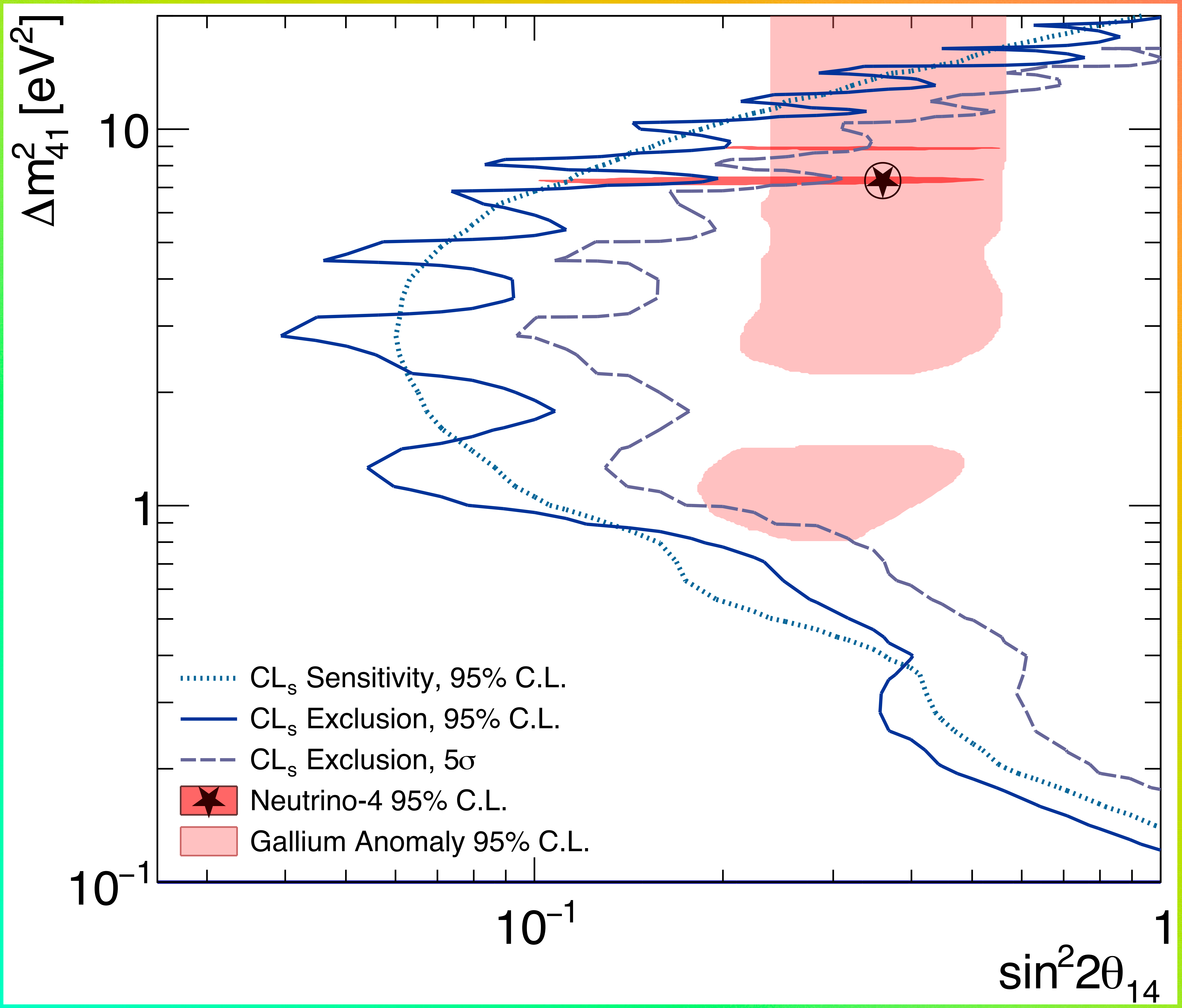

PROSPECT excludes the region below Δm^2_{14} of $10\mathrm{eV}^2$ favored by the Gallium Anomaly.

The Neutrino-4 best fit point of $(\sin^2 2\theta_{14},\ \Delta m^2_{41}) = (0.36,\ 7.3\mathrm{eV}^2)$ is disfavored at more than 3σ based on 2000 "toy" experiments.

Reactor antineutrino directionality measurement arXiv:2406.08359

- Directional neutrino measurements have been crucial in investigations of oscillation of atmospheric neutrinos and in neutrino astronomy.
- At ~MeV reactor energies, directional reconstruction is challenging. The mean neutron displacement in LS is ~1.6 cm while the spread due to scattering and diffusion is ~6 cm.
- Previous segmented detectors have observed the expected displacement with reactor $\bar{\nu}_e$ and monolithic detectors such as CHOOZ and Double Chooz have performed measurements of the incident neutrino direction using Gd as the neutron capture agent.
- PROSPECT benefits because the spatial extent of the neutron products from $^6\mathrm{Li}(n,\alpha)^3\mathrm{H}$ is greatly reduced compare to gamma production from neutron capture on Gd or H.
- In PROSPECT reconstruction, the delayed neutron candidate is required to occur within 120μs of the prompt candidate and its segment must be same as or vertically/horizontally adjacent to that of the prompt event.
- The complications due to inoperative PMTs are taken into account in reconstructing $\bar{\nu}_e$ direction.

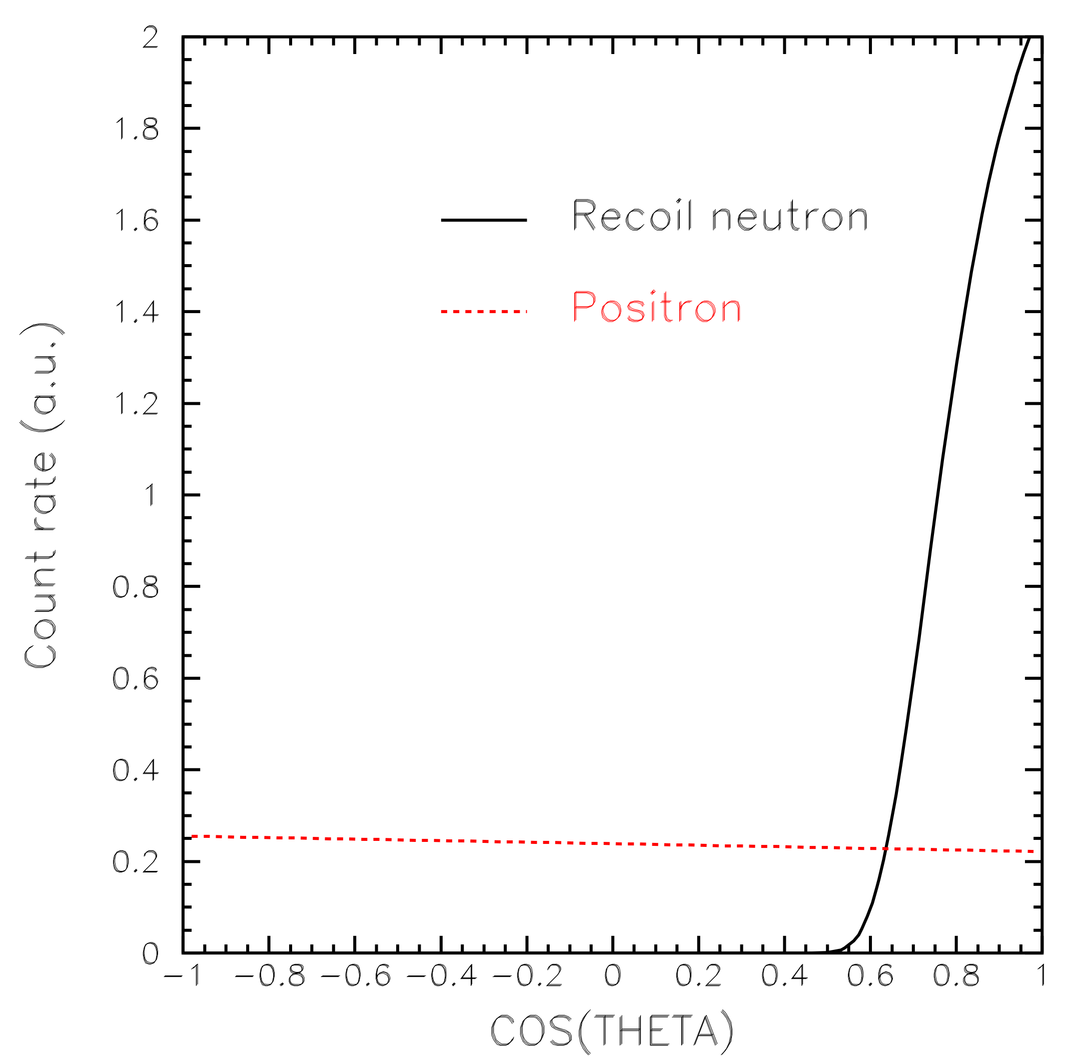

Fig. 1.6. Angular distributions of positrons and recoil neutrons from inverse beta-decay in the laboratory frame.

Vogel & Beacom, PR**D60**, 053003 (1999)

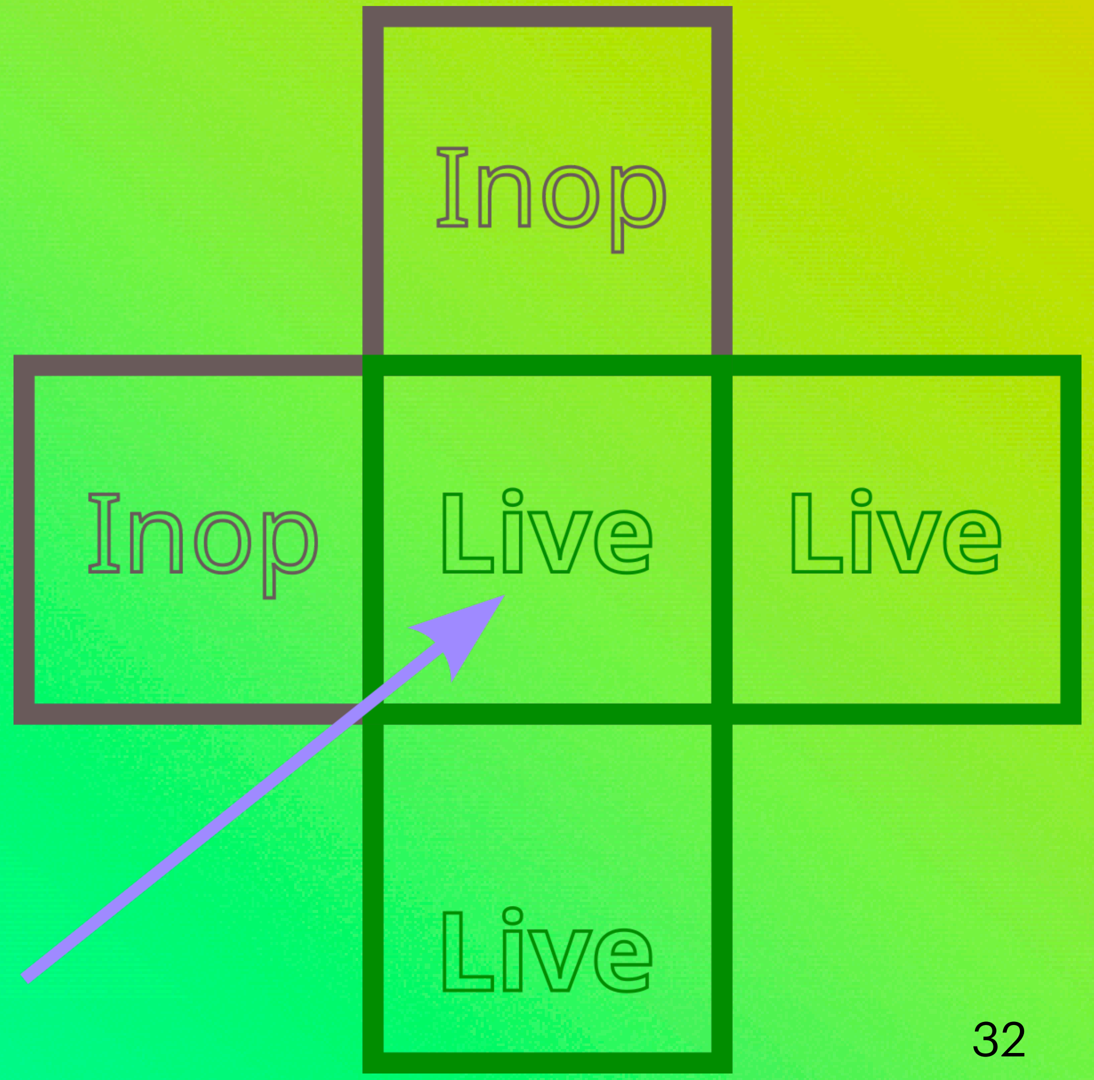

Average incident neutrino direction $\vec{p} = \frac{1}{N}\sum_{i}^{N}(\vec{s}_{d,i} - \vec{s}_{p,i})$ where $\vec{s}_{d,i}$ and $\vec{s}_{p,i}$ are the position of the delayed and prompt candidates for the i^{th} IBD candidate.

For $\alpha \in \{x, y\}$, $p_\alpha = \frac{Dn_{\alpha+} - Dn_{\alpha-}}{N}$ where D is the segment pitch; however, this expression gives a biased estimator in the presence of inactive segments.

A less biased estimator can be achieved by treating the detector as a collection of sub-detectors composed of adjacent segment pairs and using $p_x = D\frac{r_+ - r_-}{r_+ + r_- + 1}$

where $r_\pm = \frac{n_{x\pm}}{n_{0\pm} + n_{0*}}$ where $n_{0\pm}$ means the segment in the positive or negative x direction is the only active adjacent segment and n_{0*} means both adjacent segments in x are active.

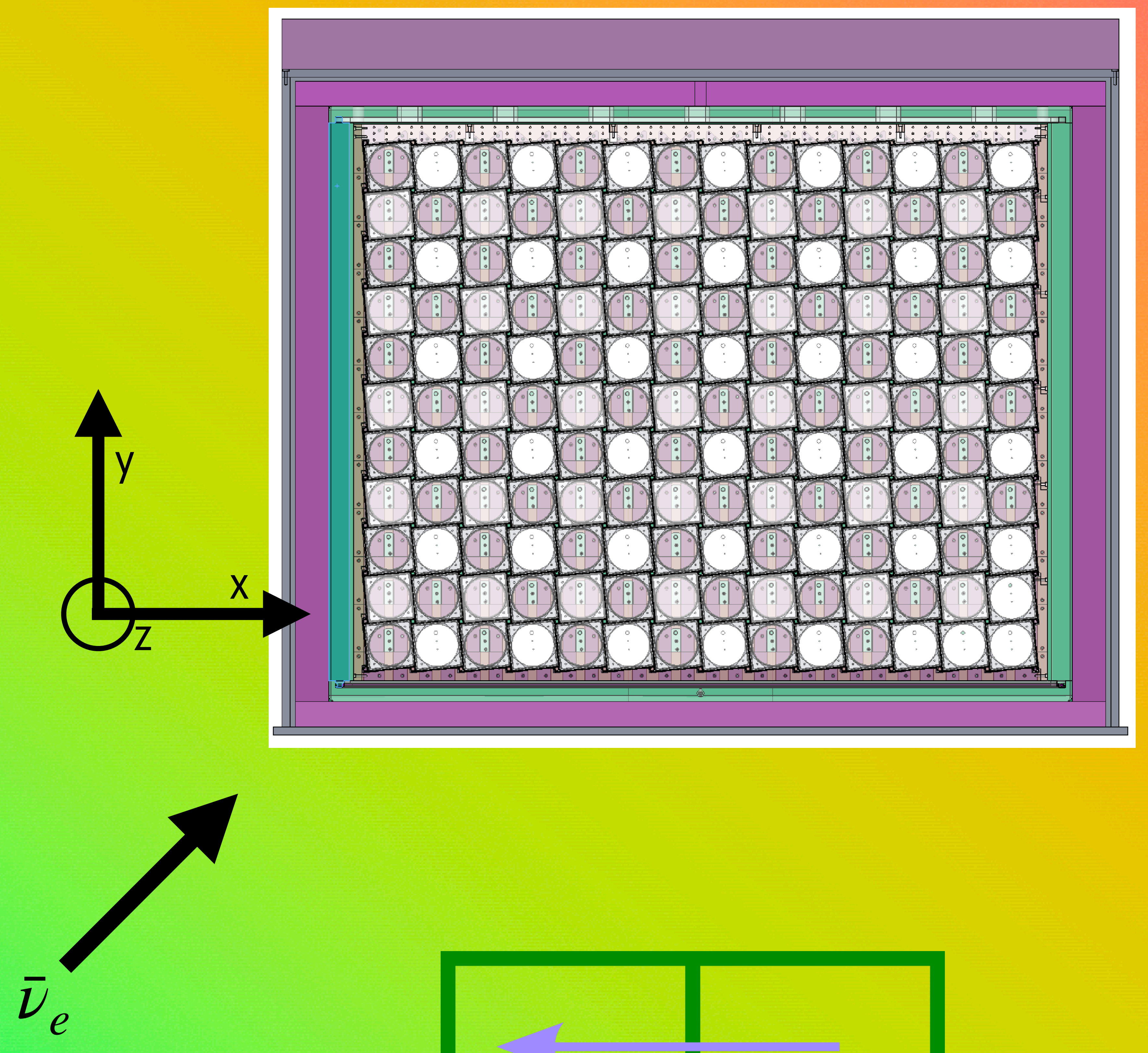

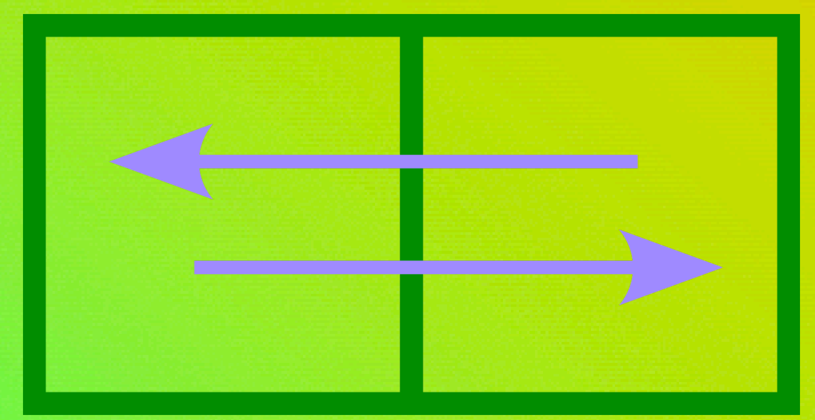

Adjacent segment pair

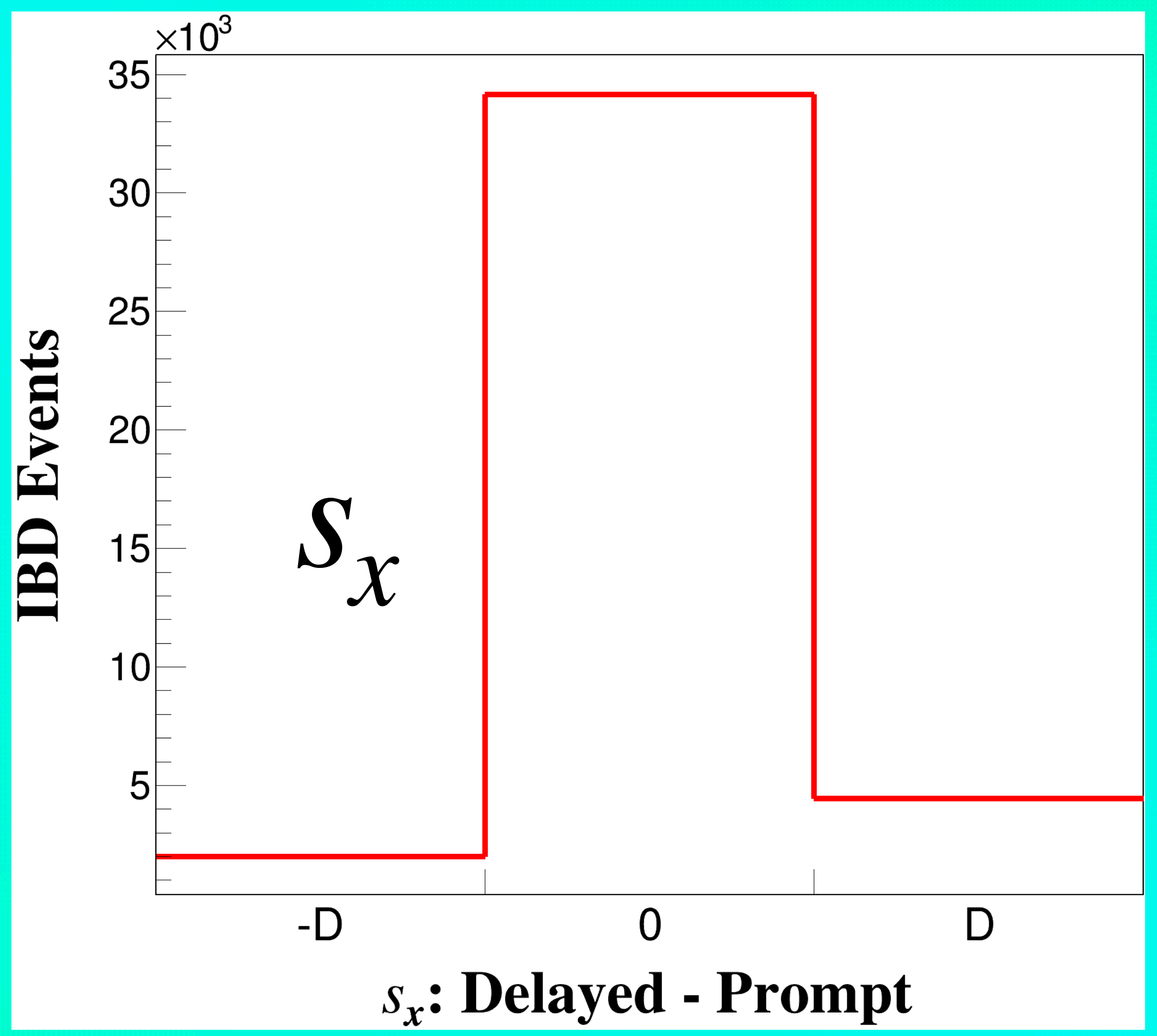

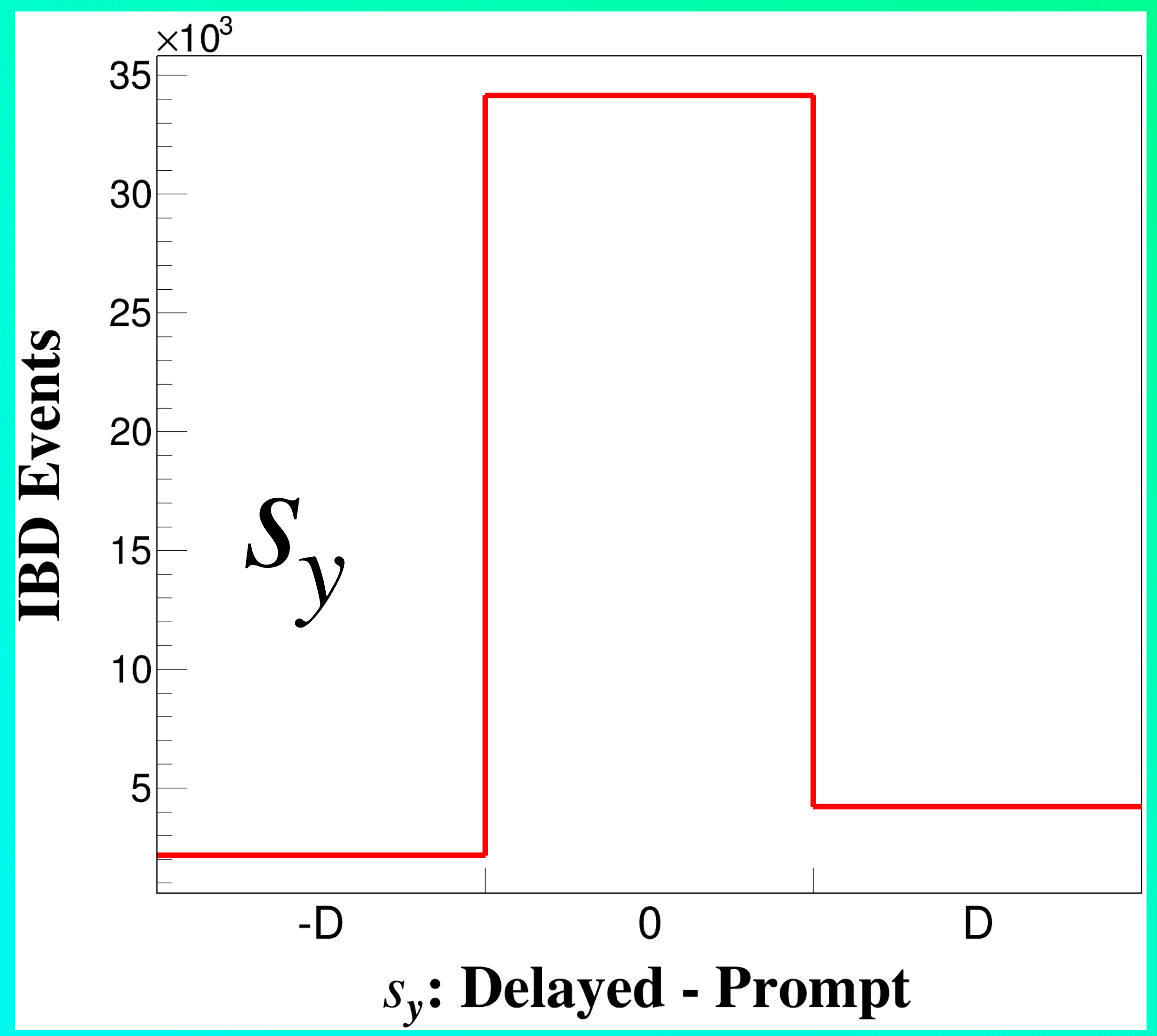

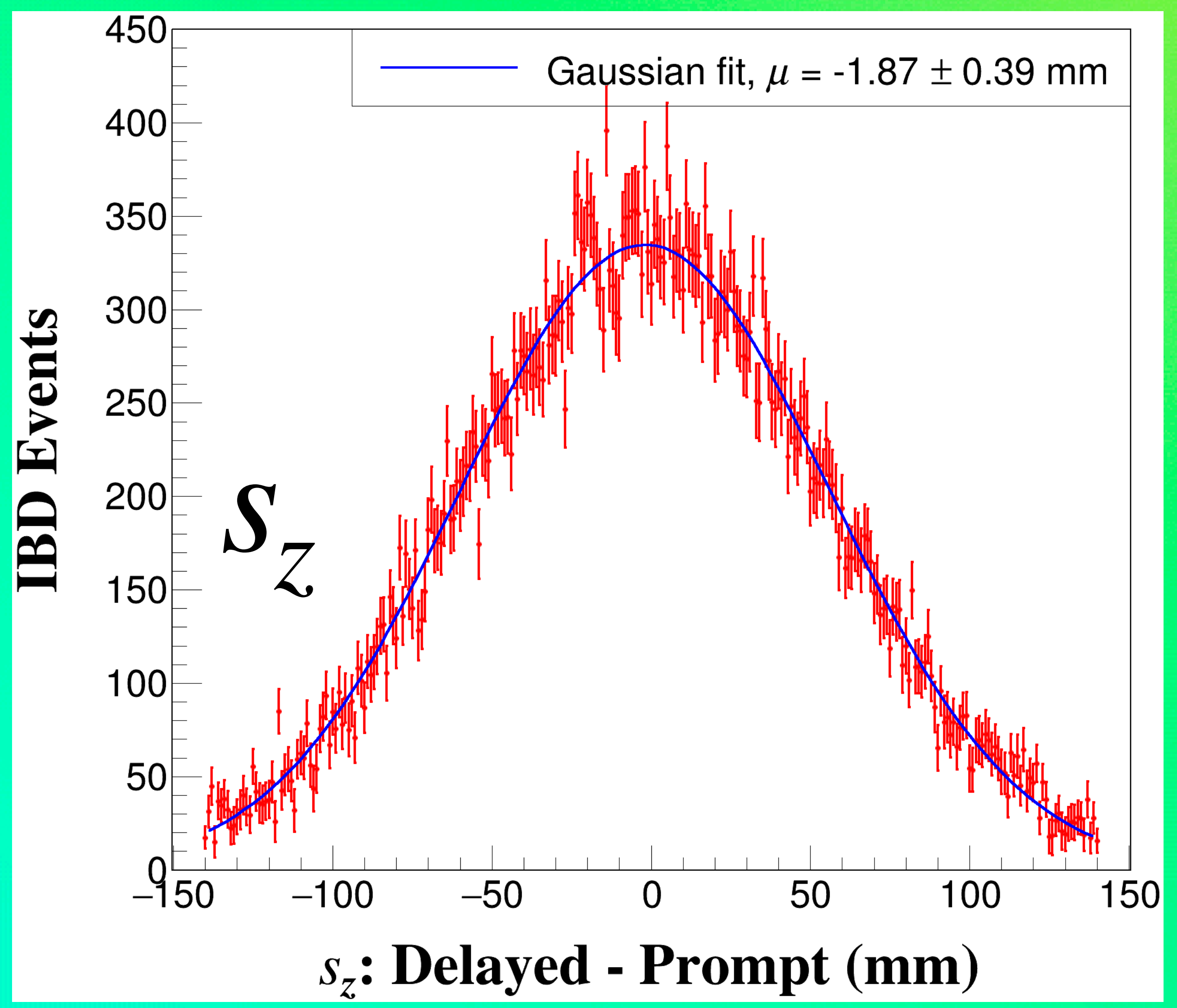

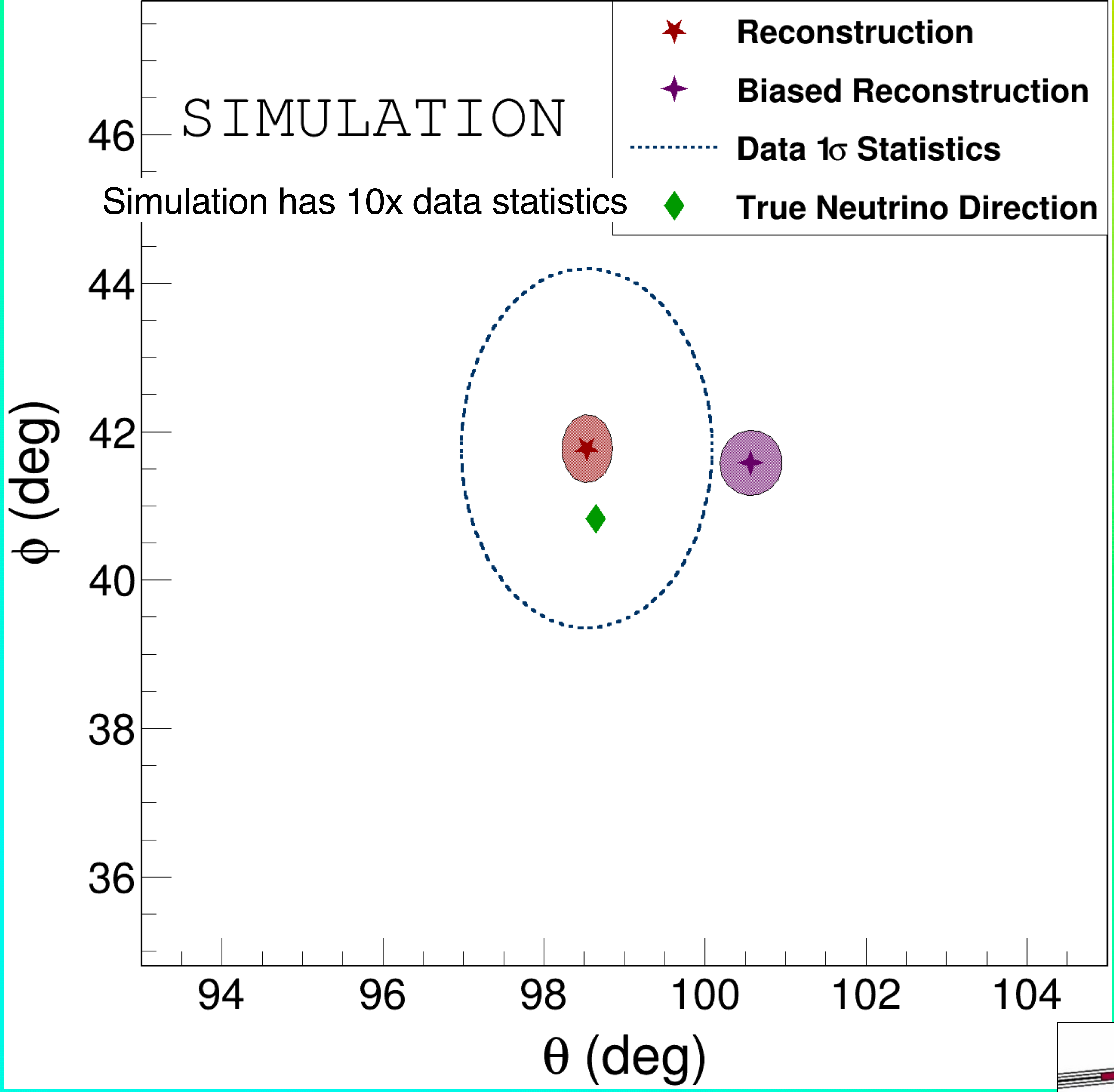

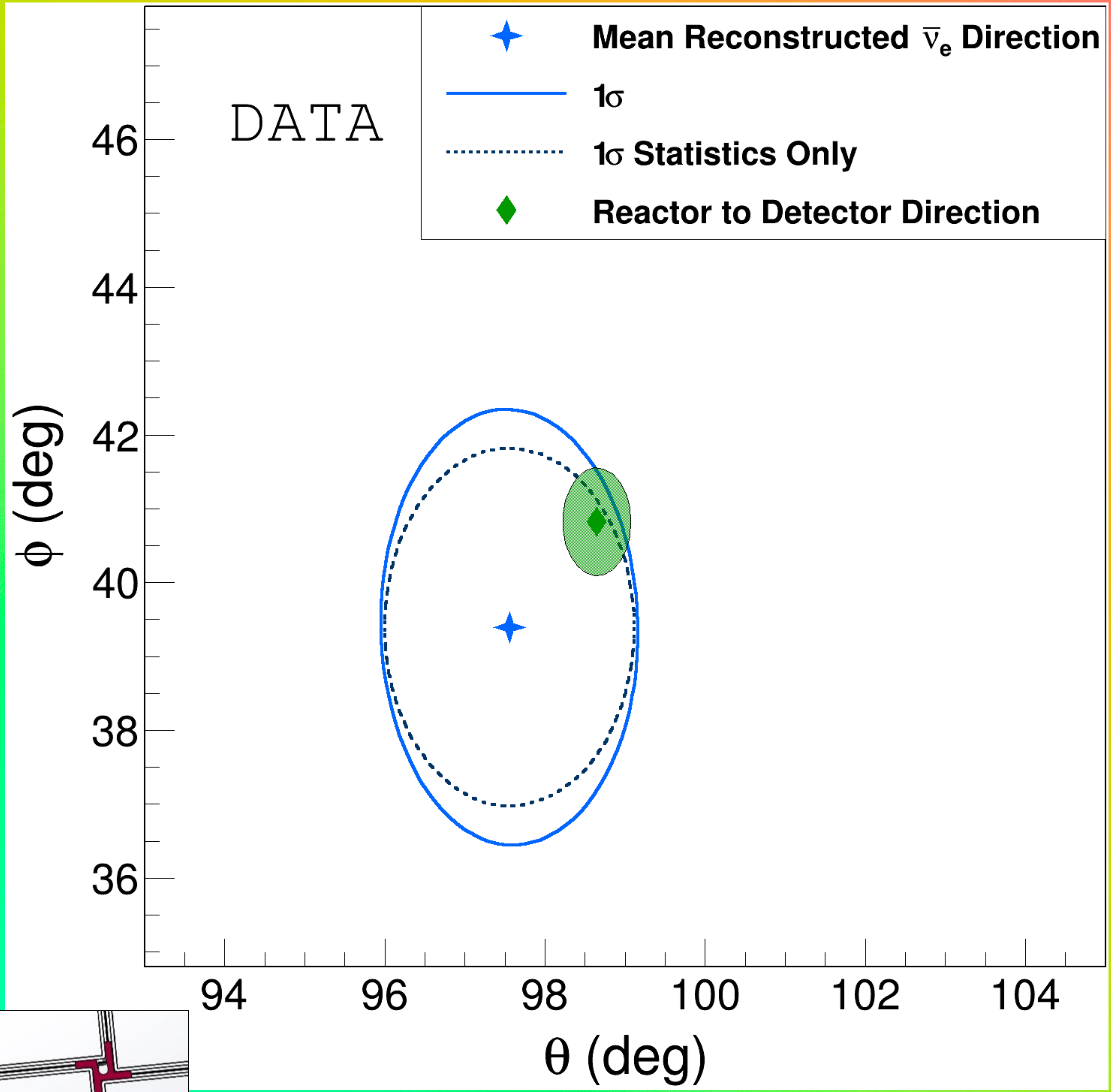

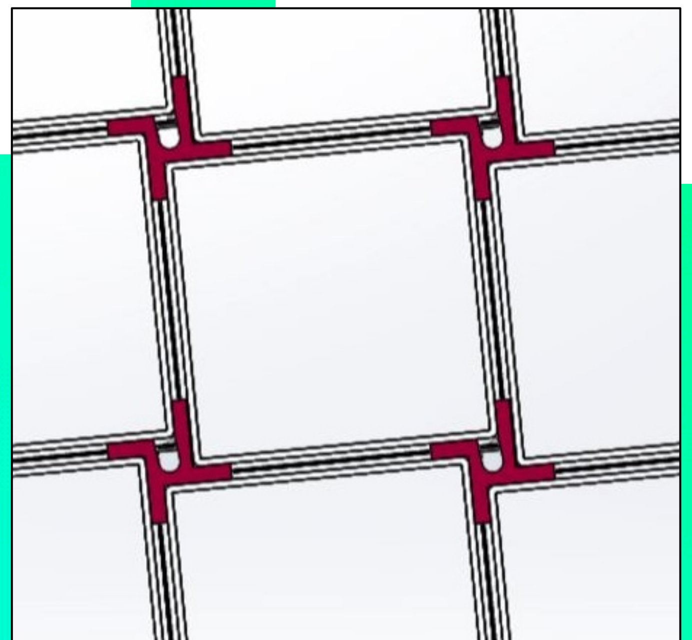

tilt for calibration access

Remaining bias of $\Delta\phi \approx 1^\circ$ is attributed to the 5.5° segment tilt to enable calibration.

Joint analyses - Oscillation

Source: David Lhuillier, Neutrino 2024

A combination of complementary datasets offers new benefits for sterile oscillation searches:

- Increased statistical power
- Accurate treatment of all experimental effects using the detector response matrices and the covariance matrices of uncertainties.
- Additional sterile sensitivity unlocked by comparison of long (commercial reactors) and short (research reactors) baseline energy spectra

The combination of all data provides neutrino fission spectra with unprecedented accuracy, challenging the predictions and associated nuclear data.

Joint analysis started late 2023 between DayaBay, Prospect and Stereo

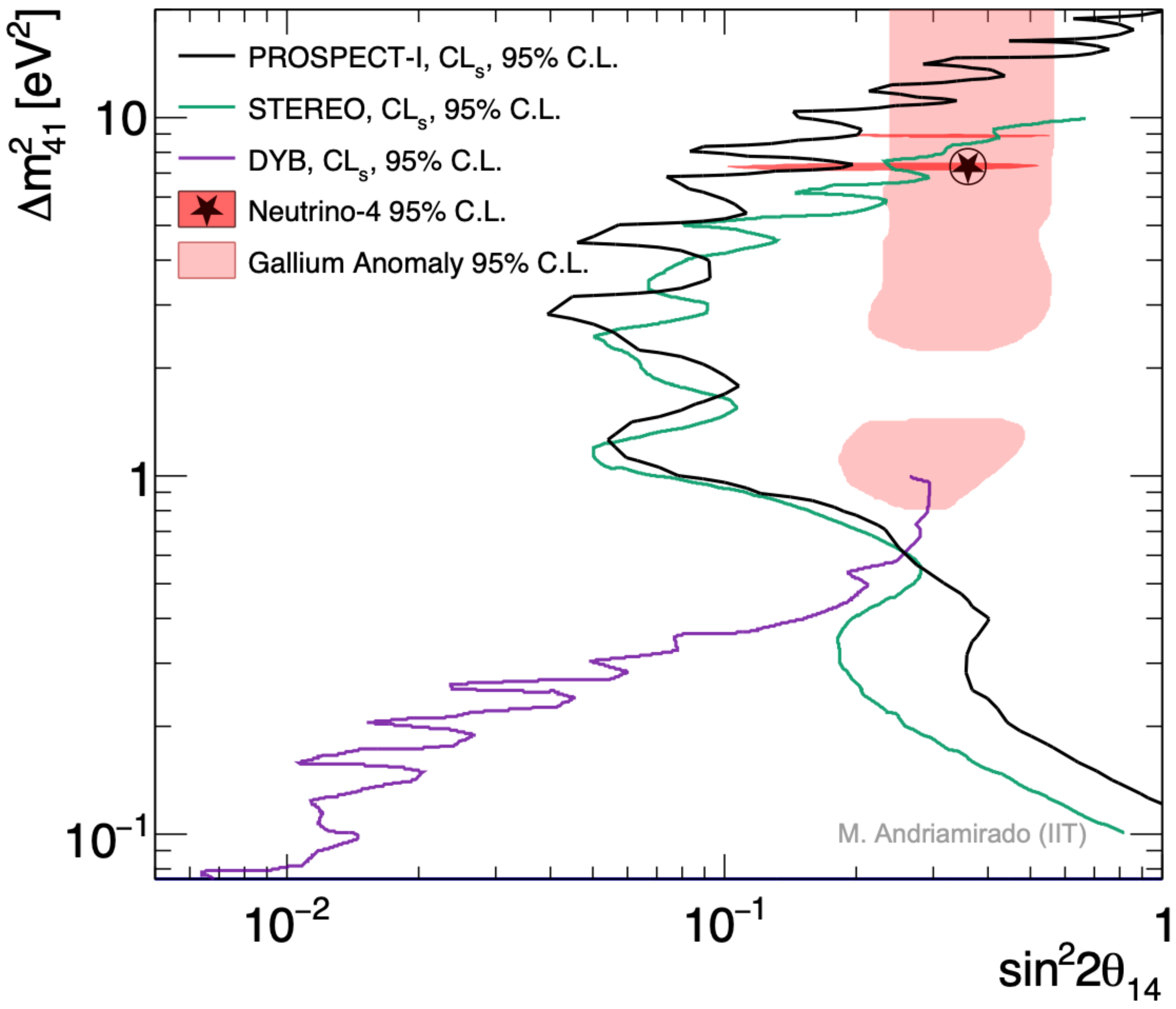

NEXT STEP: PROSPECT-II

- Goal: Match initial performance (maintain similar pitch, similar scintillator characteristics) while improving stability
- Remove PMTs from active volume
  - Eliminates main PROSPECT-1 failure mode
- Improve environmental control/isolation
  - Fewer materials in contact with LiLS
  - Improved cover gas system
  - Active cooling
- Enable emptying/refilling
  - Allows movement to multiple sites (HEU, LEU, DAR source, beam dump) unlocking a diverse potential long-term physics program

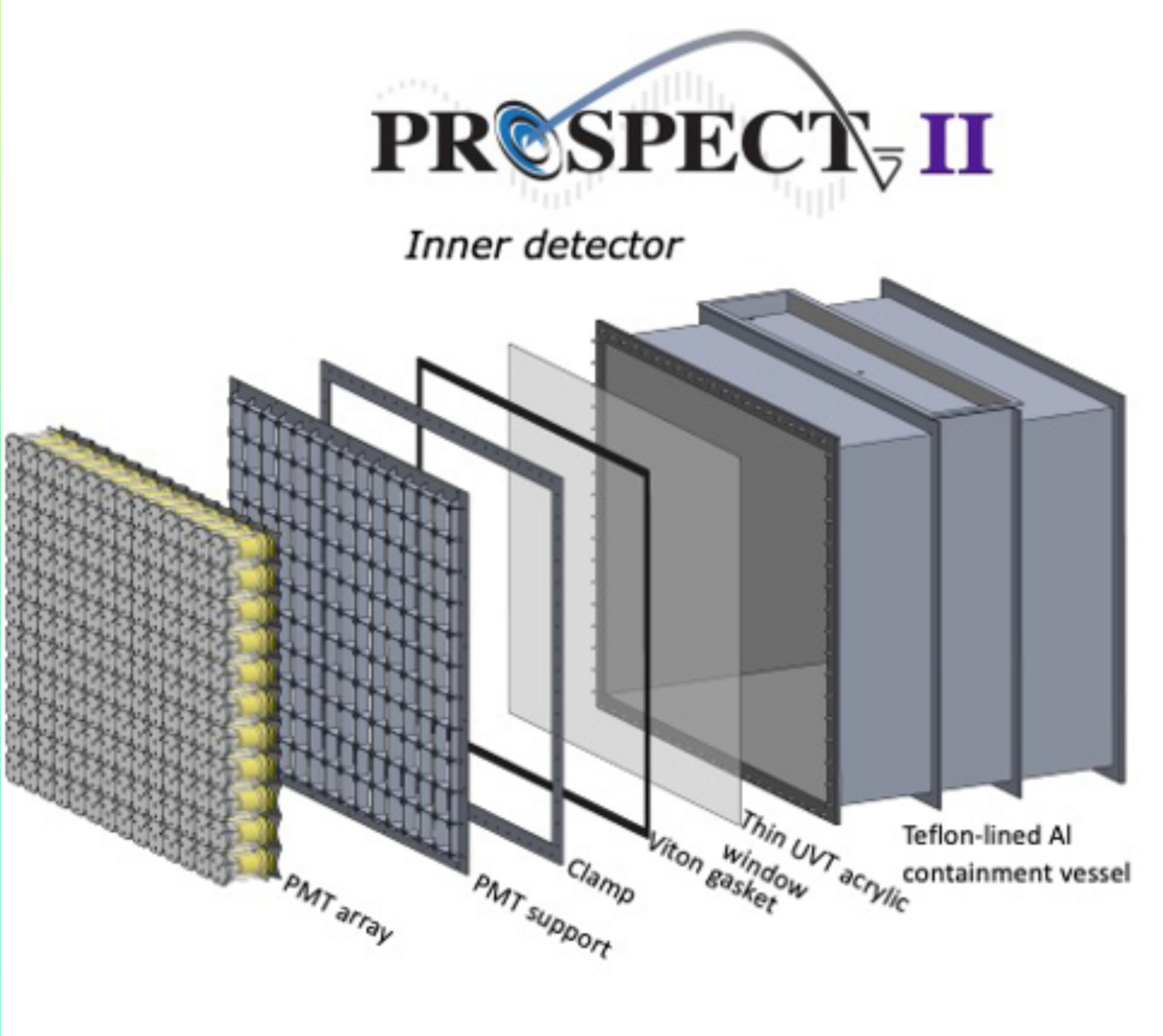

HEU = High Enriched Uranium = ^{235}U research reactor
LEU = Low Enriched Uranium = commercial reactor
DAR source = muon Decay-At-Rest source

PROSPECT-II R&D HIGHLIGHTS

Validated external calibration design JINST 18 P06010 (2023)

Retired risks associated with segment cross-talk J Phys G 49 (2022)

Completing teflon-lined inner vessel engineering design with vendor; production planned for late 2024.

Developed integration and assembly procedures

[Details: P-II IAEA presentation]

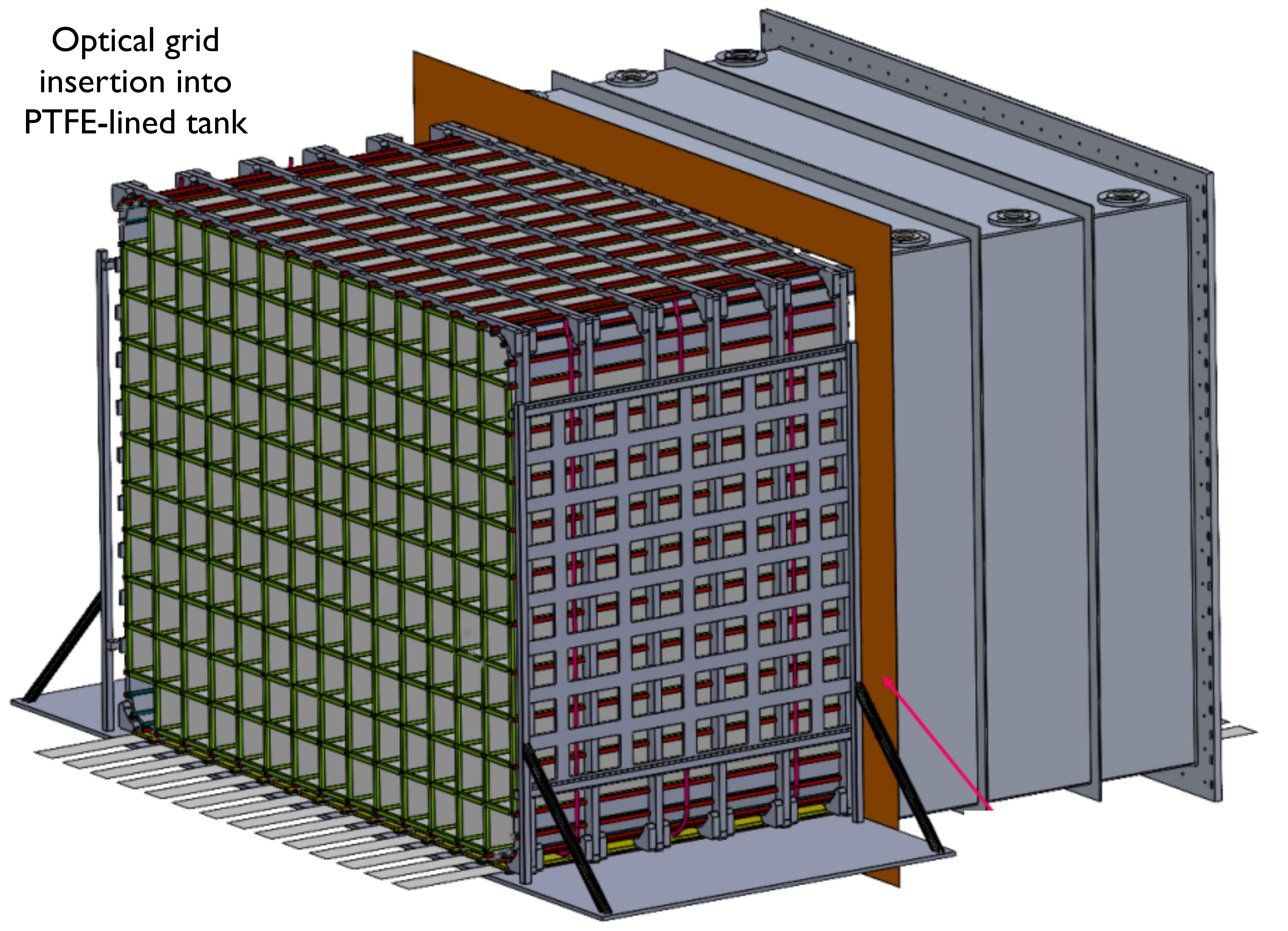

Optical grid insertion into PTFE-lined tank

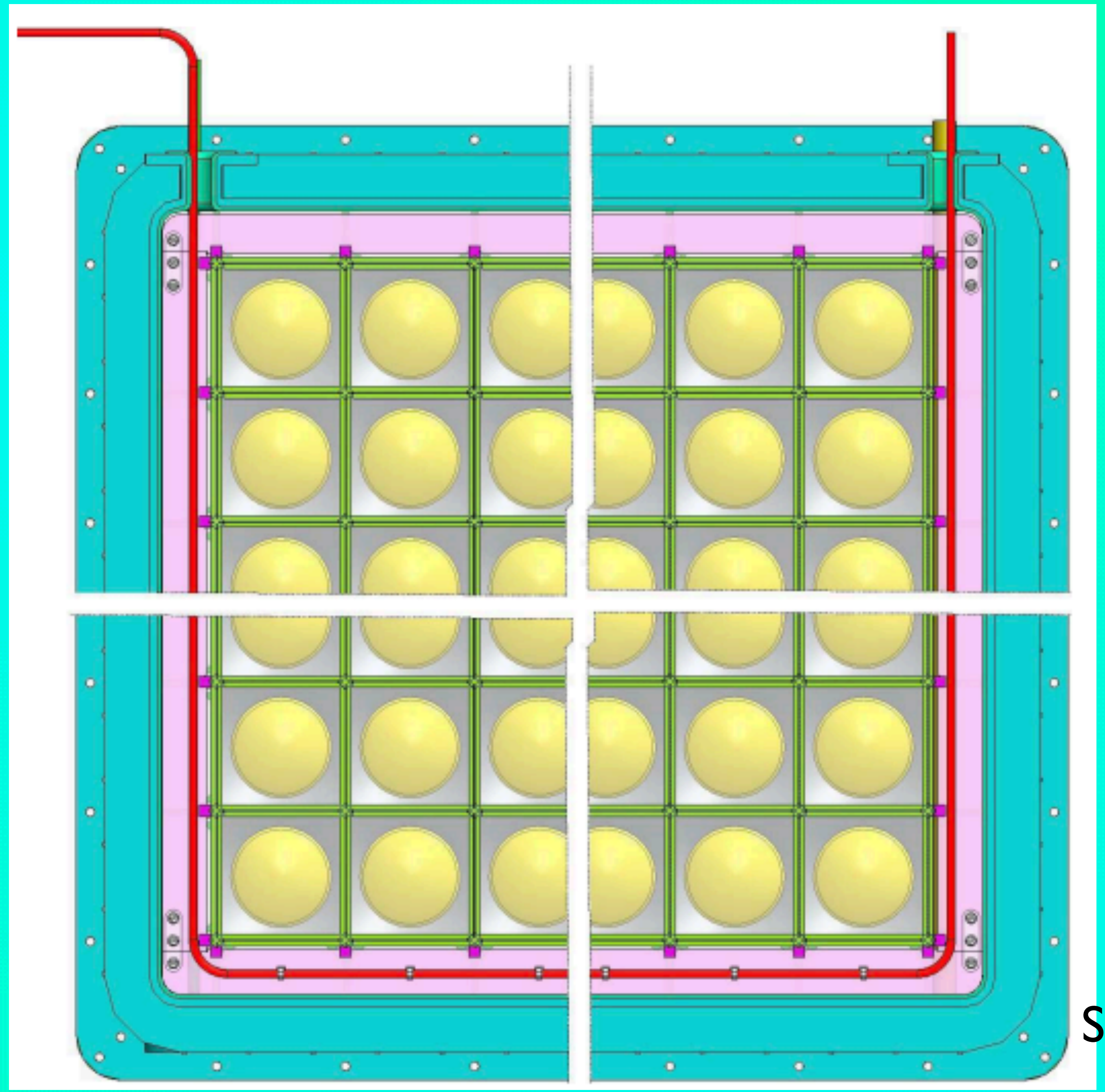

Segment-external calibration axes

Example: rotolined PTFE flange coatings

PROSPECT-II PHYSICS HIGHLIGHTS

J Phys G 49 (2022)

- HEU campaign:
  - Close out remaining BEST and Neutrino-4 suggested space below 20 eV^2
  - Pin down e-flavor disappearance to few-% level at <10 eV^2 , benefitting anomaly and long-baseline CPV interpretations
- Subsequent LEU campaign:
  - First correlated probe of HEU/LEU types
  - Delivers more precise isotopic ν_e flux/spectrum information, broadly benefiting reactor-CEvNS, nuclear data/ applications, …

Gebre, Littlejohn, Surukuchi, PRD 97 (2018)

Fujikake, Littlejohn, Benevides Rodrigues, Surukuchi, PRD 107 (2023)

Case	Description	Precision on σ_i (%)				
		^{235}U	^{238}U	^{239}Pu	^{240}Pu	^{241}Pu
-	Existing Global Data	1.3	26.4	25.2	-	42.6
1	HEU + LEU	1.6	11.1	4.6	-	10.5

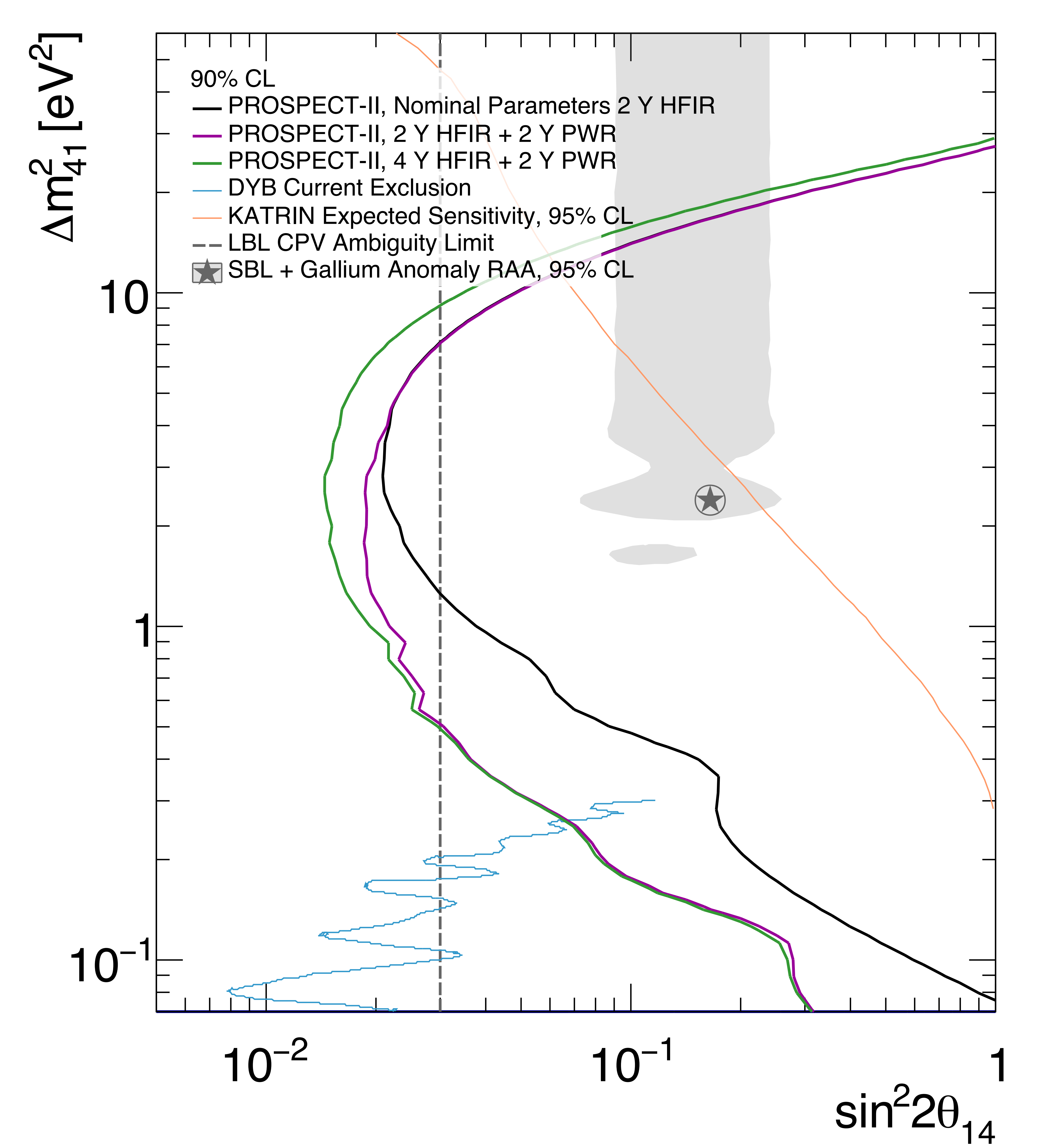

What did PROSPECT accomplish?

- PROSPECT-I physics (13 publications so far)
  - Best oscillation limits at high Δm^2_{41} with an important role in resolving reactor anomalies
  - Highest resolution measurement of the IBD antineutrino spectrum from ^{235}U fission
  - Improved understanding of non-fission contributions to the antineutrino spectrum
  - Joint analyses initiated with Daya Bay and STEREO
- Instrumentation (11 publications)
  - Highest statistics demonstration of surface neutrino detection
  - Operation of segmented detector with low inactive mass
  - Demonstrated calibration schemes for complex heterogeneous detectors
- Early career science
  - >20 undergraduates performed P-I hardware or analysis projects
  - 12 students received MS or PhDs
  - 10 postdocs with a significant fraction moving on to lab staff or university faculty

Drexel UNIVERSITY

HFIR

LE MOYNE COLLEGE A·D·1946

W&M

UNIVERSITY OF WATERLOO CONCORDIA CUM VERITATE

TEMPLE UNIVERSITY®

Lawrence Livermore National Laboratory

BROOKHAVEN NATIONAL LABORATORY

NIST

OAK RIDGE National Laboratory

Yale

Georgia Tech

ADDTIONAL SLIDES

PRD83 (2011) 073006

Neutrinos: Early 2010s - The “Reactor Antrieutrino Anomaly” (RAA)

Anomaly revealed by a re-evaluation of $\bar{\nu}_e$ production from reactors:
Experiments observe fewer $\bar{\nu}_e$ than expected from re-evaluation.

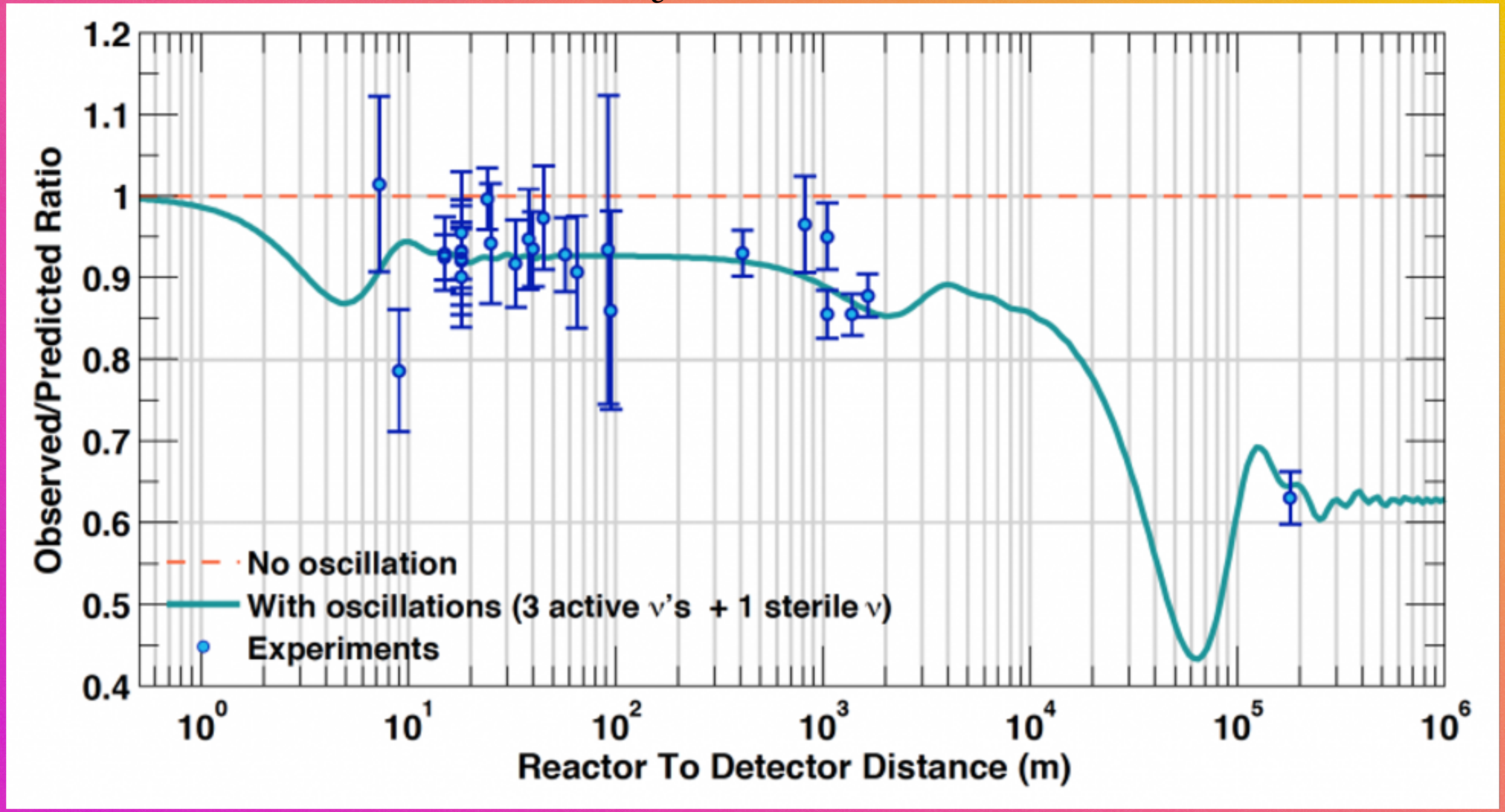

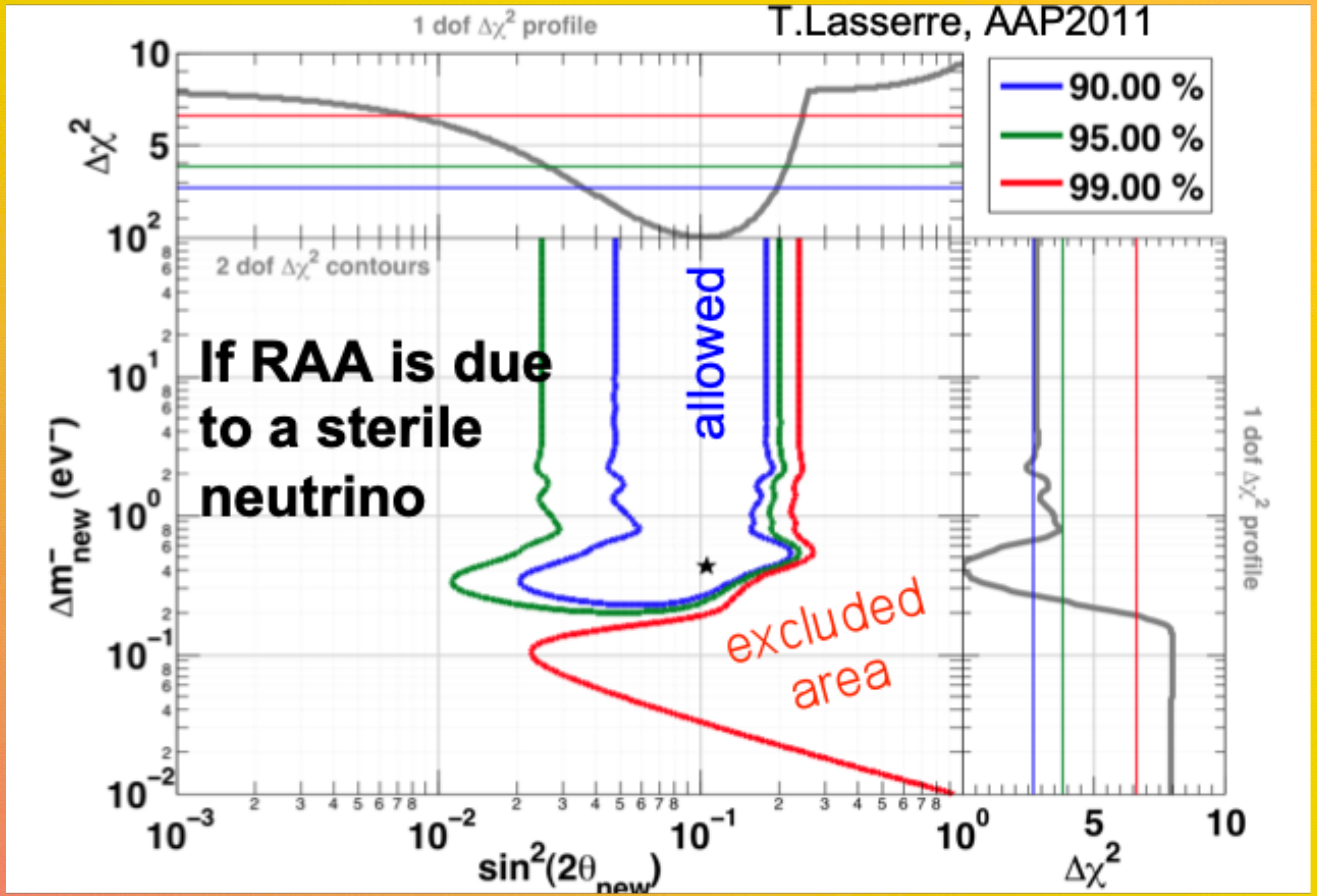

Other Backgrounds

Correlated nH followed by nLi

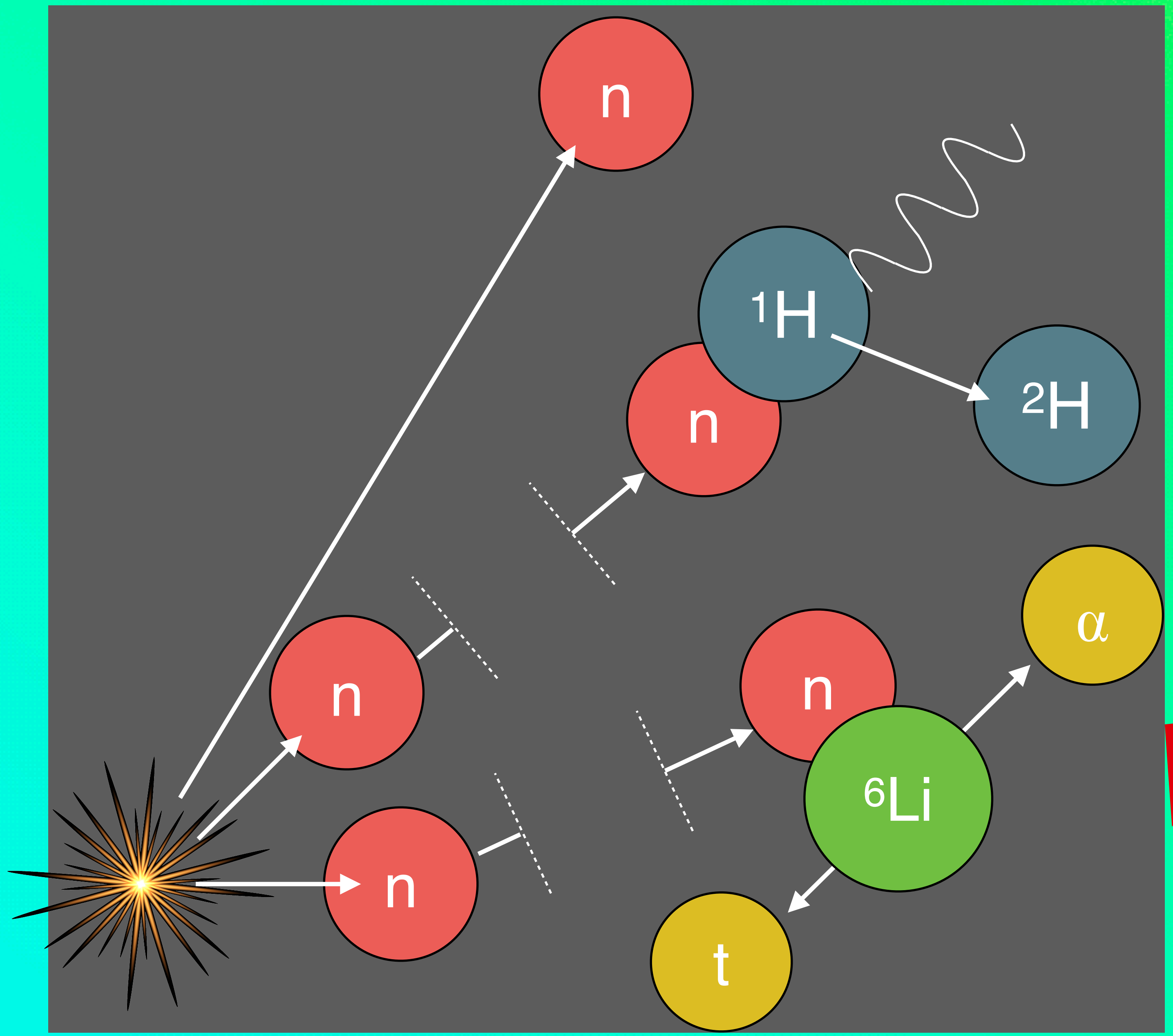

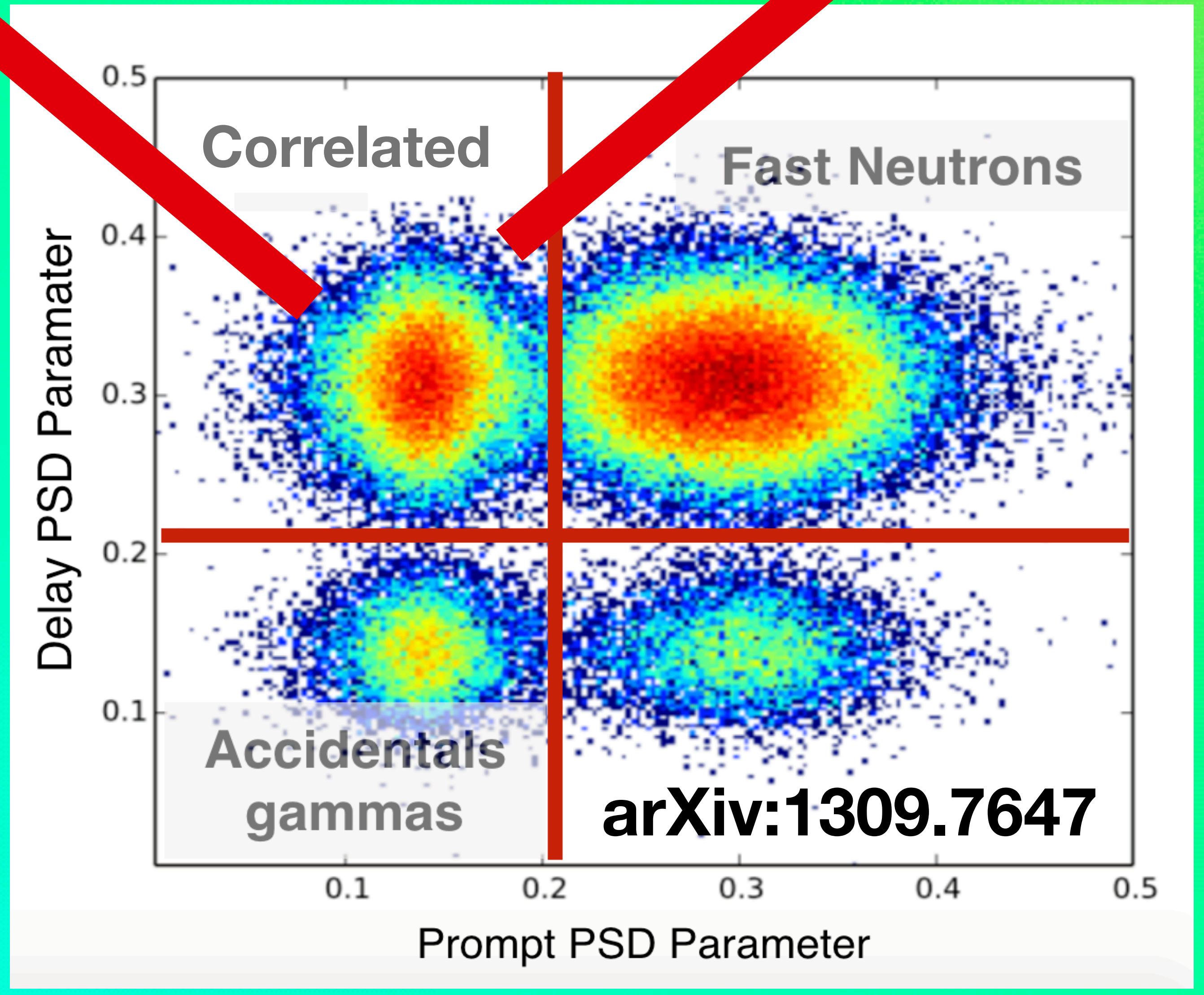

Correlated inelastic scattering on ^{12}C followed by nLi

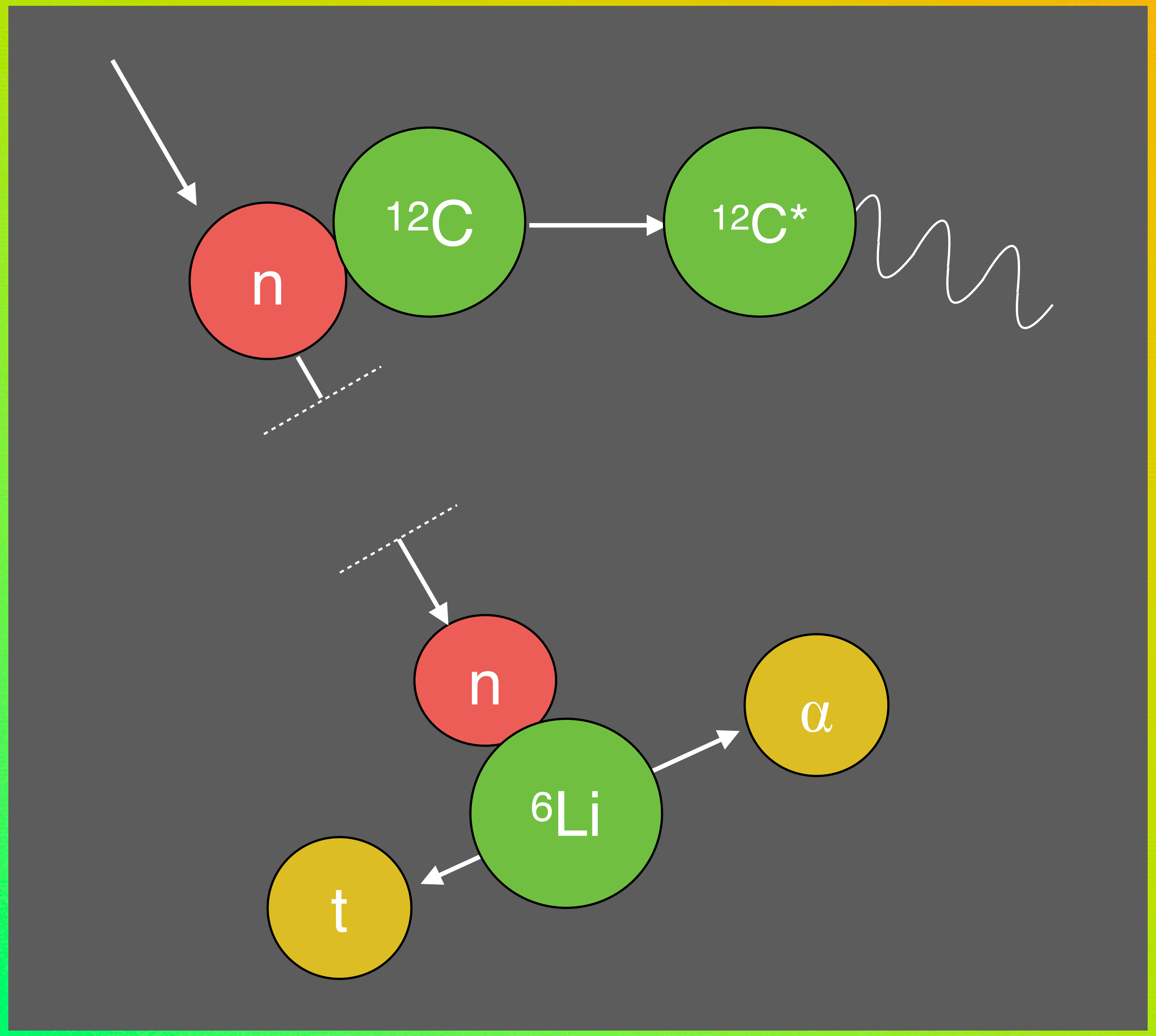

Cosmogenics are the main source for these two background classes

Neutrino oscillation: Exclusion

- Frequentist tests performed at a few key grid points:
  - Test statistic: $\Delta\chi^2 = \chi^2_{true} - \chi^2_{best\text{-}fit}$
  - 2000 toy MC experiments generated for each test point
  - $\Delta\chi^2$ observed for data is highly consistent with null-oscillation toy MC experiments (p=0.73):
  - Toy MC experiments at Neutrino-4 best-fit point provide $\Delta\chi^2$ far below that observed in the data

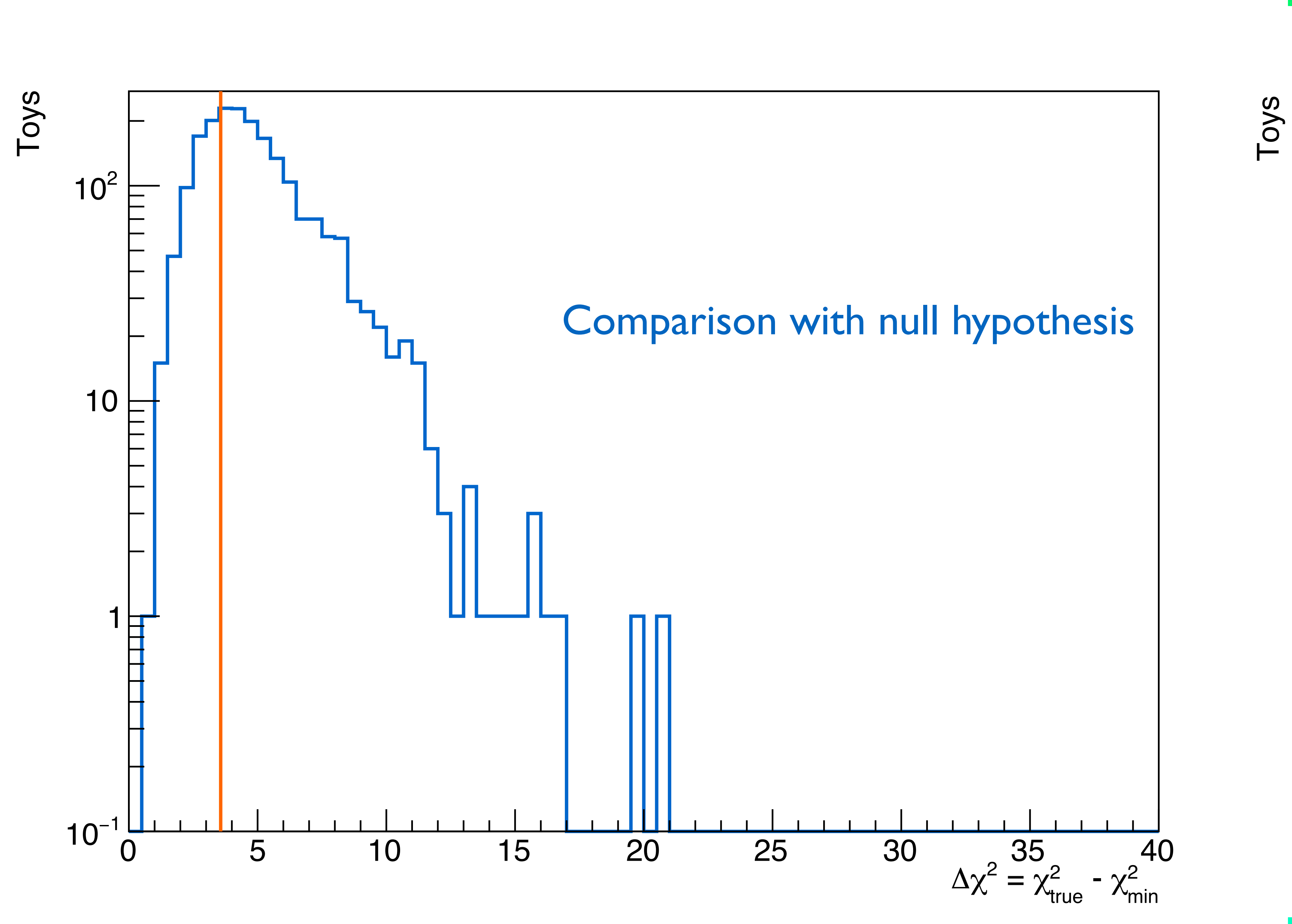

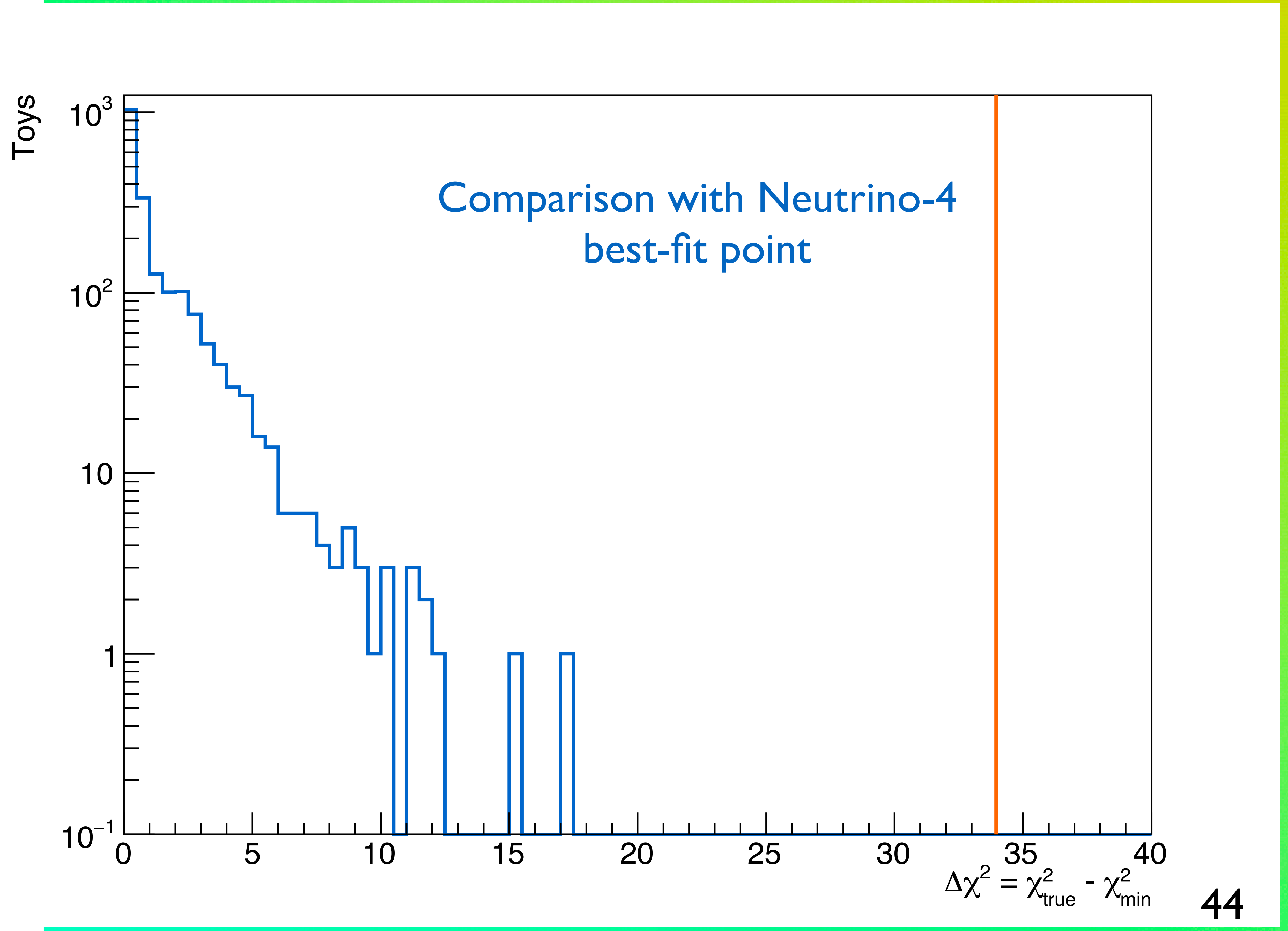

Source: David Lhuillier, Neutrino 2024

Neutrino 4

JETP 137 (2023) 1, 55-70

Reactor SM-3 Dimitrovgrad, Russia

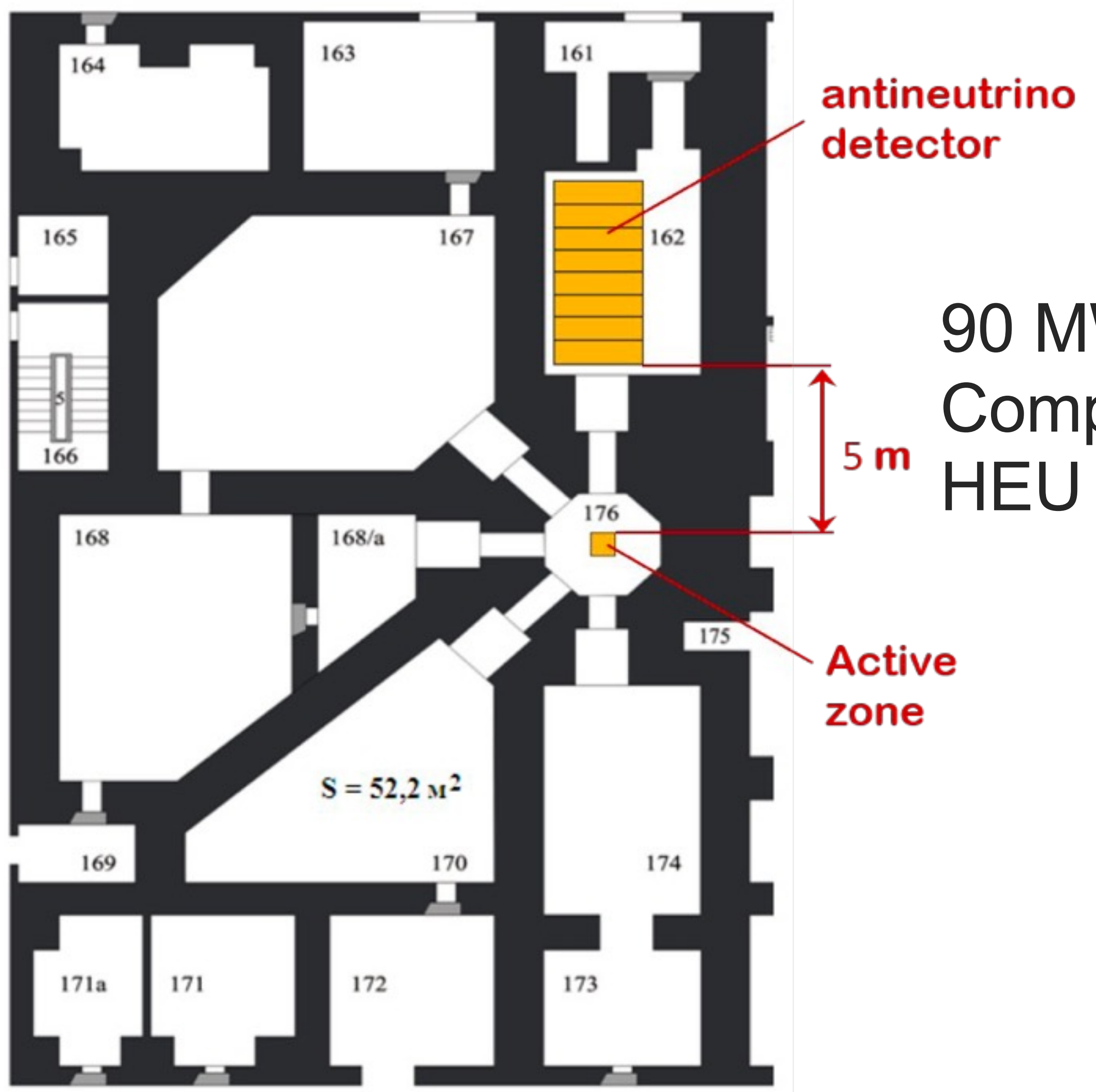

90 MW
Compact core
HEU ^{235}U fuel

Movable segmented detector filled with Gd-loaded LS
L ≈ 6.4 – 11.9m with 23 cm steps (24 positions)

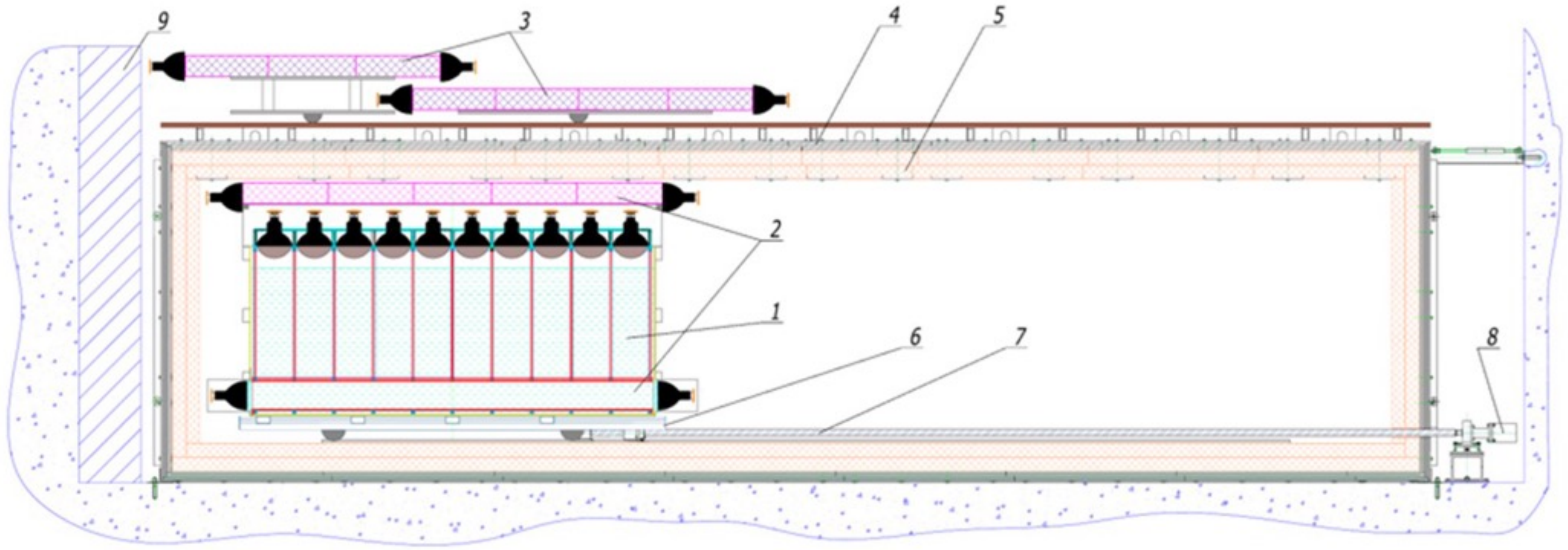

Positive oscillation signal with 2.7σ significance (FC)
Best fit parameters: $\sin^2(2\theta_{14}) \approx 0.36$, $\Delta m_{14} \approx 7.3$ eV

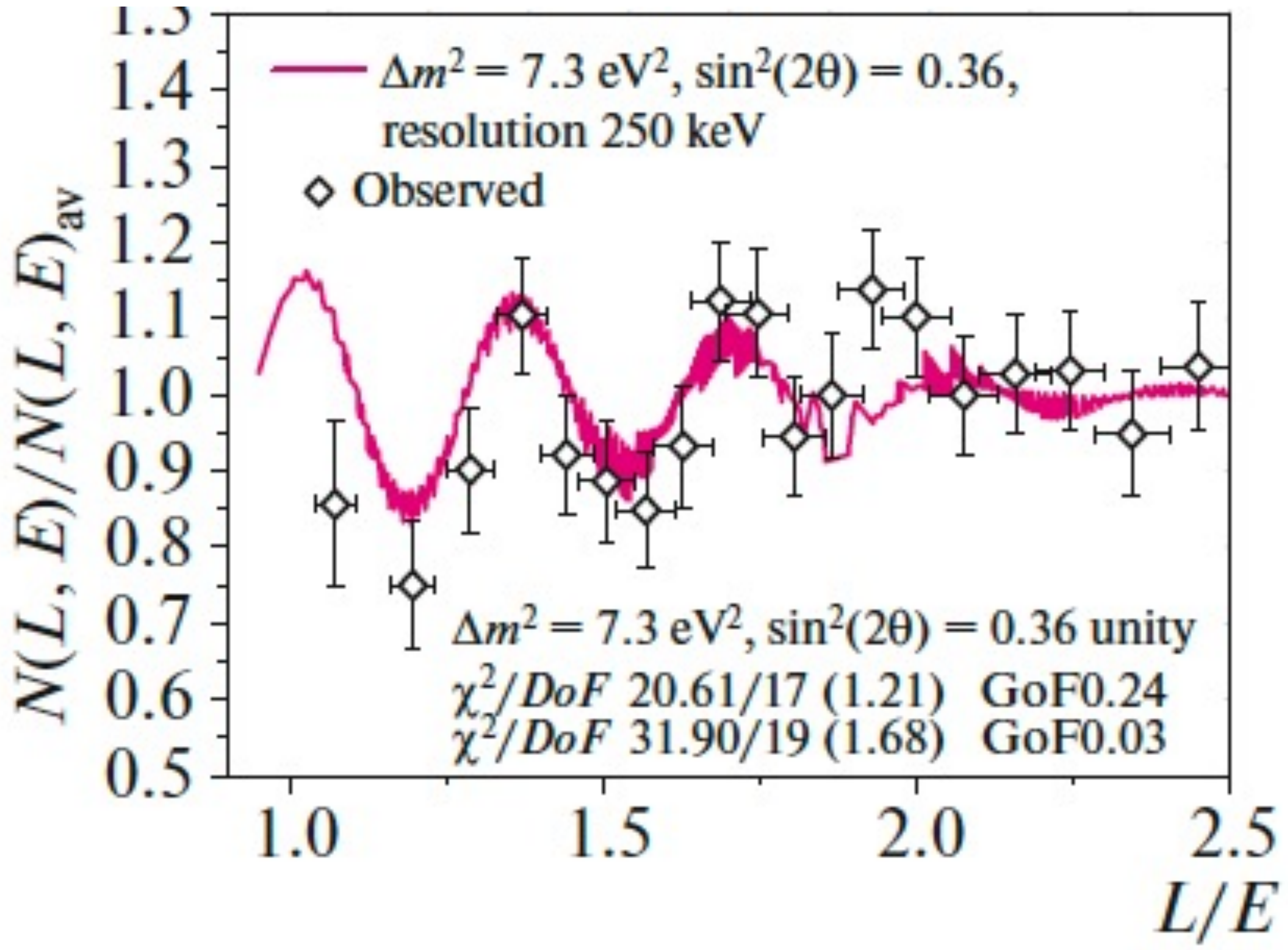

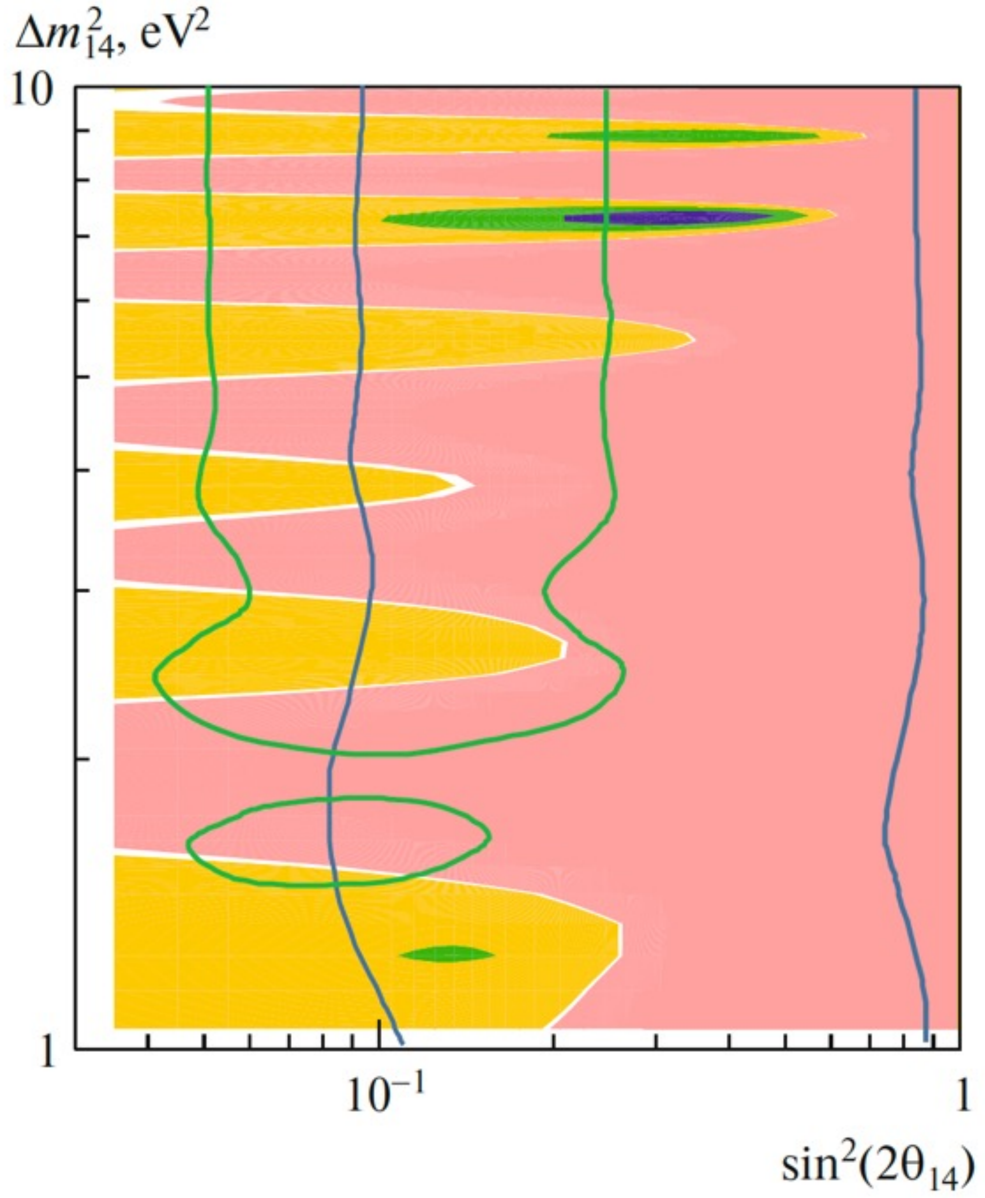

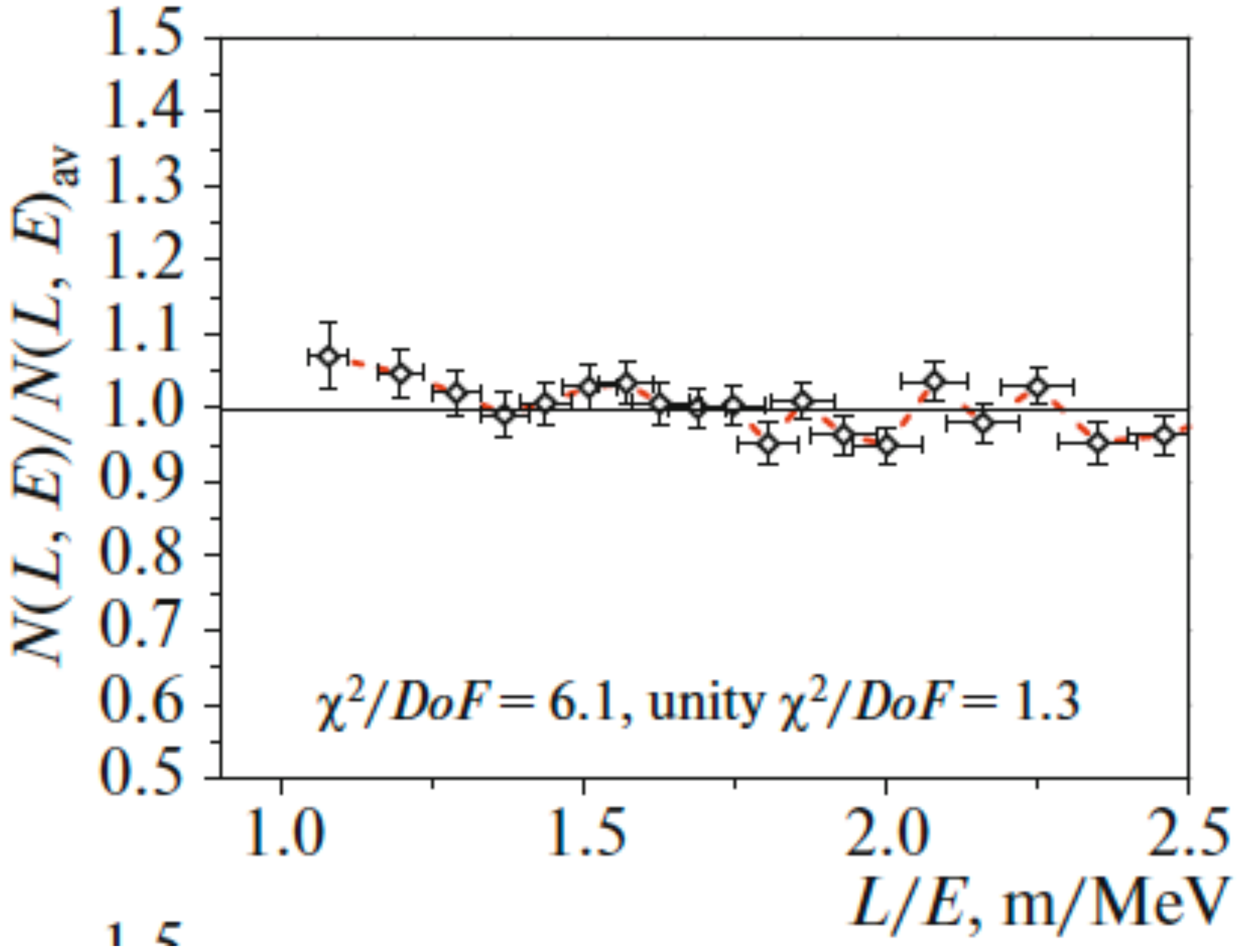

No PSD
S/B = 0.54

Source: David Lhuillier, Neutrino 2024

Neutrino 4+

Tech. Phys. 60 (2015) 12, 1863-1871

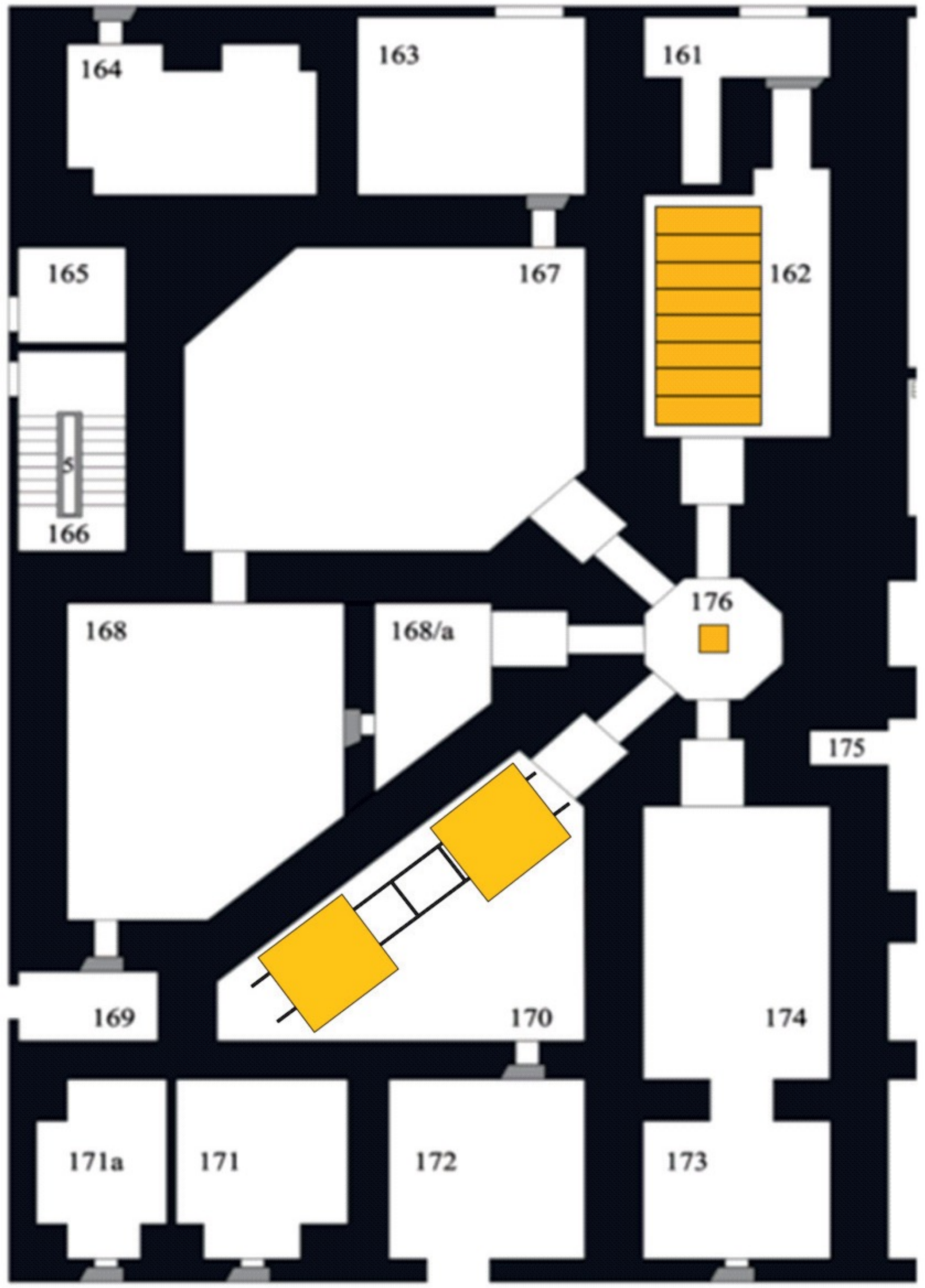

Major detector upgrade with
- Larger volume
- Improved background rejection from active and passive shielding and PSD capability
- Improved resolution from 2-sided readout of detector cells

Data collection is expected to start at the end of this year

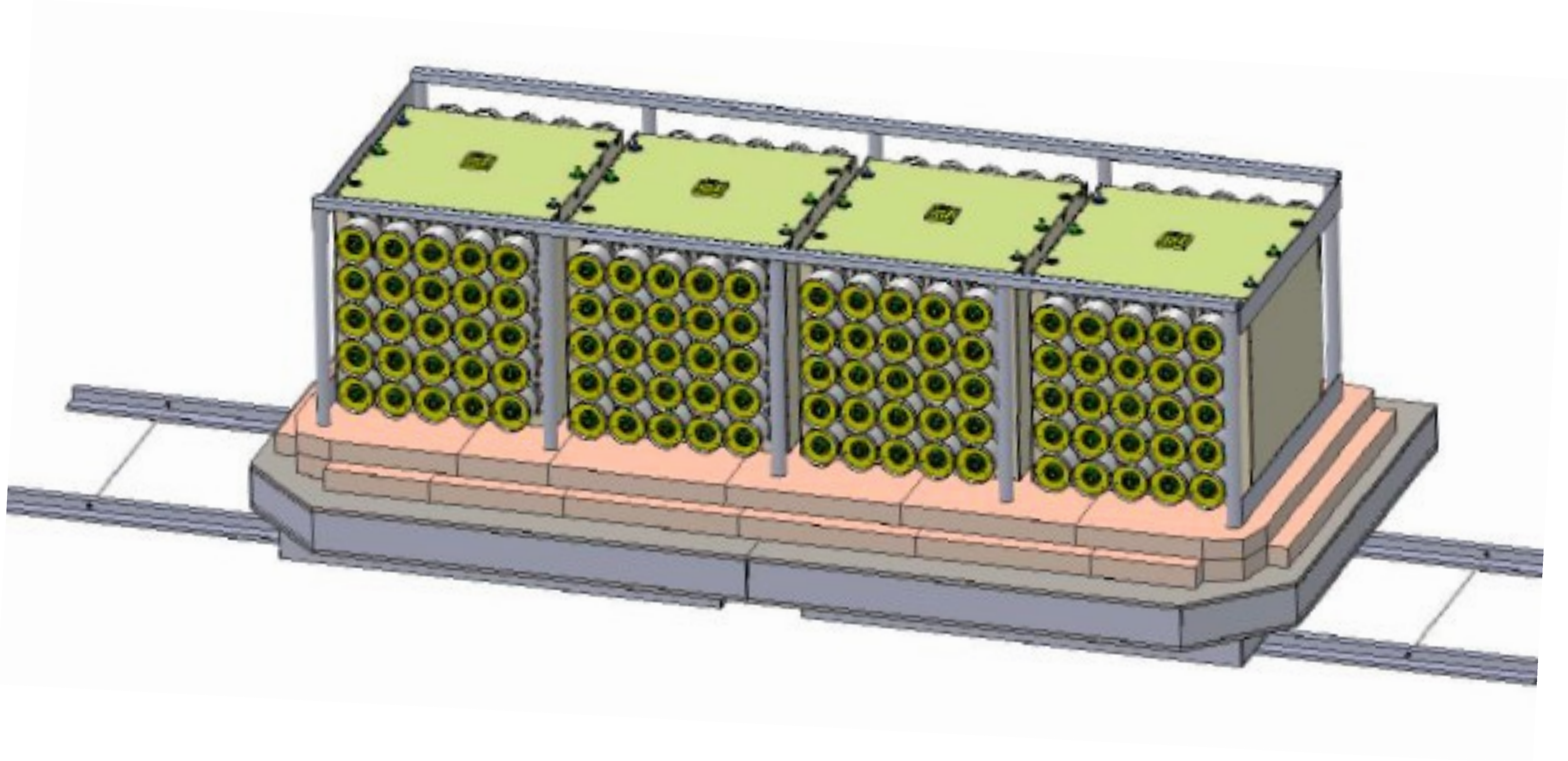

Source: David Lhuillier, Neutrino 2024

Positive Signals (?) – BEST Experiment

PRC 105 (2022)

3.4 MCi ^{51}Cr source in two concentric volumes of Gallium: $^{71}Ga(\nu,e)^{71}Ge$

"Gallium anomaly"

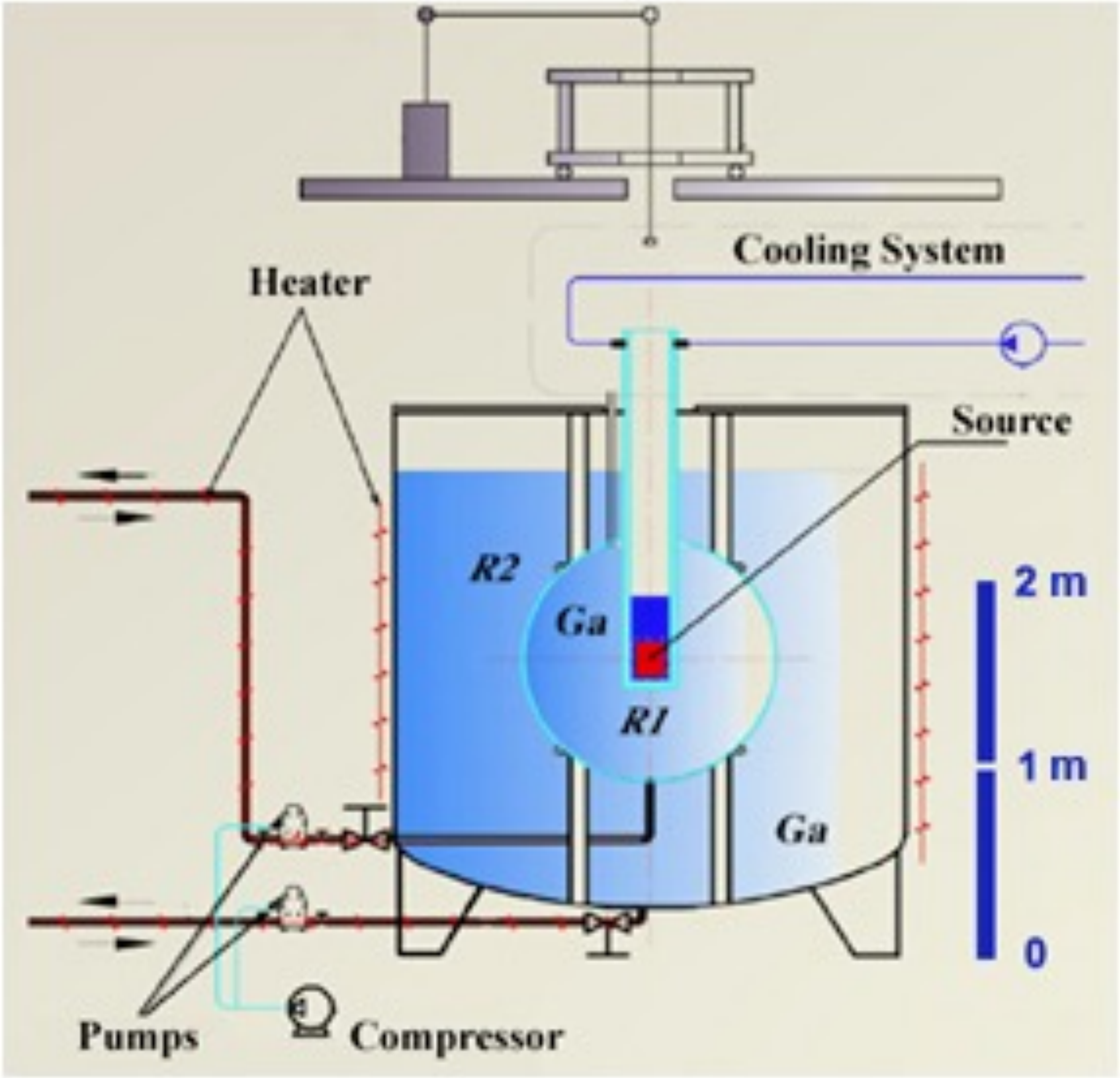

BEST+GALLEX+SAGE contour

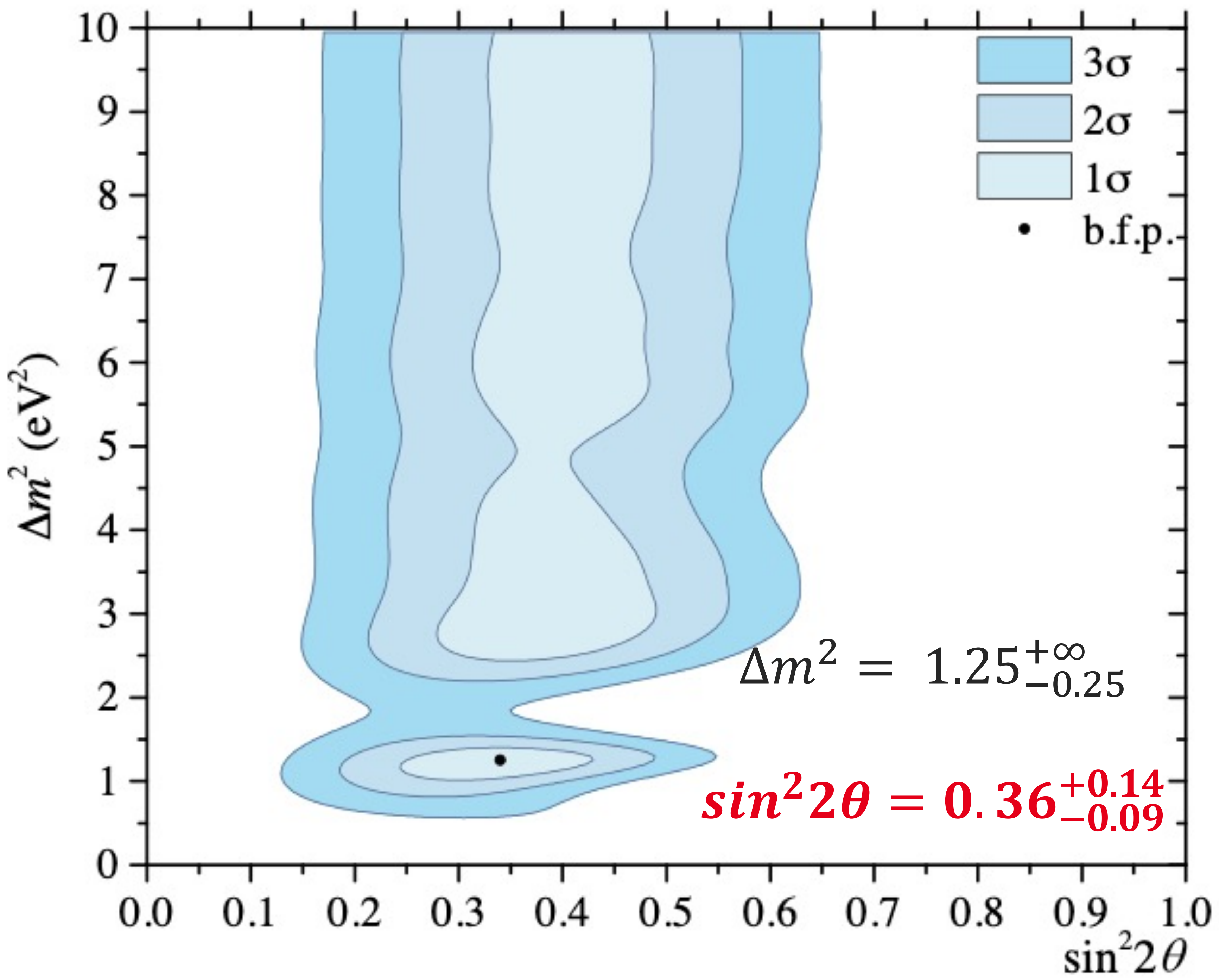

- 20% deficit confirming GALLEX and SAGE results with >5σ significance.
- Very large mixing angle.
- Rate only, no oscillation pattern → intensive search for possible normalization biases, so far unfruitful.

Ratio of observed/measured events:

R_{in} = 0.79 ± 0.05
R_{out} = 0.77 ± 0.05

Anchoring of the ν-capture cross section on the ^{71}Ge decay:

W. Hampel, L.P. Remsberg PRC, 31 (1995)

Neutrino directionality

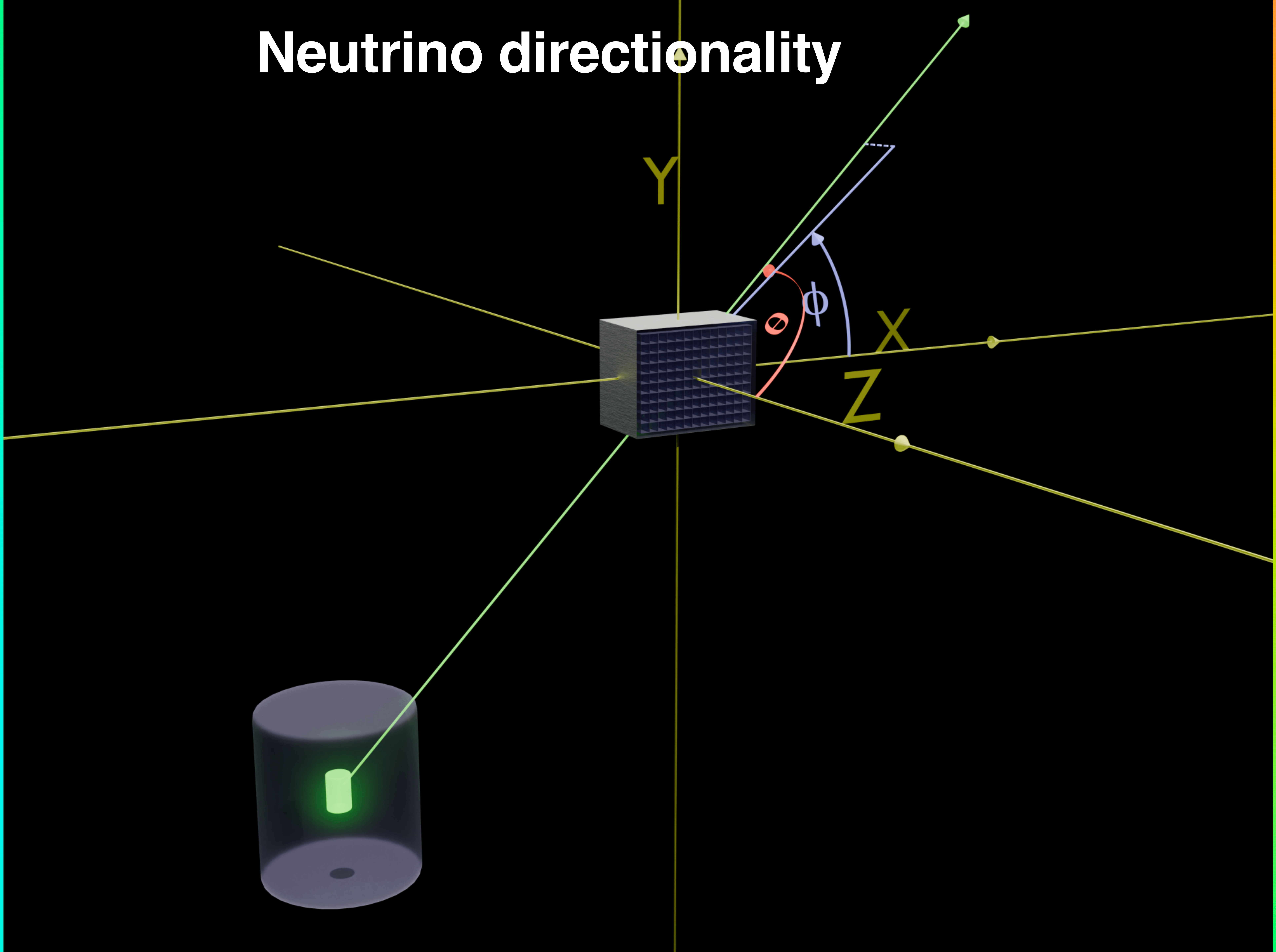

Neutrino directionality

	p_x (mm)	p_y (mm)	p_z (mm)
Data	10.84 ± 0.60	9.21 ± 0.60	-1.87 ± 0.39
Data, biased	8.70 ± 0.37	7.31 ± 0.37	-1.87 ± 0.39

TABLE I. The values of p_x, p_y, and p_z (average displacements in each direction) for the data with and without applying the modified method. "Data, biased" utilizes Equation 3 while "Data" uses Equation 5. The uncertainties on the data values are statistical only.

BiPo Displacement Mean	
p_x	-0.25 ± 0.08 mm
p_y	-0.39 ± 0.08 mm
p_z	0.06 ± 0.06 mm

TABLE II. The results for the average displacement in each direction for the BiPo events. Only the z result agrees with our expected result of 0 mm within error. However, the p_x and p_y values are only a fraction of a mm away from zero.

Null test using coincidences $^{214}\mathrm{Bi} \rightarrow ^{214}\mathrm{Po} \rightarrow ^{210}\mathrm{Pb}$ decays that produce β^-, α pairs

Detector Components

Highly reflective low mass rigid reflector system built by IIT

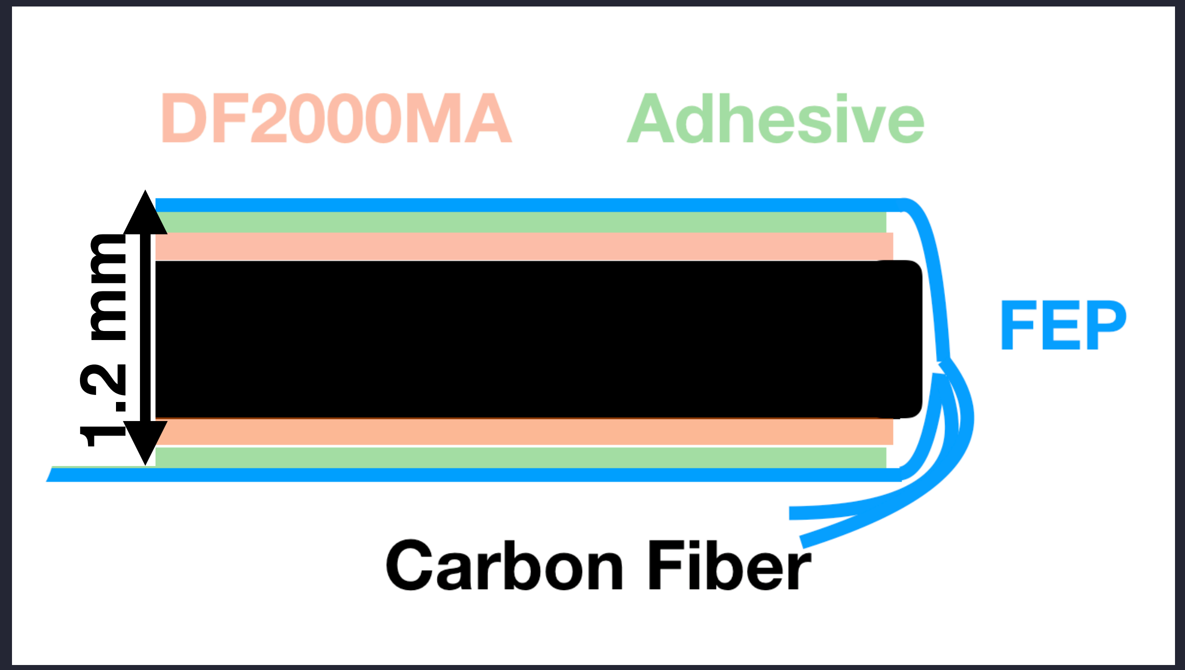

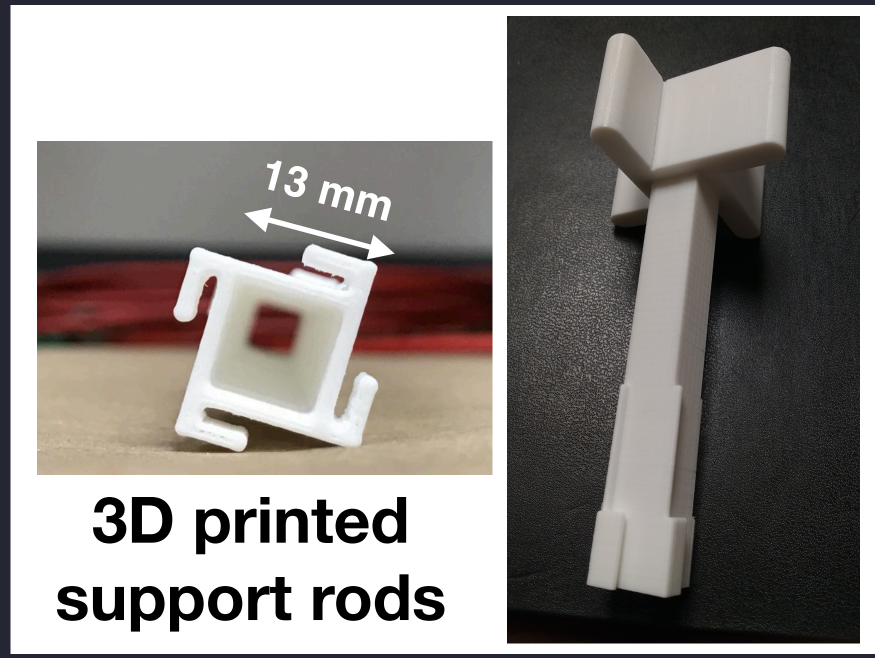

3D printed support rods

PMT housing designed for optimal light collection

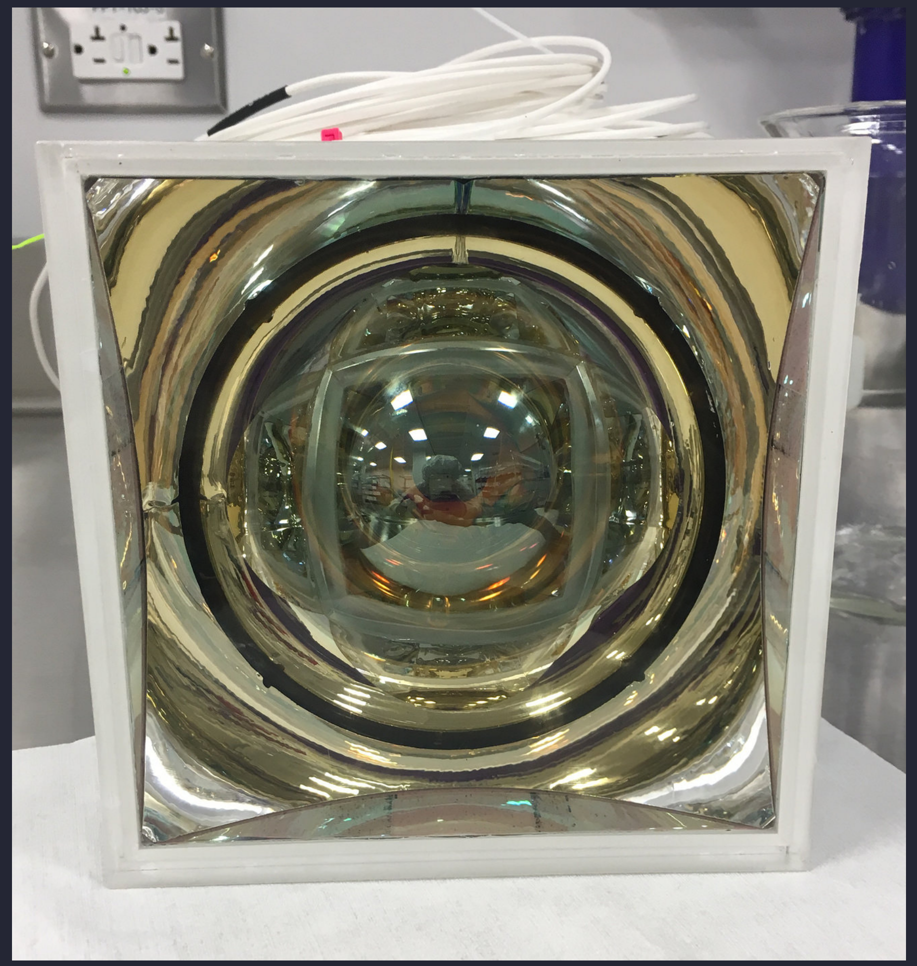

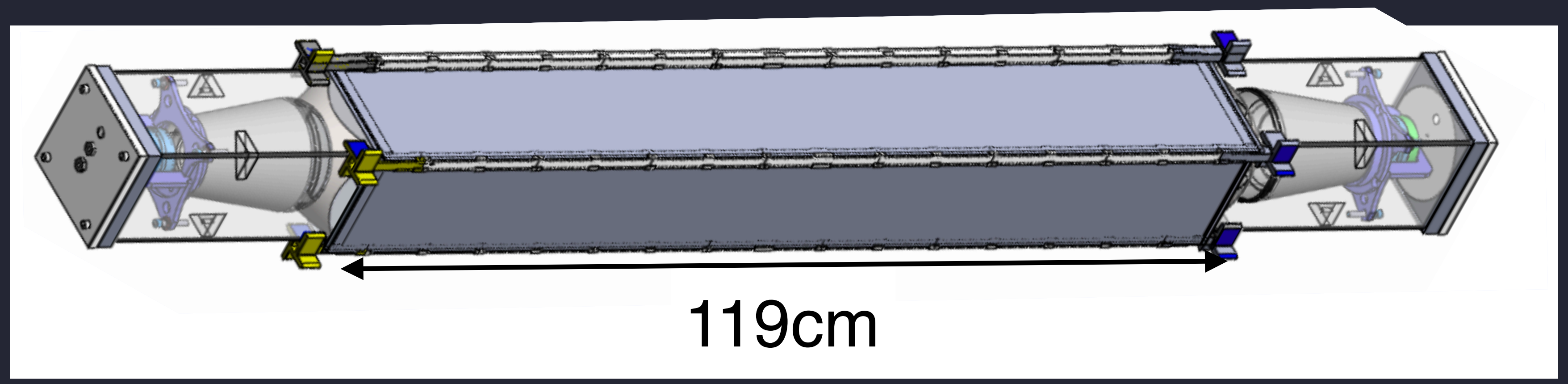

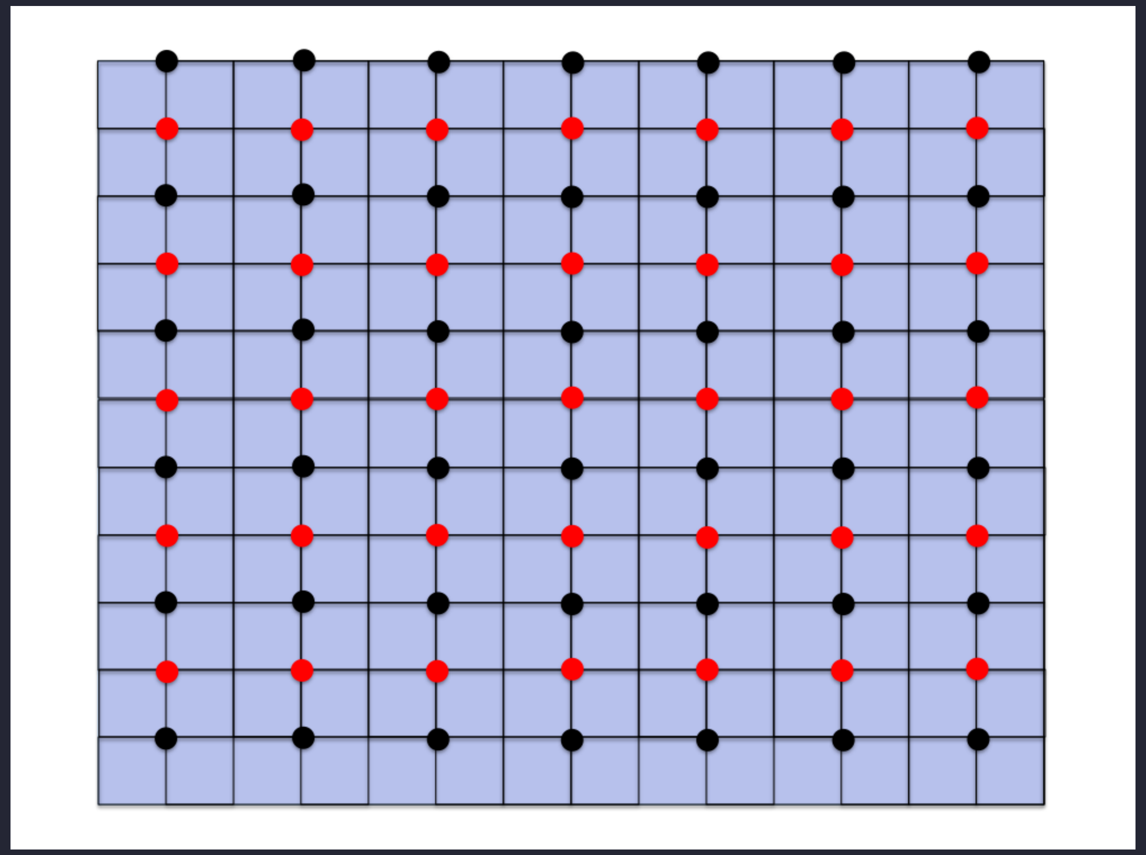

Calibration position map

All internal detector components tested for long term compatibility with the liquid scintillator

Oak Ridge National Laboratory Neutron Production Overview

Neutron Production
Outage

Revised 1/12/23. The working schedule for the Spallation Neutron Source (SNS) and the High Flux Isotope Reactor (HFIR) is subject to change in response to evolving operational and project needs. The community will be notified as soon as possible if changes occur.